National Library of Canada
Acquisitions and Bibliographic Services Branch
395 Wellington Street
Ottawa, Ontario
K1A 0N4

Bibliothèque nationale du Canada
Direction des acquisitions et des services bibliographiques
395, rue Wellington
Ottawa (Ontario)
K1A 0N4

Your file Votre référence

Our file Notre référence

NOTICE

The quality of this microform is heavily dependent upon the quality of the original thesis submitted for microfilming. Every effort has been made to ensure the highest quality of reproduction possible.

If pages are missing, contact the university which granted the degree.

Some pages may have indistinct print especially if the original pages were typed with a poor typewriter ribbon or if the university sent us an inferior photocopy.

Reproduction in full or in part of this microform is governed by the Canadian Copyright Act, R.S.C. 1970, c. C-30, and subsequent amendments.

AVIS

La qualité de cette microforme dépend grandement de la qualité de la thèse soumise au microfilmage. Nous avons tout fait pour assurer une qualité supérieure de reproduction.

S'il manque des pages, veuillez communiquer avec l'université qui a conféré le grade.

La qualité d'impression de certaines pages peut laisser à désirer, surtout si les pages originales ont été dactylographiées à l'aide d'un ruban usé ou si l'université nous a fait parvenir une photocopie de qualité inférieure.

La reproduction, même partielle, de cette microforme est soumise à la Loi canadienne sur le droit d'auteur, SRC 1970, c. C-30, et ses amendements subséquents.

Canada

University of Alberta

Glacial History and Holocene Sea Level Regression in the Foxe/Baffin Sector of the Laurentide Ice Sheet, Northwest Baffin Island, Arctic Canada

by

Matthew James Gordon Hooper

©

A thesis submitted to the Faculty of Graduate Studies and Research in partial fulfilment of the requirements for the degree of Doctor of Philosophy

Department of Earth and Atmospheric Sciences

Edmonton, Alberta

Spring, 1996

National Library
of Canada

Acquisitions and
Bibliographic Services Branch

395 Wellington Street
Ottawa, Ontario
K1A 0N4

Bibliothèque nationale
du Canada

Direction des acquisitions et
des services bibliographiques

395, rue Wellington
Ottawa (Ontario)
K1A 0N4

Your file Votre référence

Our file Notre référence

The author has granted an irrevocable non-exclusive licence allowing the National Library of Canada to reproduce, loan, distribute or sell copies of his/her thesis by any means and in any form or format, making this thesis available to interested persons.

L'auteur a accordé une licence irrévocable et non exclusive permettant à la Bibliothèque nationale du Canada de reproduire, prêter, distribuer ou vendre des copies de sa thèse de quelque manière et sous quelque forme que ce soit pour mettre des exemplaires de cette thèse à la disposition des personnes intéressées.

The author retains ownership of the copyright in his/her thesis. Neither the thesis nor substantial extracts from it may be printed or otherwise reproduced without his/her permission.

L'auteur conserve la propriété du droit d'auteur qui protège sa thèse. Ni la thèse ni des extraits substantiels de celle-ci ne doivent être imprimés ou autrement reproduits sans son autorisation.

ISBN 0-612-10595-4

Canada

University of Alberta

Library Release Form

Name of Author: Matthew James Gordon Hooper

Title of Thesis: Glacial History and Holocene Sea Level Regression in the Foxe/Baffin Sector of the Laurentide Ice Sheet, Northwest Baffin Island, Arctic Canada

Degree: Doctor of Philosophy

Year this Degree Granted: 1996

Permission is hereby granted to the University of Alberta Library to reproduce single copies of the thesis and to lend or sell such copies for private, scholarly or scientific research purposes only.

The author reserves all other publication and other rights in association with the copyright in the thesis and except as hereinbefore provided neither the thesis nor any substantial portion thereof may be printed or otherwise reproduced in any material form whatever without the author's prior written permission.

James Hooper

11034-81 Avenue
Edmonton, Alberta
T6G 0S4

University of Alberta

Faculty of Graduate Studies and Research

The undersigned certify that they have read, and recommend to the Faculty of Graduate Studies and Research for acceptance, a thesis entitled *Glacial History and Holocene Sea Level Regression in the Foxe/Baffin Sector of the Laurentide Ice Sheet, Northwest Baffin Island, Arctic Canada* here submitted by James Hooper in partial fulfilment of the requirements for the degree of Doctor of Philosophy.

Dr. John H. England

Dr. Ian A. Campbell

Dr. Arthur S. Dyke

Dr. R. Bruce Rains

Dr. M.E. Evans

Dr. James T. Teller

February 5, 1996

Natural Resources Canada | Ressources naturelles Canada

Earth Sciences Sector | Secteur des sciences de la Terre

601 Booth Street
Ottawa, Ontario
K1A 0E8

601, rue Booth
Ottawa (Ontario)
K1A 0E8

January 30, 1996

Mr. James Hooper
11034-81 Avenue
Edmonton, Alberta
T6G 0S4

Dear Mr. Hooper,

Formal permission is granted to use, on a one time basis only, the following figure from the Geological Survey of Canada:

Figure: Regional glacial reconstruction, last glacial maximum (from Dyke and Prest, 1987).

The figure should appear with an appropriate acknowledgement, for example "Courtesy of the Geological Survey of Canada (Dyke, A.S., Morris, T.F. and Green, D.E.C., 1991, Postglacial Tectonic and Sea Level History of the Central Canadian Arctic, in Geological Survey of Canada Bulletin 397)".

Sincerely,

Annette E. Bourgeois
Director
Geoscience Information Division

Acknowledgments

Logistical support for this research, provided by the Geological Survey of Canada through the Polar Continental Shelf Project, is gratefully acknowledged. Additional financial support was provided by the Canadian Circumpolar Institute in the form of grants (NSTG and BAR) covering the cost of some radiocarbon dates, shipping costs, and field assistant wages. Additional radiocarbon dates were funded by J. England's NSERC grant (A6680). The support of the Igloolik Research Station of the Science Institute of the Northwest Territories and its director, John MacDonald, during the 1991 field season was most helpful. Academic support was provided by the Geography Department of Memorial University during 1987-1990 and the Department of Geography at the University of Alberta during the years 1990-1995. Support for 2 years of academic work was generously provided by NSERC through their postgraduate scholarships program. I am sincerely grateful to Scott Wareham, Christy Taylor, Craig Machtans, and Mark Seemann, who accompanied me for one field season each, for their competent and enthusiastic help. Particular thanks are due to Dr. A.S. Dyke of the Terrain Sciences Division, Geological Survey of Canada, and Dr. John England of the University of Alberta, Earth and Atmospheric Sciences Department, for their supervision and helpful review of the thesis.

Abstract

A local ice cap, a westward flowing partly marine-based ice stream, and a land-based sector of the Foxe Dome were the main features of the Foxe (last) Glaciation on northwestern Baffin Island. The Bernier Bay Ice Stream was a major outlet for ice draining west from the Foxe Dome, and evolved into a large outlet lobe during retreat. The ice stream and peripheral areas of the Brodeur Peninsula Ice Cap and Foxe Dome were warm-based but had cold-based accumulation areas. Moraines along Bernier Bay and Berlinguet Inlet are correlatives of the Cockburn Moraines and formed between 8800 and 6500 BP during a period of protracted retreat.

Ninety-four new radiocarbon dates on shells, whalebone, walrus tusks, and driftwood were used to construct twelve emergence curves for the area. The Holocene marine limit varies from 92 m above sea level in the north to 138 m asl in the south. The relative sea level data is best accomodated by emergence curve forms having a smooth, exponential decline in the rate of emergence from its postglacial maximum. Emergence occurred at 3.5 m/century in the first 1000 years after deglaciation and dropped to 35 cm/century over the last 1000 years. Gradients of raised shorelines steepen toward the former centre of loading in the southeast, and are nearly level in the northwest. The pattern of isobases agrees with the arrangement of ice loads during the last glacial maximum and supports the interpretation that the Brodeur Peninsula Ice Cap on was a last glacial maximum, rather than a residual feature.

Marine fossils at different elevations provide a record of paleoenvironmental conditions. Between 9000 and 7000 BP, the area was colonized by molluscs but whales, walrus, and driftwood were excluded by severe sea ice. Between 7000 and 5000 BP, some bone and wood washed ashore during an interval of reduced summer sea ice. Between 5000 and 3000 BP, the number of whales peaked, recording an interval when summer sea ice was greatly reduced. After 3000 BP the number of whales declined in response to more severe ice conditions that accompanied Neoglacial cooling.

Table of Contents

Page

Chapter 1: Introduction 1
- Bedrock Geology and Physiography 4
- Topography 6
- Climate and Vegetation 8
- Regional Glacial History 10
- Cockburn Moraines 13
- References 14

Chapter 2: 17
Glacial History and Drift Dispersal Patterns in the Foxe/Baffin Sector of the Laurentide Ice Sheet 17
- Introduction 17
- Methods 18
  - Logistical Arrangements 18
  - Surficial Mapping 19
  - Drift Sampling and Description Program 20
  - Laboratory Analyses 22
  - Granule Lithological Analysis 22
- Results 23
  - Surface Materials and Landforms 23
    - Areally Extensive Units 23
    - The Bernier Bay Moraines 23
    - Interlobate Moraines 34
    - Other Moraines 37
    - Glaciofluvial Deposits 37
  - Ice Flow Indicators 39
  - Chronology of Deglaciation and Moraine Deposition 43
    - Prince Regent Inlet 46
    - Bernier Bay 47
    - Berlinguet Inlet 51
    - Bell Bay/Ivisarak Lake 51
    - Agu Bay 52
    - Fury and Hecla Strait/Foxe Basin 52
    - Summary 53
  - Till Characteristics and Dispersal 54

Lithology of Granule Fractions 56
Shield Clasts 56
Carbonate Content of Granule Fraction 61
Carbonate Content of Matrix (Chittick Analysis) 64
Sandstone 69
Grain Size 69
Discussion 73
Glacial Events 73
Ice Dynamics and Drift Dispersal 76
Summary and Conclusions 77
References 79
Chapter 3: Holocene Sea Level History 82
Introduction 82
Previous Research 82
Methods 85
Bowhead Whalebone and Driftwood 89
Shell Samples 92
Emergence Curves 92
Deglaciation and Marine Limit 93
Emergence Curves 101
Morin Point 101
Van Koenig Point 103
Bernier Bay Northeast 107
Bernier Bay Southeast 109
Berlinguet River 111
Berlinguet Inlet West 112
Berlinguet Inlet East 114
Bell Bay 116
Foss Fiord/Kimakto Peninsula 118
Nybøe Fiord 119
Crown Prince Frederick Island 121
Autridge Bay/Whyte Inlet 122
Summary 125
Emergence in Adjoining Areas 126
Pattern of Shoreline Delevelling 127

Isobase Maps 129
Discussion 135
Conclusions 140
References 141
Chapter 4: 144
Paleoclimatic Significance of Postglacial Whale and Walrus Fossils 144
Introduction 144
Past and Present Distribution of Bowheads 145
Driftwood 147
Methods 148
Results 149
Discussion 155
References 158
Chapter 5: Conclusions 161
References 165
Appendix D: Altimetry 184
Appendix E: Sample Preparation 185
Appendix F: ∂13C for dated shells, wood and bone 186
Appendix G: Radiocarbon Dates From Northwestern Melville Peninsula 188
Appendix H: Dated and Undated Whale and Walrus Samples 190

List of Tables

Page

2-1. Deglaciation dates 45
2-2. Lithic facies classification of tills 56
3-1. Radiocarbon dates on marine limit and raised shorelines 95
3-2. Shoreline elevations for southern Brodeur Peninsula 127
4-1. Paleoenvironmental conditions in the central Arctic 147

List of Figures

Page

1-1. Location of the study area 2
1-2. The study area 3
1-3. Geology of the study area..... 5
1-4. Landsat image of the study area..... 9
1-5. Reconstruction of the last glaciation in Arctic Canada 11
2-1. Location of drift sample sites. 21
2-2. Location of moraines and associated radiocarbon dates. 24
2-3. Oblique aerial photograph of multiple moraines..... 25
2-4. Steep-sided moraines south of the head of Bernier Bay..... 25
2-5. Kettle and inactive thaw flowslide 27
2-6. Embayment in moraines south of central Bernier Bay 29
2-7. Embayments in moraines south of the head of Bernier Bay 30
2-8. Ice surface profiles (ca. 9 ka BP)..... 32
2-9. Large interlobate moraine west of the head of Bell Bay. 35
2-10. Large raised deltas on both sides of the interlobate moraine..... 36
2-11. Imbricate limestone gravel flooring meltwater channel. 38
2-12. Kettle developed in glaciofluvial gravels..... 38
2-13. Drumlins and Rogen moraines 41
2-14. Deglaciation of the study area..... 44
2-15. Marine limit delta at 110 m asl north of Bernier Bay 48
2-16. Marine limit delta at 111 m asl 49
2-17. Locally-derived sandstone felsenmeer..... 55
2-18. Distribution of Precambrian clasts 57
2-19. Distribution of carbonate clasts 62
2-20. Distribution of carbonate (acid-soluble) minerals 65
2-21. Calcite/dolomite ratios for tills 66
2-22. Percent carbonate content of till matrix..... 67
2-23. Percent carbonate clasts in till granule fractions 67
2-24. Distribution of sandstone clasts..... 70
2-25A. Sand content of tills..... 71
2-25B. Silt content of tills..... 72
2-25C. Clay content of tills..... 72
3-1. Flights of raised beaches near Easter Cape 87

3-2. Ice-pushed ridges on the north side of Bernier Bay 89
3-3. Collecting bone fragments from bowhead skull 91
3-4. Scatter of whalebone on raised beach 91
3-5. Large ice-contact delta north of Bernier Bay 94
3-6. Locations of radiocarbon-dated samples 100
3-7. Emergence curve for Morin Point 102
3-8. Emergence curve for Van Koenig Point 104
3-9. Walrus skull 104
3-10. Emergence curve for Bernier Bay northeast 107
3-11. Emergence curve for southeast Bernier Bay 110
3-12. Emergence curve for Berlinguet River 112
3-13. Emergence curve for Berlinguet Inlet west 113
3-14. Emergence curve for Berlinguet Inlet east 115
3-15. Emergence curve for Bell Bay 117
3-16. Emergence curve for Foss Fiord and Kimakto Peninsula 119
3-17. Emergence curve for Nybøe Fiord 120
3-18. Emergence curve for Crown Prince Frederick Island 122
3-19. Emergence curve for Autridge Bay and Whyte Inlet 123
3-20. Emergence curve for northern Melville Peninsula 126
3-21. Equidistant diagram showing the gradient of the 8500, 8000, 7500, 7000 and 6000 BP shorelines 128
3-22. Isobases on the 8500 BP shoreline 130
3-23. Isobases on the 8000 BP shoreline 131
3-24. Isobases on the 7500 BP shoreline 132
3-25. Isobases on the 7000 BP shoreline 133
3-26. Isobases on the 6000 BP shoreline 134
3-27. Predicted emergence curve for Bernier Bay southeast 136
4-1. Abundance of whale bones on raised beaches 152
4-2. Paleogeography of the study area at 6500 BP 152
4-3. Relative abundance of walrus during the postglacial interval 154

List of Maps

1. Surficial Geology, Agu Bay and Easter Cape Mapsheets, Baffin Island, Northwest Territories, Geological Survey of Canada Map, scale 1:250,000. (Map pocket).

Chapter 1: Introduction

This thesis presents the results of research on the glacial and sea level history of northwest Baffin Island. Chapter 2 discusses the glacial history based on mapped landforms, surface materials, drift dispersal patterns and fifteen radiocarbon dates pertaining to deglaciation and the formation of the marine limit. Chapter 3 reconstructs the emergence history of the area based on 94 new radiocarbon dates on shells, marine mammal bones and driftwood. The dates were used to construct 10 emergence curves and two partial curves for different parts of the area. Paleoenvironmental conditions controlling driftwood penetration into marine channels bordering the study area and occupation of these channels by bowhead whales and walrus over the last 7000 years are reconstructed from the relative abundance of marine mammal bones on dated shorelines (Chapter 4).

The research includes a surficial geology map (Map 1, pocket) for a 16,000 km^2 study area (Fig. 1-1) extending from the base of Brodeur Peninsula southward across Bernier Bay to Crown Prince Frederick Island, a small island at the west end of Fury and Hecla Strait (Fig. 1-2). Fieldwork began in 1988 and constituted an M.Sc. thesis at Memorial University of Newfoundland (Hooper, 1990). This dissertation includes the results of subsequent doctoral research, supported by the Geological Survey of Canada, concerned with drift sampling, Quaternary mapping and deglaciation chronology. The areal coverage of the drift sampling program was greatly extended during fieldwork in 1989-1991. This enlargement of the field area also allowed the collection of additional samples of dateable materials from previously unexamined parts of Baffin Island.

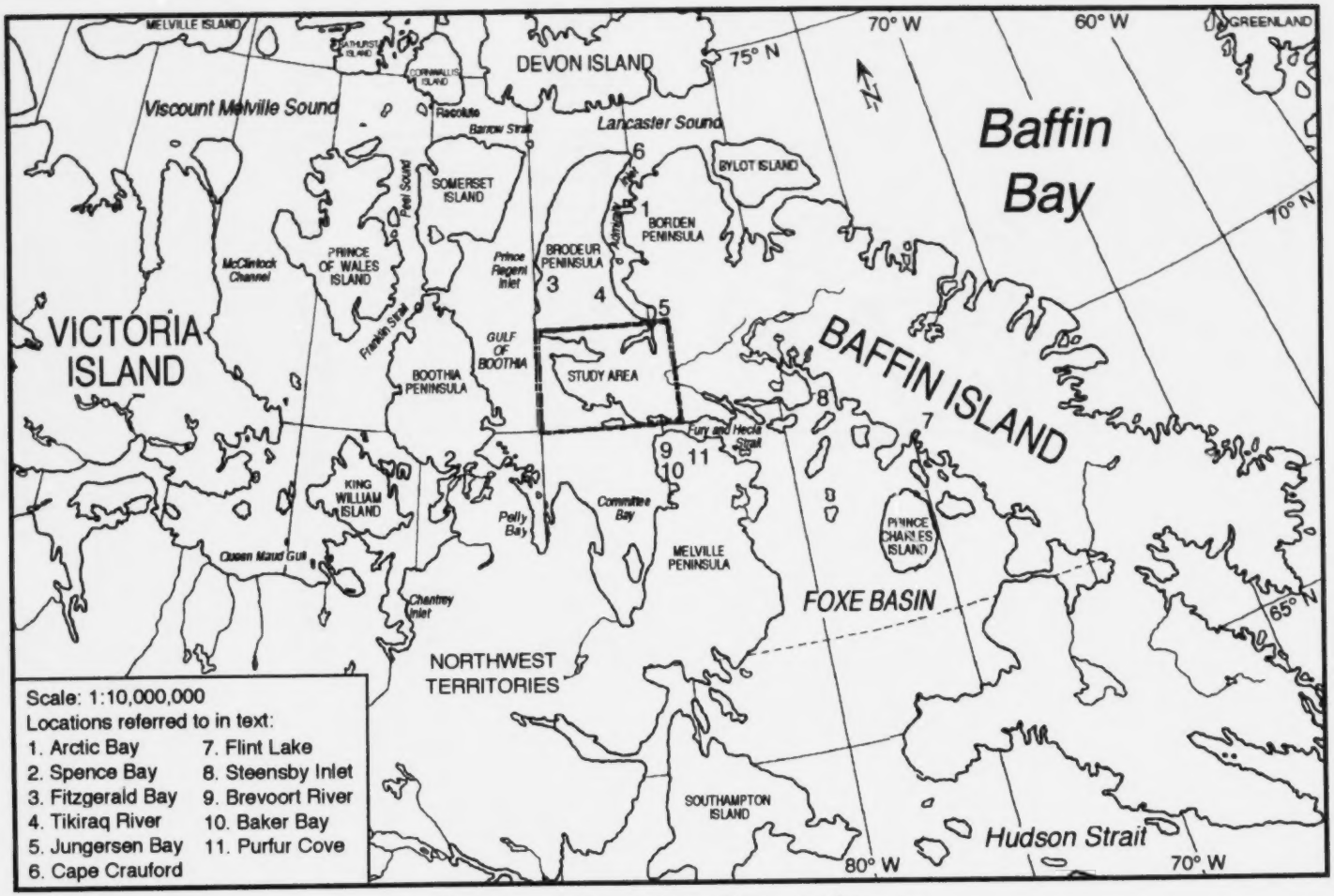

Figure 1-1. Location of the study area.

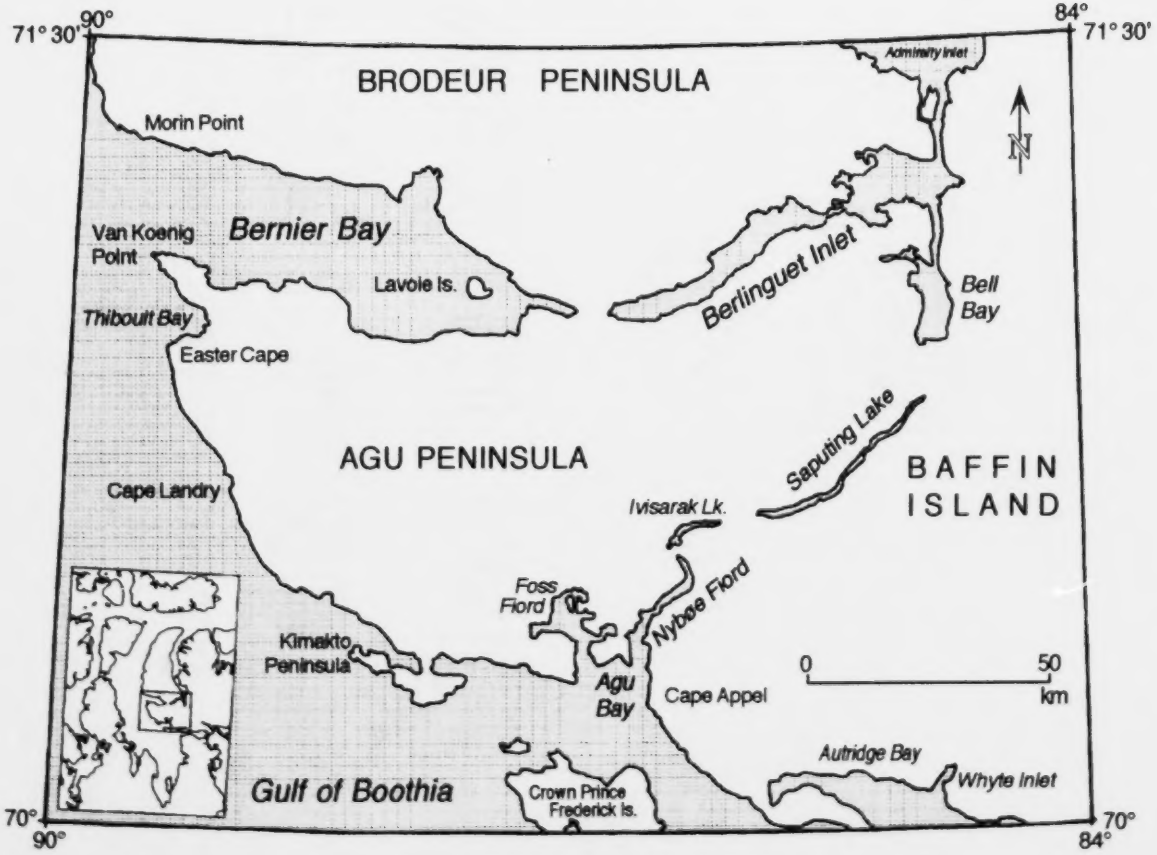

Figure 1-2. The study area.

Bedrock Geology and Physiography

The study area (Fig. 1-3) consists of horizontally-bedded Paleozoic dolostones and limestones in the west, and a northward extension of the Canadian Shield (Precambrian) in the east. The shield rocks are mainly gneiss, overlain in places by Precambrian sandstone. The shield hosts local diabase dykes and gabbro sills, also of Precambrian age. The structural geology of the area is described by Blackadar (1970) who notes the existence of numerous faults in the Precambrian rocks.

The carbonate rocks (Fig. 1-3) consist of flat-bedded lower Paleozoic dolomite and dolomitic limestone of the Ship Point, Baillarge, and Cape Crauford formations (Trettin, 1969). These formations record fine sediment deposition in a shallow marine basin. Fossils from these rocks are occasionally abundant and include corals, brachiopods, gastropods, cephalopods, stromatoporoids and trilobites. Precambrian rocks underlie the eastern part of the area and are intruded by northwest-trending gabbro dykes of Neohelikian age. The contact between Paleozoic and Precambrian rocks runs north from Agu Bay to the head of Admiralty Inlet (Fig. 1-3) and the contrasting geology across Admiralty Inlet suggests that a fault lies along it (Trettin, 1969). East and north of the contact the area is underlain by gneiss whereas in the southeast corner of the study area the gneissic basement is unconformably overlain by stratified quartzite and quartzitic sandstones (Blackadar, 1970). Around Autridge Bay the sandstone is locally overlain by gabbro sills up to 183 m thick (Blackadar, 1970). The peninsula that forms the south shore of Autridge Bay is one such sill.

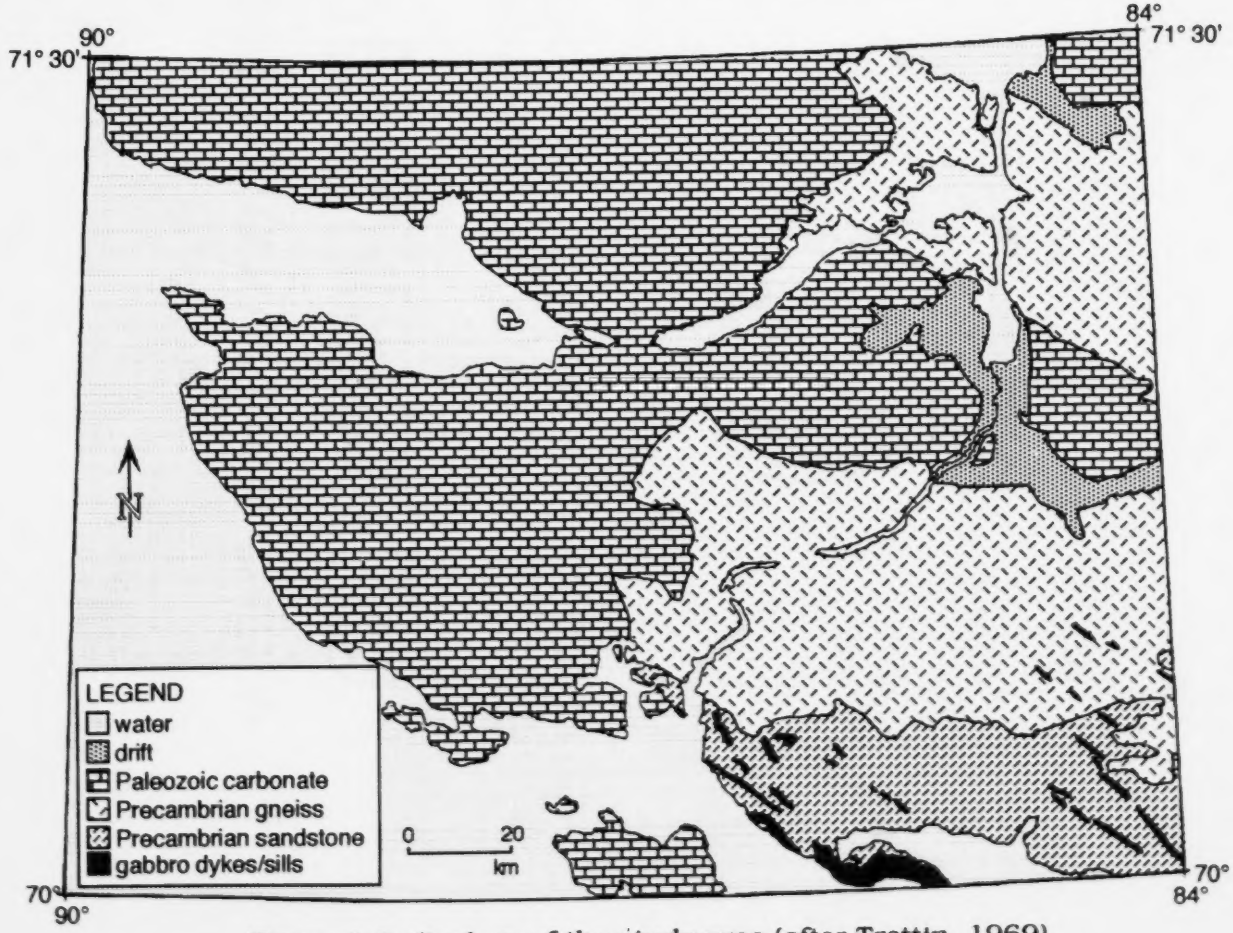

Figure 1-3. Geology of the study area (after Trettin, 1969).

Small fault blocks, resembling those shown in Lemon and Blackadar (1963) were observed in the sandstone terrain north of Autridge Bay. The age of the faults is unknown. Trettin (1969) noted fracture patterns in the sandstone and gneiss terrains and measured the orientation of linear elements, streams, etc, visible on aerial photographs. He observed numerous steeply dipping fractures especially in the southeast part of the study area. The fractures affect the Precambrian basement rocks as well as the overlying Paleozoic strata. Pleistocene and Recent unconsolidated sediments appear to have also been displaced (Trettin, 1969). Hence, it is possible that tectonic activity is still occurring. To the west the Boothia Horst (Kerr, 1980) is amongst the most seismically active areas in Canada east of the Cordillera (Basham et al., 1977).

Topography

The origin of large scale topographic elements remains uncertain. These include the Bernier Bay/Berlinguet Inlet trough and other marine channels bordering northwest Baffin Island: Admiralty Inlet, Prince Regent Inlet, the Gulf of Boothia, and Fury and Hecla Strait. These may be ancient fluvial valleys overdeepened by glaciation (Bird, 1967). The plateau of Brodeur Peninsula is similar in elevation and appearance to the Barrow surface, a ancient, formerly contiguous surface of fluvial planation best developed on Somerset Island, Boothia and Brodeur Peninsulas (Bird, 1967) but is south of its proposed southern margin. Also, the Brodeur Peninsula surface differs in its consistent westward dip.

On a regional scale, Fortier and Morley (1956) suggested that the channels of the Arctic Archipelago represented a dendritic fluvial system which had been enlarged and overdeepened by glacial erosion. However, Kerr (1980) proposed a tectonic origin for Lancaster Sound. Similarly, Prince Regent Inlet may also be a fault-bounded rift valley which propagated from Lancaster Sound. However, until bounding faults have been mapped it would be premature to attribute the origin of the large, parallel-sided valleys to faulting, glacial erosion or both. In contrast, the Bernier Bay/Berlinguet Inlet trough is meandering and lacks the cliffed

margins, characteristic of Prince Regent Inlet and Lancaster Sound, suggesting an erosional origin. Large meandering valleys, likely of Tertiary fluvial origin have been mapped on Prince of Wales Island (Dyke et al., 1992).

Hills and valleys cut in resistant bedrock in the southeastern part of the area are the result of lengthy fluvial dissection prior to the onset of glaciation. The flat to gently undulating plateau on the unnamed peninsula to the west, hereafter unofficially named Agu Peninsula (Fig. 1-2), and the plateau of Brodeur Peninsula, are likely products of prolonged post-Paleozoic fluvial planation (cf. Bird, 1967, Barrow Surface). The large, sinuous valley crossing the eastern part of the area, containing Nybøe Fiord, Ivisarak and Saputing lakes (Fig. 1-2), and extending to the head of Bell Bay, is also likely be a preglacial fluvial valley. Parts of this valley lie along the contact between the Paleozoic and Precambrian bedrock where differential erosion would be favoured.

The most rugged terrain corresponds with the Precambrian uplands in the southeast where some summits are above 400 m elevation. Both Bird (1967) and Trettin (1969) suggest that this landscape is an exhumed fluvial erosion surface of late Precambrian or early Paleozoic age. The surface is classified as stepped plains and dissected uplands by Andrews (1989). Coastal lowlands may represent younger physiographic elements or simply places where the gently tilted, older plains descend to the coast. These are narrow or non existent in the area of Precambrian rock but extensive in areas of limestone.

The limestone terrain consists of coastal lowlands with flights of raised beaches rising to the interior plateaux. The plateaux comprise broad plains and low hills, generally less than 30 m high, with broad rounded summits and occasional bedrock outcrops in the form of low cuestas and shallowly incised canyons.

Climate and Vegetation

The climate of the field area is characterized by short, cool summers and long, severe winters. Seasons are ill-defined, with the exception of winter. Arctic Bay and Spence Bay (Fig. 1-1) are the closest weather stations to the study area. Arctic Bay, on northwestern Borden Peninsula, has a mean annual temperature of -14°C and precipitation of 126 mm. Spence Bay, on central Boothia Peninsula to the west, has a mean annual temperature of -15°C and precipitation of 153 mm (Atmospheric Environment Service 1973, 1982). Despite low annual precipitation, soil moisture is often high due to the blockage of subsurface drainage by permafrost (cf. Church, 1974).

The mid to high arctic tundra vegetation of the area has not been studied extensively. Ground cover is usually sparse, consisting of patchy *Dryas*, grass, willows, bryophytes and lichens. Poorly drained areas have the greatest cover, many attaining 100%; mainly sedge and grass. The plants are sensitive to the availability of soil nutrients as well as moisture. For example, they are least abundant on soils derived from nutrient-deficient dolostone or sandstone and increase progressively with increasing amounts of shield-derived material. Intermediate cover values occur where shield rocks have been dispersed westward across limestone plateaux. Ice-rafted shield material has also increased the nutrient content of calcareous beach gravels. The effects of nutrient availability on the vegetation, largely a product of till dispersal, is visible on Landsat images (Fig. 1-4).

Figure 1-4. Landsat image of the study area (scale 1:5,000,000). Dark-toned areas along Bernier Bay and Berlinguet Inlet trough (upper third of box) are caused by westward glacial dispersal of erratics from Precambrian source rocks (reddish brown area right of box).

Regional Glacial History

During the last glaciation, the area was crossed by westward flowing Laurentide ice from a dispersal centre over Foxe Basin, the Foxe Dome (Ives and Andrews, 1963; Dyke and Prest, 1987; Fig. 1-5). Recognition of this independent dispersal centre was a major departure from the widely accepted view proposed by R.F. Flint (1943) of a single-domed Laurentide Ice Sheet since Tyrrell (1898). In the north, Foxe ice was excluded by a local ice cap on Brodeur Peninsula, the Brodeur Peninsula Ice Cap.

Little information is available on events prior to the last glaciation in the study area. One non-finite radiocarbon date was obtained on surface shells collected by B.G. Craig at 101 m asl in 1963. The sample is from the crest of a moraine ridge north of the head of Bernier Bay and dated >30,580 BP (GSC-189; Dyck et al., 1965). The date records reworking of preexisting shell-bearing marine sediments by the last glaciation.

At the last glacial maximum (LGM), flow of Foxe ice across the area involved two glaciologically distinct regimes. In the north, the Bernier Bay/Berlinguet Inlet trough contained a warm-based ice stream about 80 km wide, here named the Bernier Bay Ice Stream. The ice stream was grounded well below sea level and fed into an extensive ice stream, or ice shelf, in the Gulf of Boothia and Prince Regent Inlet (Dyke and Prest, 1987). At the same time, the plateau of Agu Peninsula was entirely covered by westward flowing ice, also from the Foxe Dome.

North of the Bernier Bay Ice Stream, Brodeur Peninsula supported an independent ice cap with a north-south trending axial ice divide (Dyke and Prest, 1987). At the last glacial maximum, radial flow from this divide blocked Foxe ice from southern Brodeur Peninsula. Dyke (1993), in his discussion of local ice caps in the central Arctic, estimates that these ice caps persisted for at least 10,000 years and likely more than 20,000 years, based on the time required for the removal of underlying permafrost (from the bottom up) by geothermal heating. Over time, the ice caps developed warm-based peripheral zones. Thus, the local ice caps were "not merely brief transients during the demise of a preceding regional ice sheet" (Dyke, 1993; p.243).

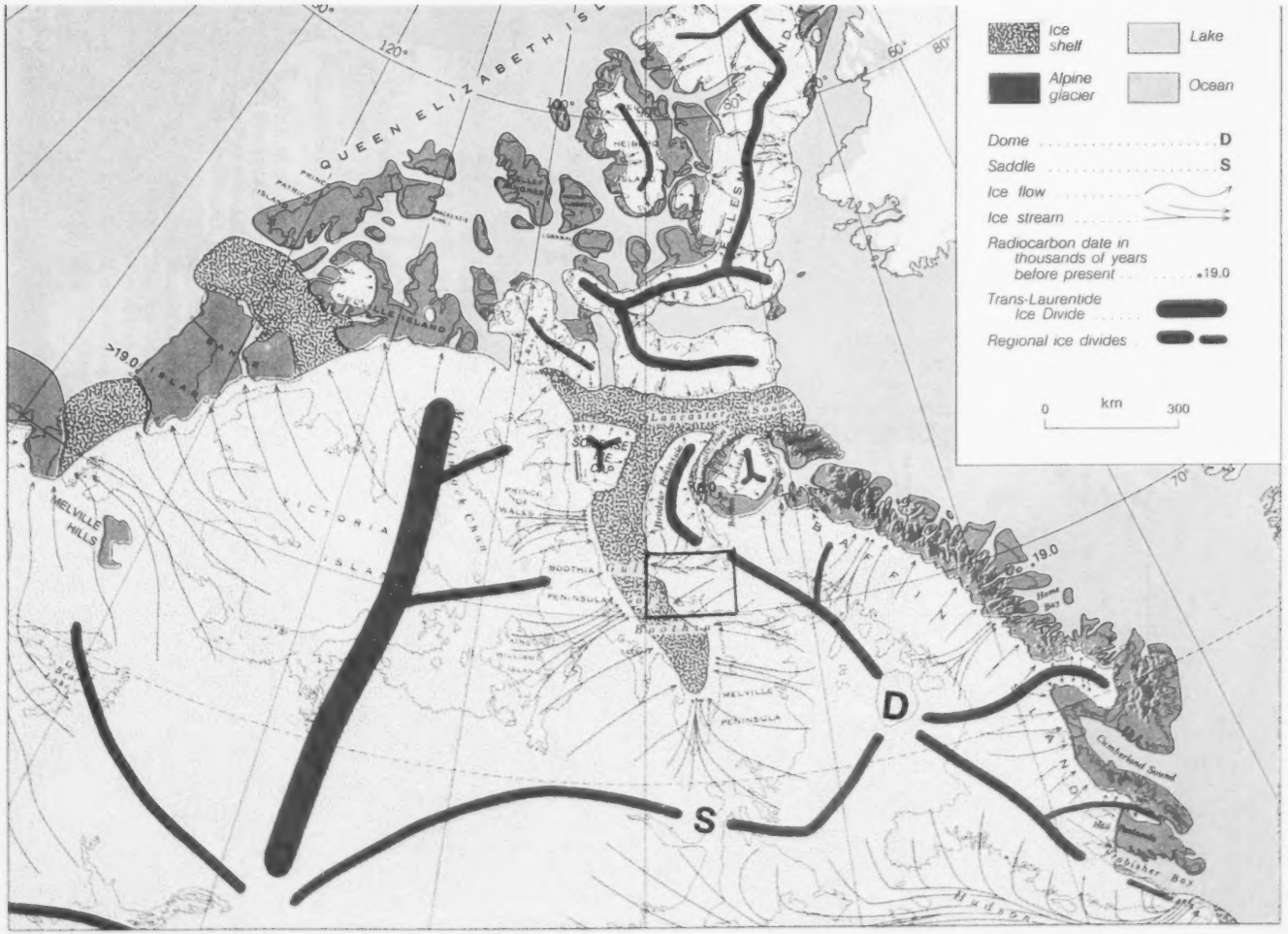

Figure 1-5. Reconstruction of the last glacial maximum in Arctic Canada (18-13 ka BP; Dyke and Prest, 1987).

The area was deglaciated from northwest to southeast beginning with the disintegration of ice in Prince Regent Inlet and the Gulf of Boothia shortly before 9000 BP (see Fig. 1-1 for locations). This was followed by a halt in retreat during which large moraines were deposited along Bernier Bay and Berlinguet Inlet, here named the Bernier Bay Moraines. The moraines delineate the former margin of a lobe of grounded ice, the Bernier Bay Lobe. Eastward retreat of Foxe ice resumed about 8000 BP and the ice in Foxe Basin disintegrated by 6900 BP (Craig, 1965; Dredge, 1990, 1991). Numerous younger dates (Sim, 1964; Blake, 1966; Andrews, 1970) are available from around Foxe Basin. Fury and Hecla Strait became ice-free between 6900 and 6600 BP (Dredge, 1990). Ice on the interior plateau probably retreated beyond the eastern margin of the study area by 5500 BP. Residual ice caps cut off from the main body of retreating ice were rare, or simply hard to detect. Such isolated remnants probably persisted in narrow valleys in the southeastern part of the area, north of Whyte Inlet, for some time after the rest of the area was deglaciated.

Cockburn Moraines

Research on the Quaternary history of the area began in the early 1960s by the Geological Survey of Canada and the former Geographical Branch of of the Department of Mines and Technical Surveys, Ottawa. This work included airborne reconnaissance and mapping of moraines (Falconer et al., 1965) and the first radiocarbon dates for the area (Craig, 1965). These authors recognized that the Bernier Bay Moraines were correlative with an extensive series of end moraines, collectively called the Cockburn Moraines, which occupy the fiord heads along the east coast of Baffin Island. The Cockburn Moraines were first mapped by Ives and Andrews (1963) who also outlined the general retreat of Foxe Ice. This ice retreat pattern included a marine incursion into Foxe Basin when the eastern margin of Foxe ice stood at or just behind the Cockburn Moraines. Falconer et al. (1965) proposed that the moraines delineated a late Wisconsinan remnant of the Laurentide Ice Sheet. The Bernier Bay Moraines mark the western margin of a residual Laurentide Ice Sheet. Other moraines then thought to be correlatives of the Cockburn system included the Melville Moraine on western Melville Peninsula (Sim;1960) and the MacAlpine and Cree Lake Moraines on the mainland.

References

Andrews, J.T., 1970. Differential crustal recovery and glacial chronology (6700-0 BP), west Baffin Island, N.W.T., Canada. *Arct. Alp. Res.* 5:185-200.

Andrews, J.T., 1989. Quaternary geology of the northeastern Canadian Shield; In Chapter 3 of *Quaternary Geology of Canada and Greenland.* R.J. Fulton (ed.) Geological Survey of Canada, Geology of Canada No. 1, pp. 276-317.

Andrews, J.T. and Ives, J.D., 1978. "Cockburn" nomenclature and the Late Quaternary history of the eastern Canadian Arctic. *Arct. Alp. Res.* 10:617-633.

Atmospheric Environment Service, 1973. Canadian Climate Normals: Precipitation, 1941-1970. Volume 2, Environment Canada.

Atmospheric Environment Service, 1982. *Canadian Climate Normals: Temperature,* 1941-1980. Volume 2, Environment Canada.

Basham, P.W., Forsyth, D.A. and Wetmiller, R.J., 1977. The seismicity of northern Canada. *Can. J. Earth Sci.* 14:1646-1667.

Bird, J.B., 1967. *The Physiography of Arctic Canada with Special Reference to the Area South of Parry Channel,* John Hopkins Press, Baltimore, 336 p.

Blackadar, R.G., 1970. Precambrian geology, northwestern Baffin Island, District of Franklin. *Geol. Surv. Can. Bull.* 191. 89 p.

Blake, W., Jr., 1966. End moraines and deglaciation chronology in northern Canada with special reference to southern Baffin Island. *Geol. Surv. Can. Pap.* 66-26, 31 p.

Bryson, R.A., Wendland, W.M., Ives, J.D. and Andrews, J.T., 1969. Radiocarbon isochrones on the disintegration of the Laurentide Ice Sheet, *Arct. Alp. Res.* 1:1-14.

Church, M., 1974. Hydrology and permafrost with reference to northern North America. Canadian National Committee, *International Hydrological Decade, Workshop Seminar Proceedings,* p. 7-19.

Craig, B.G., 1965. Notes on moraines and radiocarbon dates in northwest Baffin Island, Melville Peninsula and northeast District of Keewatin. *Geol. Surv. Can. Pap.* 65 20, 7 p.

Dredge, L.A., 1990. The Melville Moraine: sea-level change and respnse of the western margin of the Foxe Ice Dome, Melville Peninsula, Nothwest Territories. *Can. J. Earth. Sci.* 27: 1215-1224.

Dredge, L.A., 1991. Raised marine features, radiocarbon dates, and sea level changes, eastern Melville Peninsula, Arctic Canada. *Arctic* 44(1):63-73.

Dyck, W., Fyles, J.G. and Blake, W., Jr., 1965. Geological Survey of Canada Radiocarbon Dates V. *Radiocarbon* 7:24-46.

Dyke, A.S. 1993. Landscapes of cold-centred Late Wisconsinan ice caps, Arctic Canada. *Progress in Physical Geography* 17(2):223-247.

Dyke, A.S. and Prest, V.K., 1987. Late Wisconsinan and Holocene history of the Laurentide Ice Sheet. *Geographie physique et Quaternaire* 41(2):237-263.

Dyke, A.S., Morris, T.F., Green, D.E.C. and England, J., 1992. Quaternary Geology of Prince of Wales Island, N.W.T. *Geol. Surv. Can. Mem.* 433, 142 p.

Falconer, G., Ives, J.D., Løken, O.H. and Andrews, J.T., 1965. Major end moraines in eastern and central Arctic Canada. *Can. Dept. Mines Tech. Surv., Geog. Bull.* 7:137-153.

Flint, R.F., 1943. Growth of the North American Ice Sheet during the Wisconsin Age. *Geological Society of America Bulletin* 54:325-362.

Fortier, Y.O. and Morley, L.W., 1956. Geological unity of the Arctic Islands. *Transactions of the Royal Society of London*, v. 50, p. 3-12.

Hooper, J.M., 1990. *Late Quaternary Glacial and Sea Level History of the Bernier Bay Area, Northwest Baffin Island, N.W.T.*, unpublished M.Sc. thesis, Memorial University of Newfoundland, 98 p.

Ives, J.D. and Andrews, J.T., 1963. Studies in the physical geography of north-central Baffin Island, N.W.T., *Geog. Bull.* 19:5-48.

Jackson, G.D., Ianelli, T.R., Narbonne, G.M. and Wallace P.J., 1978. Upper Proterozoic sedimentary and volcanic rocks of northwestern Baffin Island, *Geol. Surv. Can. Pap.* 78-14, 15 p.

Kerr, J.W., 1980. Structural framework of the Lancaster Aulocogen, Arctic Canada. *Geol. Surv. Can. Bull.* 319, 24 p.

Lemon, R.R.H. and Blackadar, R.G., 1963. Admiralty Inlet area, Baffin Island, District of Franklin. *Geol. Surv. Can. Mem.* 328. 84 p.

Miller, G.H. and Dyke, A.S., 1974. Proposed extent of Late Wisconsin Laurentide ice on Baffin Island. *Geology* 2:125-130.

Sim, V.W., 1960. A preliminary account of late Wisconsin glaciation in Melville Peninsula, N.W.T. *Canadian Geographer* 17:21-34.

Sim, V.W., 1964. Terrain Analysis of west-central Baffin Island, N.W.T. *Geog. Bull.* 21:66-92.

Trettin, H.P., 1969. Lower Paleozoic sediments of northwestern Baffin Island, District of Franklin, *Geol. Surv. Can. Bull.* 157, 70 p.

Tyrrell, J.B., 1898. The glaciation of north central Canada. *Jour. Geol.*, 6:147-160.

Chapter 2:
Glacial History and Drift Dispersal Patterns in the Foxe/Baffin Sector of the Laurentide Ice Sheet

Introduction

During the last glaciation, the southern part of the study area was inundated by ice flowing from a dispersal centre over Foxe Basin to the southeast, the Foxe Dome (Ives and Andrews, 1963; cf. fig. 1-5). This Laurentide ice covered most of the study area with the exception of southern Brodeur Peninsula where it was excluded by ice of the coalescent Brodeur Peninsula Ice Cap. The distribution of surface materials and landforms (Map 1, pocket) is primarily the product of these events. This chapter discusses the glacial and deglacial history of the area based on its glacial landforms, the set of deglacial radiocarbon dates, and the pattern of drift dispersal.

The largest glacial landforms in the study area are sets of moraines of Cockburn age (Craig, 1965; Falconer et al., 1965; Andrews and Ives, 1978), which mark the former location of an ice lobe in Bernier Bay and Berlinguet Inlet. This large trough contained a topographically controlled ice stream which flowed westward into Prince Regent Inlet during the last glacial maximum (Dyke and Prest, 1987). The moraines record the marginal position of Foxe ice during the Cockburn Substage (8000 and 9000 BP) and its subsequent retreat. Over parts of the system, the moraines arguably mark the maximum Late Wisconsinan extent of the Laurentide Ice Sheet (Dyke, 1974; Miller and Dyke, 1974; Andrews and Ives, 1978). Together with lateral meltwater channels and younger moraines, they provide a detailed record of the retreat of Foxe ice. Chronological control is based on a series of radiocarbon dates which provide minimum ages on deglaciation. The pattern of drift dispersal, described below, indicates which areas were covered by Foxe ice, and allows estimates of transport distances and the degree of comminution of debris.

Although the late glacial climate was probably similar throughout the study area, the basal thermal regime of the ice cover, controlled

primarily by flow rate, was not uniform. Uplands covered by cold-based ice during the last glaciation were little modified. These include the interior of Agu Peninsula (Foxe ice), and the interior of Brodeur Peninsula (Brodeur Peninsula Ice Cap). Around the margin of these ice masses, flow by internal deformation was sufficiently rapid to compensate for atmospheric cooling (from the top down) after which geothermal heating (from the bottom up) slowly remove subglacial permafrost, allowing a warm-based marginal fringe to develop (Dyke, 1993). In areas formerly under cold-based ice, surface sediments record the effects of previous glaciations in the form of widely dispersed erratics. In some instances, the preglacial mantle of subaerially weathered residuum appears to have survived largely intact (cf. Dyke, 1993). Surfaces formerly covered by warm-based ice were more extensively altered. Alteration usually consisted of the removal of preexisting sediment and scouring of bedrock. Due to its rapid flow rate, the Bernier Bay Ice Stream likely maintained a warm-based condition during all but the inception of the last glaciation. The presence of the large moraines and other deposits, indicates that other areas alongside and under warm-based ice may have been zones of net deposition. Here older sediments may still exist beneath more recent deposits.

Methods

Logistical Arrangements

Fieldwork was conducted from 16 camps located at coastal sites in order to provide access to sea level for altimeter surveys. From these camps, traverses were carried out on Honda ATC's to collect drift samples and dateable material from raised marine shorelines, to survey marine limit and key sample sites, and to verify air photo interpretations of surficial materials. Daily traverses were up to 80 km long but commonly in the 20 to 50 km range.

Surficial Mapping

Surficial materials and landforms were initially mapped on air photographs at 1:60,000 scale and were subsequently verified, as much as possible, by ground truthing. The final version of the map was compiled at a scale of 1:125,000 and reduced photographically to 1:250,000 (Map 1, pocket). The area north of Bernier Bay and Berlinguet Inlet was mapped by A.S. Dyke of the Terrain Sciences Division, Geological Survey of Canada, as part of a regional mapping project that included both Brodeur and Borden Peninsulas but ground checking here was by the author. Due to the difficulty of access, some interior areas above marine limit were not visited. The lack of samples from these areas complicates overall reconstruction of till dispersal.

For mapping purposes, till is subdivided into veneer (< 2 m thick) and blanket (> 2 m thick). Till thickness was assessed by the number of bedrock outcrops and the degree of tundra polygon development. For example, numerous rock outcrops occur within till veneers, whereas bedrock topography is muted or obscured by till blankets. Till forming end and lateral moraines is mapped as a separate facies.

Other mapped glacigenic sediments include proglacial outwash and glaciofluvial gravel deposited in ice-contact settings. Proglacial outwash consists of coarse gravel plains which typically floor meltwater channels. The channels often terminate at large raised deltas graded either to Holocene marine limit or the level of former proglacial lakes. Ice-contact gravels comprise kames and eskers and contain variable amounts of silt and sand.

Marine sediments are widespread below the marine limit but are rarely > 2 m thick. Flights of raised beaches occur along most coastlines and are composed of gravel, sandy gravel and sand derived from reworked till and outwash. Coastal lowlands and valley floors are typically mantled by marine silty clay, silt and sand with numerous dropstones and reflect proglacial deposition in deep water. Like tills, these form veneers (< 2 m thick) and blankets (> 2 m thick).

Proglacial lake sediments record the temporary impoundment of lakes where valleys were blocked by the retreating ice margin. Lacustrine veneers and blankets are easily recognized above marine limit, and the

position of the impounding ice margin is usually obvious. The sediments consist of nonfossiliferous silt, silty clay and sand with dropstones. In some instances, the Holocene marine limit and proglacial lake limits can be traced over considerable distances.

Fluvial sediments form floodplains, alluvial fans, and terraces above modern floodplains. The sediments consist of moderately to well sorted gravel and sand. Fluvial gravel typically becomes coarser in the upper reaches of river valleys whereas large alluvial fans along coastlines contain the coarsest sediment.

Mapped glacial landforms include moraines, kames, kettles, drumlins, eskers and meltwater channels (subglacial and ice marginal). Lichen-free areas, each about 5 km^2 in extent, were mapped surrounding two small glaciers that still exist in the southeastern part of the area. These record the former extent of the glaciers during the Neoglacial.

Drift Sampling and Description Program

Drift samples, mostly till (N=241), were collected from shallow pits. Their locations were recorded on air photographs (1:60,000). At each sample site (Fig. 2-1) observations were made of: dominant clast types and sizes, texture and color of the matrix, estimated content of large clasts, local drainage conditions, estimated percentage of Precambrian erratics in the drift, estimated percentages of the surface covered by boulders and vegetation, respectively, (as opposed to bare soil) and type of patterned ground (i.e. net diameter, relief, and degree of sorting).

Estimates made of the stoniness and boulder cover at each site are useful adjuncts to the laboratory grain size analysis because it is impractical to collect samples large enough to meaningfully measure the content of cobbles and boulders. Drainage conditions are relevant to considerations of trafficability and may also reflect the clay content of the matrix. In limestone terrain, local vegetation cover is a good indicator of the amount of Precambrian material in the drift (except in bogs) because vegetation is very sparse on nutrient-deficient tills derived solely from dolostone.

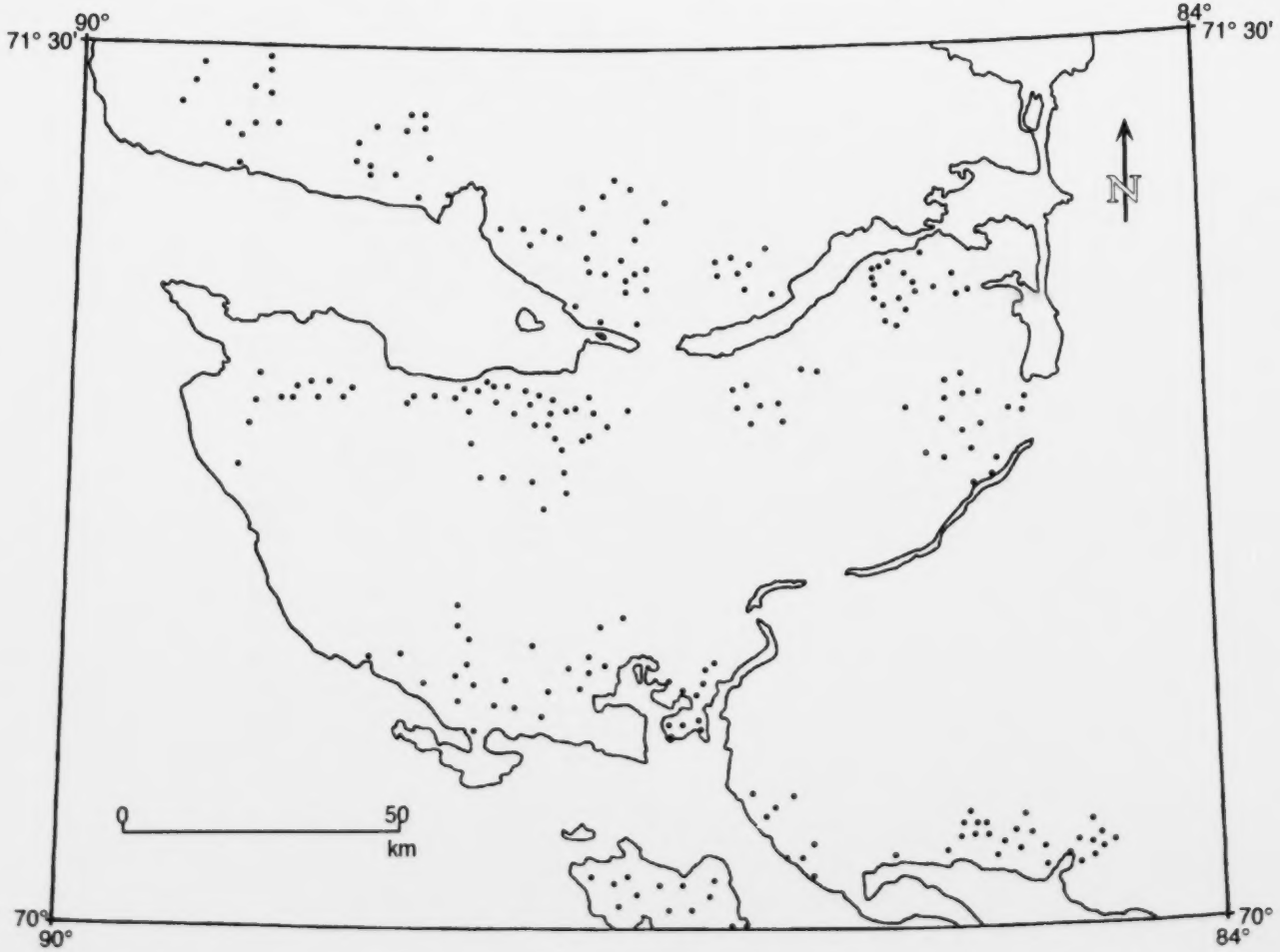

Figure 2-1. Location of drift sample sites.

Patterned ground includes small scale sorted and nonsorted nets, circles and desiccation polygons. These landforms are ubiquitous on all but the coarsest substrates. The distributions of ice wedges and peat mounds are controlled by drainage conditions (slope) and water retentiveness of the substrate (clay content). Small peat mounds (palsen) are common in bogs and shallow ponds. The best developed patterned ground forms occur on level, poorly drained diamict surfaces. Large ice wedge polygons on the surface of thick till, and bounded by troughs up to 2 m deep, probably indicate buried glacier ice (Dyke et al., 1992).

Laboratory Analyses

Standard grain size analysis was conducted on the samples at the GSC laboratory in Ottawa. The silt and clay content of the samples was measured using a Sedigraph, with the exception of samples collected in 1988 which were analyzed with a Coulter apparatus. Carbonate content of the samples was measured using a Chittick apparatus in which the sample is reacted with a known quantity of HCl. The volume of carbon dioxide evolved is then used to calculate the total carbonate and the rate of the reaction is a measure of the relative amounts of the calcite and dolomite. Since calcium carbonate (calcite) reacts more quickly than magnesium carbonate (dolomite), the gas produced in the first part of the reaction reflects the amount of calcite present while the gas evolved as the reaction proceeds to completion indicates the amount of dolomite.

Granule Lithological Analysis

To determine the lithological composition of the drift samples, the 2-5.6 mm fraction was retained after sieving. Clasts from these subsamples (generally less than 50 grams) were washed in water, sorted visually according to lithology, and weighed. Lithological categories were based on the local geology, since the aim was ultimately to define the pattern of drift dispersal. The results of the analysis were then expressed as a percentage of the total weight of the 2-5.6 mm fraction.

Results

Surface Materials and Landforms

Areally Extensive Units

Bedrock and till veneer (i.e. <2 m thick) over bedrock are the most extensive surface materials in the area (Map 1). Large areas of rock in the interior lack striae or other indications of glacial erosion. This indicates that ice covering these areas during the last glaciation was largely non-erosive, and hence likely cold-based. The possible existence of protective ice suggests that till veneers may contain preexisting weathered residuum, colluvium or older till which has been only minimally reworked. If this is true, the trace amounts of Precambrian erratics on these surfaces were deposited during earlier glaciation(s).

Landsat images of the area (Fig. 1-4) show a regional till sheet boundary along the north side of Bernier Bay and Berlinguet Inlet. The boundary marks the former location of the contact between the Brodeur Peninsula Ice Cap, which lacked a source of Precambrian material, and the Bernier Bay Ice Stream. The main cause of this tonal contrast is increased vegetation cover on tills with greater quantities of Precambrian material, i.e. tills deposited by the Bernier Bay Ice Stream. Other factors contributing to increased plant cover in this area, hence darkening parts of the image in Fig. 1-4, are its numerous bogs and relatively warm microclimate.

The Bernier Bay Moraines

Belts of large lateral moraines along the north and south sides of the Bernier Bay/Berlinguet Inlet trough (Fig. 2-2, Map 1) are approximately 130 km long and composed of multiple ridges up to 60 m high (Fig. 2-3, 2-4). The moraines are smaller in the west, becoming less distinct north and south of the mouth of Bernier Bay. Here, broad ridges form an obvious continuation of the system where it descends below marine limit to the coast. Surface material on these ridges has been extensively reworked into flights of sand and gravel beaches. In the east, large moraines terminate abruptly in a single large ridge west of the head of Bell Bay. North of Berlinguet Inlet, numerous moraines wrap the

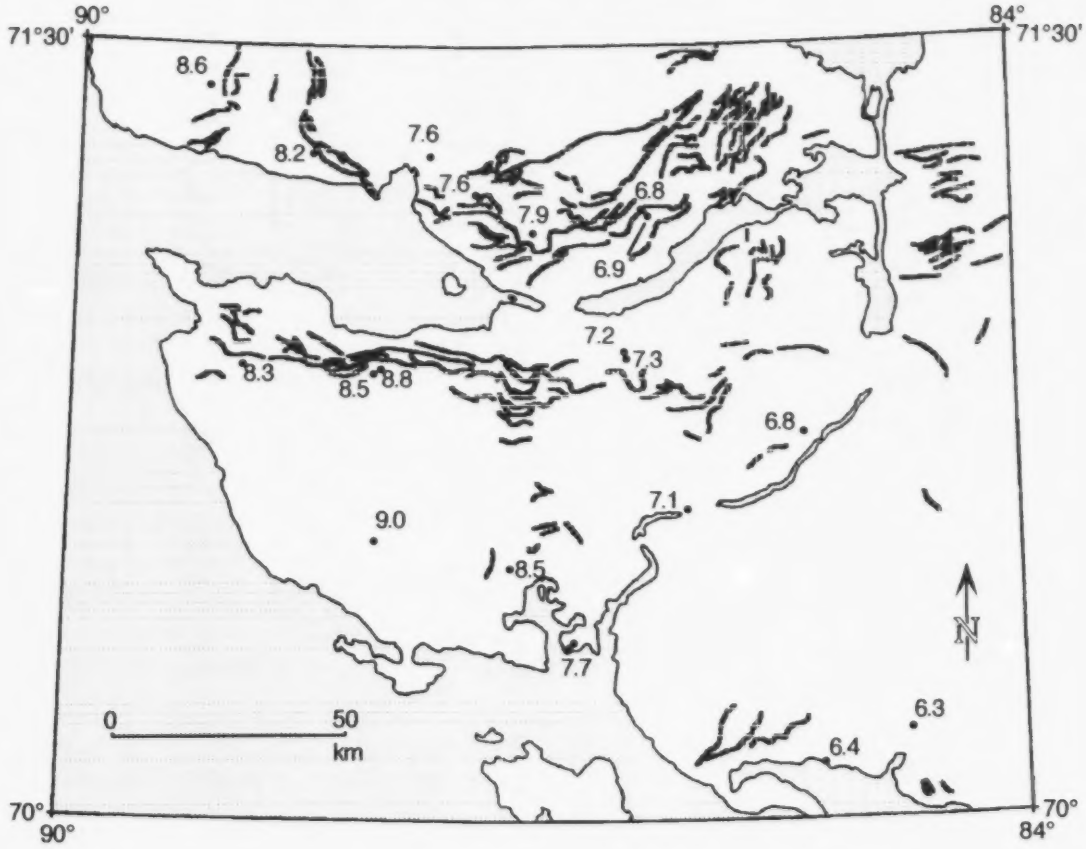

Figure 2-2. Location of moraines (grey lines) and limiting radiocarbon dates

Figure 2-3. Oblique aerial photograph of multiple moraines flanked by marine silts south of the head of Bernier Bay.

Figure 2-4. Steep-sided moraines south of the head of Bernier Bay.

south end of Brodeur Peninsula with a few extending beyond the northern limit of the field area along the west side of Admiralty Inlet.

With one exception, all the Bernier Bay moraines were deposited by ice of the Bernier Bay Lobe. The large moraine north of the bay was deposited by a readvance of the southern margin of the Brodeur Peninsula Ice Cap immediately after deglaciation of Bernier Bay.

The moraines are mainly composed of locally-derived (from bedrock or residuum) till. The till also contains glacially reworked marine sediment as recorded by shell fragments observed above marine limit at several sites. In addition, the granule fractions of till samples, including those from above marine limit, usually contain trace shell fragments. The presence of shells antedating the last glaciation is demonstrated by a date of >30,580 BP (GSC-189; Dyck et al., 1965) obtained on a surface collection of shells.

Other sediments were deposited simultaneously along the same ice margin. These include glaciomarine sediments deposited in shallow seas alongside the Bernier Bay Lobe and glaciofluvial deposits. The latter record large quantities of meltwater released into the early Holocene sea while the ice stood at the moraines and during its subsequent retreat. Significant portions of the moraines and some till blankets contain buried cores of relict glacier ice which has survived up to the present day below the active layer. Indirect evidence for this buried ice includes unusually large tundra polygons and ice wedge troughs crossing till surfaces, flowslides in the sides of moraines (Fig. 2-5) and numerous kettles (cf. Dyke et al., 1992).

Figure 2-5. Kettle and inactive thaw flowslide in side of moraine north of the head of Berlinguet Inlet.

Numerous loops and embayments in the Bernier Bay Moraines (Fig. 2-6) were described by Falconer et al., (1965). The development of these marginal features was controlled by the topography encountered by ice flowing out of the trough. Where the ice encountered relatively steep slopes, the band of deposition was compressed into one or two large ridges, whereas, on gentler slopes, multiple ridges formed. For example, south of the head of Bernier Bay, nine successive ice marginal positions can be defined where a small lobe of ice flowed south, out of the main trough, backfilling a shallow side valley (Fig. 2-7). Similarly, the Berlinguet River valley, which descends toward Berlinguet Inlet from the interior of Brodeur Peninsula, is crossed by a large semicircular moraine loop. The loop is convex upvalley and could only have been formed by ice flowing upslope out of Berlinguet Inlet. Headlands along the main trough acted as obstacles to flow which restricted the width of the moraine system and shifted the locus of deposition toward the axis of the trough. The correlation between the loops/embayments in the moraines and valleyside topography indicates that ice on the adjoining plateaux, which would otherwise have buttressed ice flowing out of the main trough, had, with few exceptions, already thinned or melted entirely.

Extending flow likely enhanced deposition along the margins the Bernier Bay Lobe by lowering debris in the basal ice to the bed through attenuation. This flow pattern is recorded by drumlins, flutings and striations which splay outwards from the axis of the trough toward the moraines. The emergent part of the floor of the trough lacks moraines and has a thin cover of bouldery postglacial marine mud over bedrock which suggests it was a zone of net erosion during the last glaciation.

Figure 2-6. Embayment in moraines south of central Bernier Bay. Six successive ice-marginal positions can be defined (beaded lines). The surface of the delta (outlined) is at 125 m asl. Two dates on surface shells GSC-183 (A) and GSC-4721 (B) yielded ages of 8830 ± 170 and 8470 ± 100 BP, respectively.

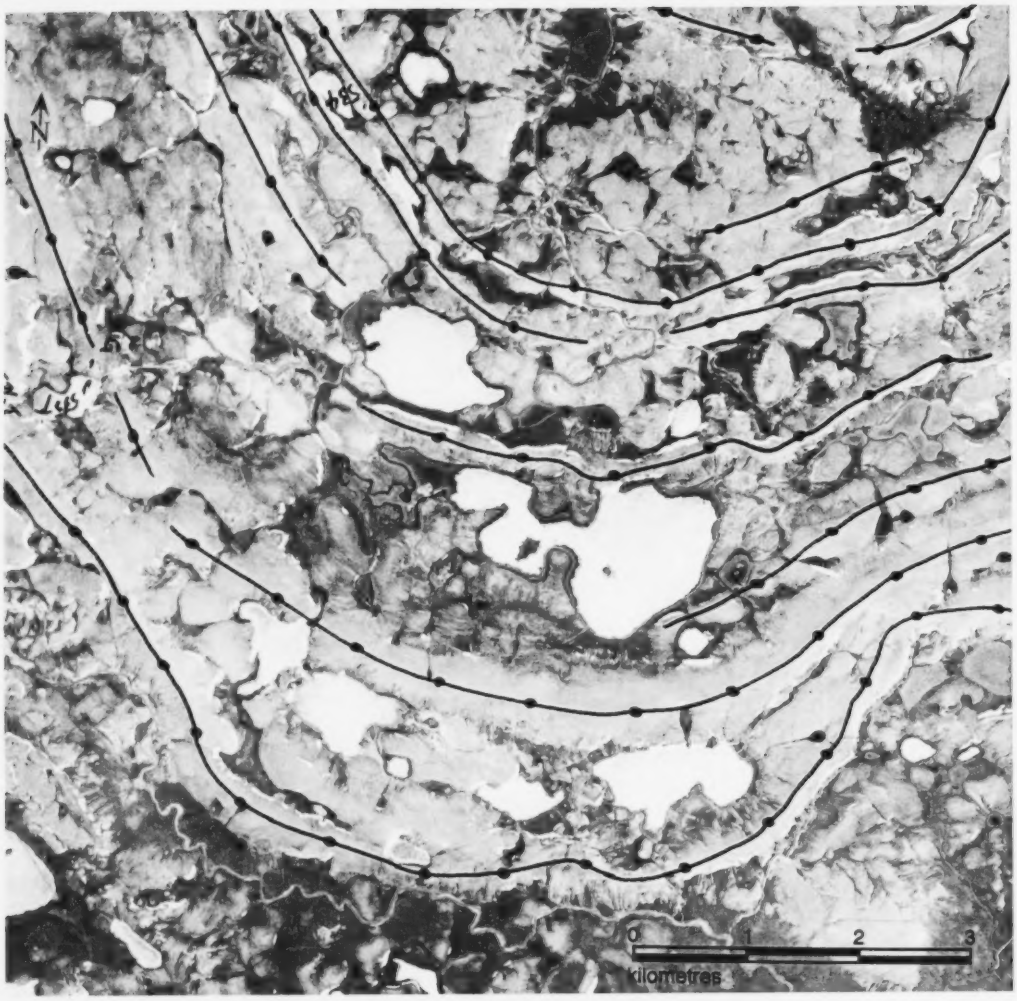

Figure 2-7. Embayments in moraines crossing a shallow side valley south of the head of Bernier Bay. Nine successive ice marginal positions (beaded lines) can be defined.

On both the north and south sides of the trough, moraines were deposited below, at and above marine limit (Map 1). The longitudinal gradient of the highest moraines is low, about 2 m/km over the entire system, declining westward. This initially led to an interpretation that the moraines marked a former ice shelf (Hooper, 1990). However, moraine crests commonly extend 30 m or more above marine limit. Ice shelf moraines can be deposited no higher than the freeboard (i.e. the height of the ice shelf surface above the waterline) of the ice shelf with the amount of freeboard being equal to about 10% of ice shelf thickness. For a hypothetical ice shelf in Bernier Bay to have a freeboard of 30 m requires a 300 m thick slab of floating ice. Water depths in the bay are 60 m or less at present, or about 180 m prior to isostatic recovery, and hence insufficient to float an ice shelf of the required thickness.

The gradient of the moraines and channel bathymetry were used to estimate the position of the former grounding line for an extensive ice shelf in Prince Regent Inlet which disintegrated about 9100 BP (Fig. 2-8). South of the head of Bernier Bay, the highest moraine crests extend up to 100 m above marine limit and drop westward at about 5 m/km. The ice surface is shown above this in Fig. 2-8 because the top of the depositing ice was higher than the moraines. The profile approaches marine limit about 20 km west of the head of Bernier Bay, slightly inside the mouth of the bay where the water was less than 180 m deep (before isostatic recovery). Hence, a likely location for the former grounding line of the ice shelf, at the LGM, is at or slightly beyond the bay mouth where water depths increase rapidly to over 200 m (or 320 m previously) in only 40 km. This reconstruction relies on the assumption that ice in Bernier Bay did not thin significantly and maintained a similar surface profile between the disintegration of ice in Prince Regent Inlet and the subsequent moraine-building episode. This assumption is warranted because radiocarbon dates (discussed below) on the breakup of the ice shelf are only slightly older than the oldest dates on the moraines.

At the LGM, global sea level was about 121 m below present (Fairbanks, 1989). This roughly equals the minimum amount of crustal depression (as recorded by the height of the marine limit) in the study area such that, at LGM, sea level in the study area would have been at or above its modern level (Fig.2-8). If there was significant regional

unloading prior to deglaciation at 9000 BP, then sea level at LGM would have been higher than present, which also favours an ice shelf in Prince Regent Inlet. Hence, it is likely that an ice shelf occupied Prince Regent Inlet throughout the last glaciation.

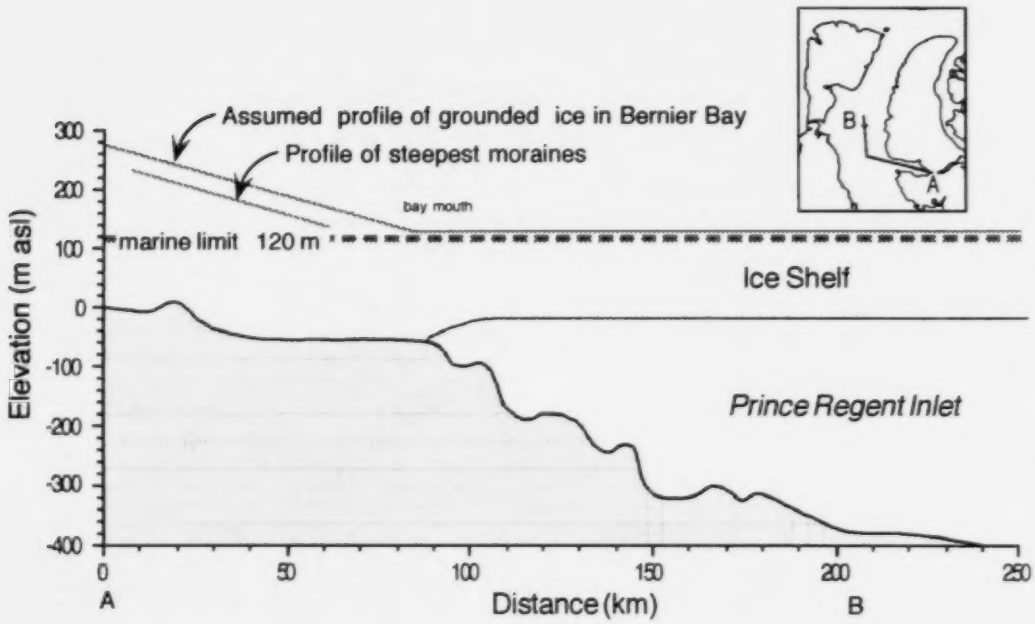

Figure 2-8. Ice surface profiles (ca. 9 ka BP) for the Bernier Bay Lobe and channel bathymetry of Prince Regent Inlet.

The gradient of 5 m/km (from the moraines) can also be used to estimate the ice thickness at the head of Bernier Bay required to maintain grounded ice in central Prince Regent Inlet during the LGM. If the ice in the centre of the inlet was grounded in 300 m of water, it would have a minimum thickness of 330 m (i.e. the top of the ice would be at 30 m asl). Extending the profile 150 km east to the head of Bernier Bay yields a minimum ice thickness there of 780 m. Ice of this thickness would have easily overcome the topographic control imposed by the sides of the Bernier Bay/Berlinguet Inlet trough, which are everywhere below 300 m asl. However, the data on drift dispersal, discussed below, indicate that ice in Bernier Bay was confined to the trough throughout the last glaciation and did not spread laterally onto southern Brodeur or Agu Peninsulas.

The Van Koenig Point ridge forms a possible continuation of the moraine system below marine limit. Surface material on the ridge consists of sand and gravelly sand which has been extensively reworked into raised beaches. The internal composition of the ridge is unknown but the unusual lack of outcrops suggests that much of the ridge consists of unconsolidated sediment. Differences between the form of this ridge and the moraines further inland, notably the lack of multiple steep sided ridges, could be due to deposition in a subaquatic setting. Here fines were winnowed by currents and the material was reworked by debris flows producing low slopes. Large sandy deposits covered by numerous beach ridges have been described from other areas. A noteworthy example, of much larger extent, is the Great Beach, an extension of the Burntwood-Knife interlobate moraine near Churchill, Manitoba. This feature is also interpreted as a former grounding line deposit (Dredge and Cowan, 1989).

INTERLOBATE MORAINES

Small interlobate moraines were deposited north of Berlinguet Inlet where the Bernier Bay Ice Lobe was buttressed by the Brodeur Peninsula Ice Cap (Fig. 2-2). To the west, the location of the contact between these ice masses is marked only by the boundary between till sheets of different lithologic composition, visible on satellite imagery. This sharp tonal change likely marks the stable position of the flowline separating parallel-flowing Laurentide and Brodeur ice, both locally warm-based.

The highest moraine crests south of the head of Bernier Bay are at 230 m asl. East (upice) of this, the height of moraine crests in the southern moraine belt decreases, contrary to the expected configuration of moraines which typically increase in elevation upice. This is due to confinement of the Bernier Bay Lobe by plateau ice to the south. Hence, these moraines were deposited in interlobate settings where their positions were controlled by the dynamics of the two ice masses rather than one ice margin controlled solely by the local topography.

The southern moraine belt terminates abruptly west of the head of Bell Bay at a large interlobate moraine (Fig. 2-9). Till in this moraine is extremely coarse, containing numerous angular boulders, and the top of the moraine is relatively flat. A large esker occurs south of the moraine's eastern end. Further west, channels and eskers connect to large ice-contact deltas on *both* sides of this moraine (Fig. 2-10). These must have been deposited from separate meltwater sources, and prove the moraine formed in an interlobate setting.

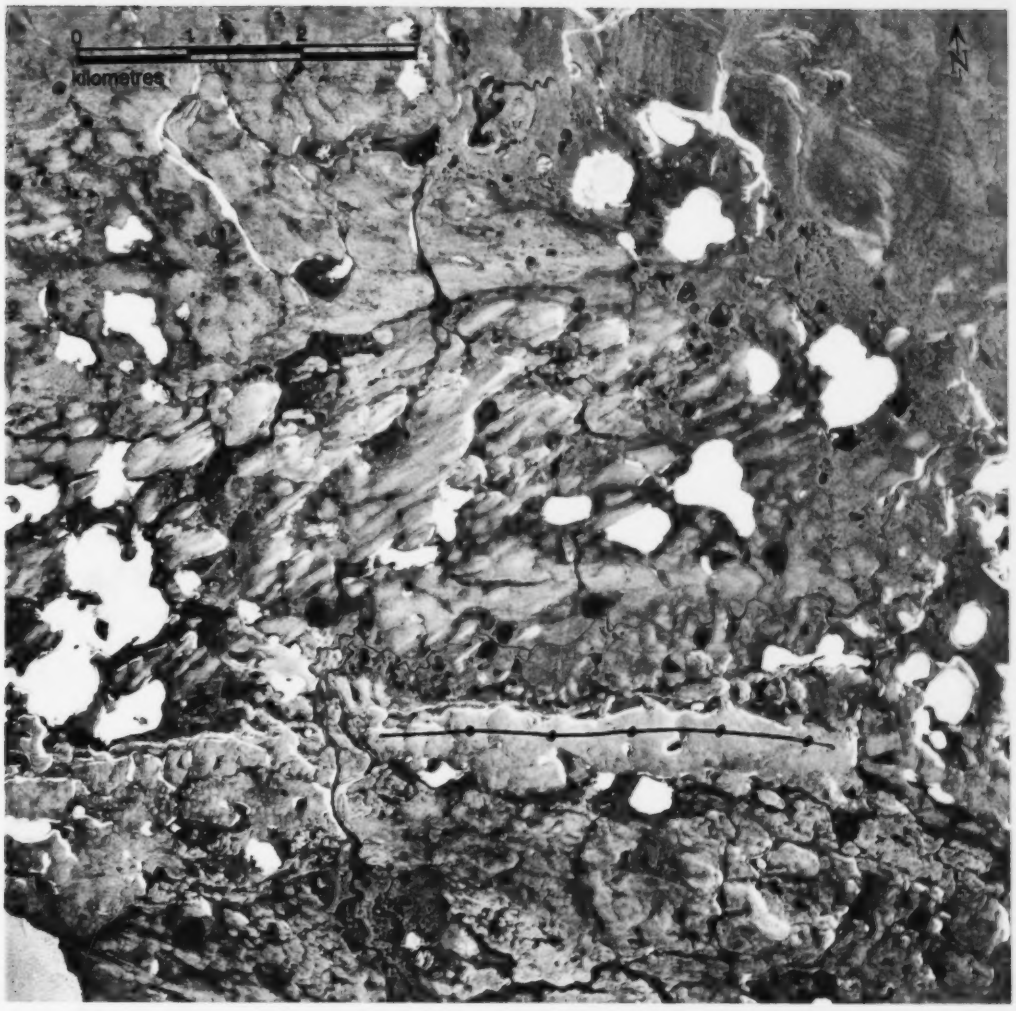

Figure 2-9. Large interlobate moraine composed of bouldery till west of the head of Bell Bay.

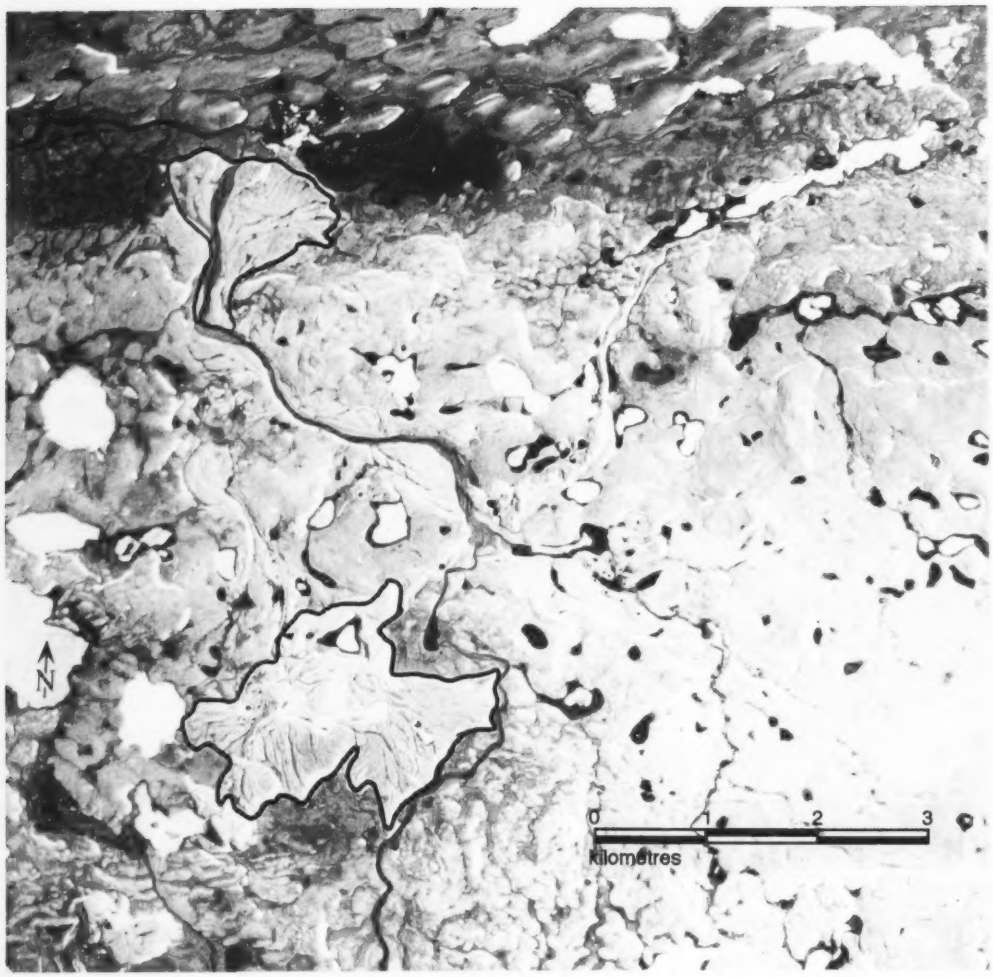

Figure 2-10. Large raised deltas (outlined) on both sides of the interlobate moraine. The southern delta was measured at 134 m asl.

Other Moraines

A few small moraines were mapped in interior locations south of Berlinguet Inlet (Fig. 2-2). The complete lack of recessional moraines on uplands in this area suggests that cold-based conditions prevailed during retreat. Minor terminal moraines crossing some valleys in this area show where local flow into depressions during deglaciation was sufficiently vigorous to trigger a shift to warm-based conditions.

The largest moraines other than the Bernier Bay Moraines are a set of lateral moraines north of Autridge Bay (Map 1). These are 10-15 m high, composed of bouldery till, and mark the former western margin of an ice lobe buttressed by the peninsula on the south side of the bay (Fig. 2-2). Together with the drumlin field north of Whyte Inlet, these moraines record the existence of a warm-based fringe along the margin of the Early Barnes Ice Cap (cf. Dyke, 1993).

Glaciofluvial Deposits

Deposits of glaciofluvial gravel are locally significant, forming eskers and kames up to 60 m high, but more commonly between 5 and 20 m. Small, isolated, conical kames, likely recording moulins, are common in the interior. Ice-contact glaciofluvial sand and gravel and sandy gravel occur in association with the Bernier Bay Moraines. These gravels form steep-sided eskers, conical kames and deltas and occasionally connect with large meltwater channels. Outwash plains, graded to marine limit or former lake levels floor the larger meltwater channels. In some cases, imbrication of the surface clasts is well preserved (Fig.2-11). Raised gravel deltas within the moraine complex occur on the ice-distal side of gaps in the moraines and record the location of the meltwater source as well as the height of marine limit, discussed below. The deltas are often kettled and, like the moraines, probably contain quantities of buried glacial ice as evidenced by thaw flowslides and ponds (Fig. 2-12).

In the north, glaciofluvial deposits are small compared to the size of associated moraines whereas in the south, along the Autridge Bay coast, raised deltas are the largest ice marginal deposits. Between Autridge Bay and Whyte Inlet, a series of ice-contact deltas mark the position of the ice margin and Holocene marine limit. Moraines deposited along the same ice margin are limited to small, discontinuous ridges.

Figure 2-11. Imbricate limestone gravel flooring meltwater channel.

Figure 2-12. Kettle developed in glaciofluvial gravels from the melting of buried ice.

Glaciofluvial landforms of the interior consist of small, widely scattered kames, eskers formed during retreat. The existence of these deposits is not inconsistent with the interpretation of protective cold-based ice on the plateaux which melted from the top down during deglaciation. The small scale of the deposits suggests that these features formed along parts of the margin that attained a warm-based condition possible triggered by localized, topographically-controlled flows as the ice melted. By far the best record of ice retreat in the interior is provided by numerous lateral meltwater channels that record the progressive retreat of cold-based ice across the plateau and frequently extend to the underlying bedrock. The former locations of smaller ice-marginal streams are occasionally marked by gravel lines crossing valley sides. On the north side of Autridge Bay, where the ice was warm-based some valley sides are covered by extensive networks of small eskers. Throughout the field area, ice-marginal channels formed along the retreating edge of the Foxe Dome provide the primary means of mapping that margin above marine limit or where moraines are scarce (Map 1).

Ice Flow Indicators

Small scale erosional features, such as striae and grooves, are rare in limestone terrain because, if formed, they were either covered by till or been erased by Holocene solution weathering. In limestone and sandstone terrains, striae were often found at sections where the rock surface had been recently exhumed by streams. This suggests that, in areas formerly covered by warm-based ice, most bedrock had been scoured prior to the deposition of the overlying till. Granular disintegration during the Holocene also removed some striae from the surface of crystalline rocks, but the greater resistance of these rocks has allowed striae to persist on most exposed surfaces.

Because striae were often difficult to find, the direction of the most recent ice flow was easier to ascertain from drumlins and flutings visible on aerial photographs. Striae observed in the field indicated the same ice flow pattern as adjacent streamlined till. No striae derived from earlier ice flows were recognized, however, the record of earlier ice flows in the area may be confined to such striae.

Several small drumlin and fluting fields occur in the study area. North of Bernier Bay, the Bernier Bay Moraines are interupted by a field of small, north-south trending drumlins formed by a readvance of the southern margin of the Brodeur Peninsula Ice Cap (Fig. 2-13). This drawdown flow was initiated by the retreat of buttressing Foxe ice in the bay. The surfaces of the drumlins are composed of diamict but no sections were found that reveal their internal composition. The field extends below marine limit where its eastern side is bounded by a field of Rogen moraines. Individual ridges within this moraine field are about 2-5 m high, much smaller and shorter than the terminal moraines described above.

A large field of drumlins and flutings occurs near the coast northwest of Whyte Inlet (Map 1). These drumlins trend northeast to southwest. Surface material in this area is bouldery diamict. Extensive bedrock outcrops in this area have been well scoured by ice flowing in the same direction.

South of the head of Berlinguet Inlet is a field of drumlins, many of which are below marine limit. These are oriented nearly east-west. A similar group of small drumlins occurs west of the head of Bell Bay. There are numerous scattered small drumlins on the proximal side of the moraines south of Bernier Bay and Berlinguet Inlet (Fig. 2-9). As they approach the moraines the drumlins tend to become perpendicular to the long axes of moraines. This indicates that the drumlins and the moraines formed at the same time.

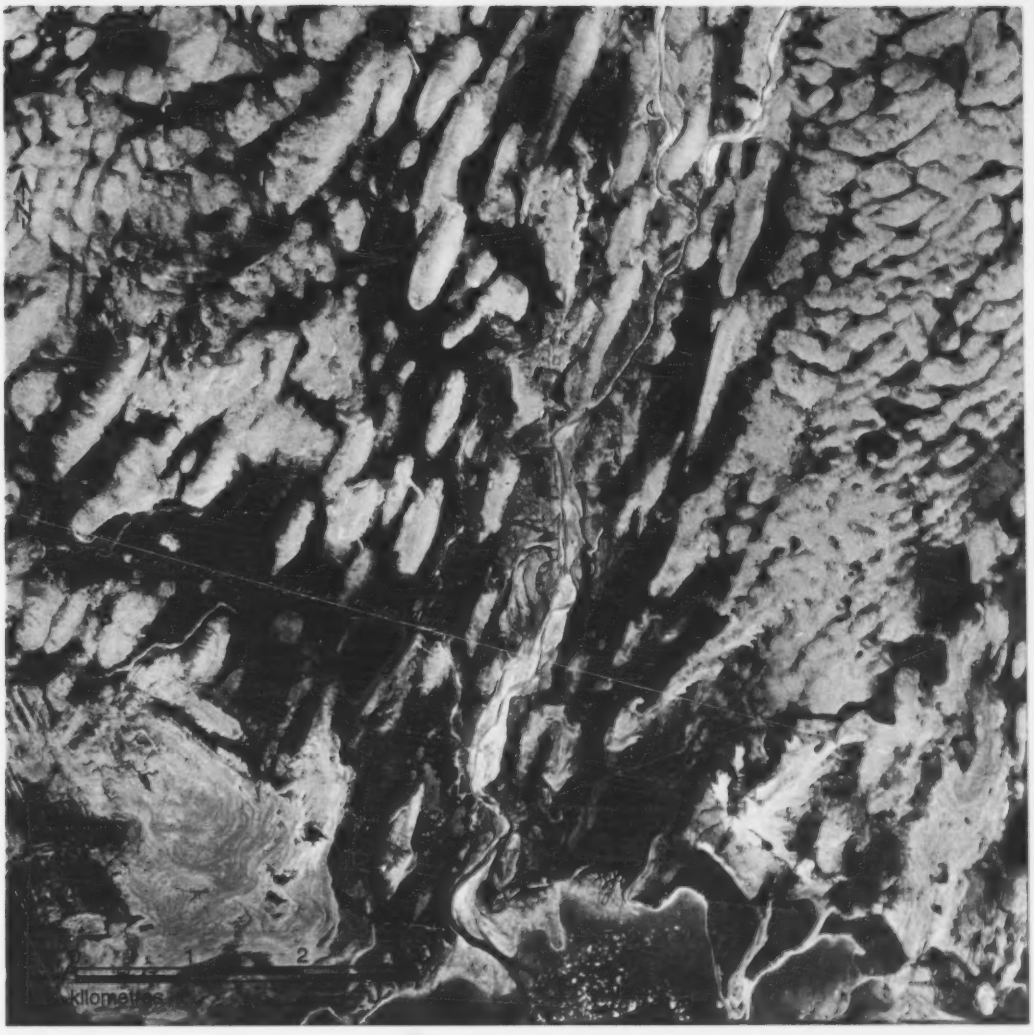

Figure 2-13. Drumlins and Rogen moraines on the north side of Bernier Bay.

No drumlins or flutings occur on the plateau east of Agu Bay. To the west, several areas of streamlined till were mapped on Agu Peninsula south of the Bernier Bay Moraines (Map 1). The largest of these is a field of east-west trending drumlins and flutings that record a westward flow of Foxe ice of unknown age. These are up to 1 km in length and 10 m (est.) or less in height. A field of smaller flutings occur to the northeast of the drumlins and have a northwest-southeast orientation, recording flow toward the moraines. The eastern limit of these flutings is marked by a small field of northeast-southwest trending flutings north of the head of Foss Fiord. The latter two groups of flutings are interpreted as products of topographically controlled flows during deglaciation.

An unusual ice flow feature occurs on the north side of Bernier Bay. Here, a flat-topped ridge of stony silt is almost perfectly straight over its northeast trending 10 km length. The top of the ridge is 130 m asl. The feature is interpreted as a fluting since it lies within and at right angles to, a terminal moraine formed by the Brodeur Peninsula Ice Cap (Map 1). Several small flutings occur adjacent to the south end of this feature and trend north-northeast to south-southwest.

The scarcity of moraines, drumlins and flutings on the interior plateaux of Brodeur and Agu Peninsulas is noteworthy. Dyke (1993) updates the discussion of the influence of basal thermal regime on the evolution of the landscape of southern Brodeur Peninsula. He concludes that local upland ice caps in the south-central Arctic had cold-based centres and warm-based peripheries. Hence, the interior plateaux are ancient surfaces mainly covered by weathered residuum and colluvium. This hypothesis applies equally well to the plateau south of the Bernier Bay/Berlinguet Inlet trough even though the area was covered by Foxe, rather than local ice. All the glacial landforms discussed above, with the exception of the ice-marginal channels of the interior, are indicators of warm-based conditions. Streamlined till forms on western and southern Agu Peninsula and north of Agu Bay indicate that these areas were within the warm-based marginal fringe of Foxe ice. The transition to cold-based conditions on the southern plateau is marked by the eastern limit of flutings and a corresponding increase in the number of lateral channels cut in the plateau surface during retreat.

Chronology of Deglaciation and Moraine Deposition

Radiocarbon dates on marine shells (Table 2-1) and the distribution of moraines and meltwater channels were used to establish the age and sequence of deglaciation (Fig. 2-14). Gaps in the dataset include: 1) the pattern of retreat offshore, where the record remains uninvestigated; and 2) the chronology of ice retreat above marine limit where radiocarbon dates are unavailable. The 15 radiocarbon dates included here are a subset of 92 new dates used to discuss the emergence history of the area (see Chapter 3). The dates provide minimum age estimates for deglaciation of their respective sample sites.

All of the dates discussed below are GSC shell dates corrected to $\partial^{13}C = 0‰$ (the PDB standard for marine carbonate). Thus they incorporate a -400 year correction for the reservoir effect. A further correction for isotopic fractionation was made in cases where the ^{13}C content of the sample was measured. The corrected ages are used in the discussion when available. Further explanation of corrections applied to the radiocarbon dates is given in Chapter 3.

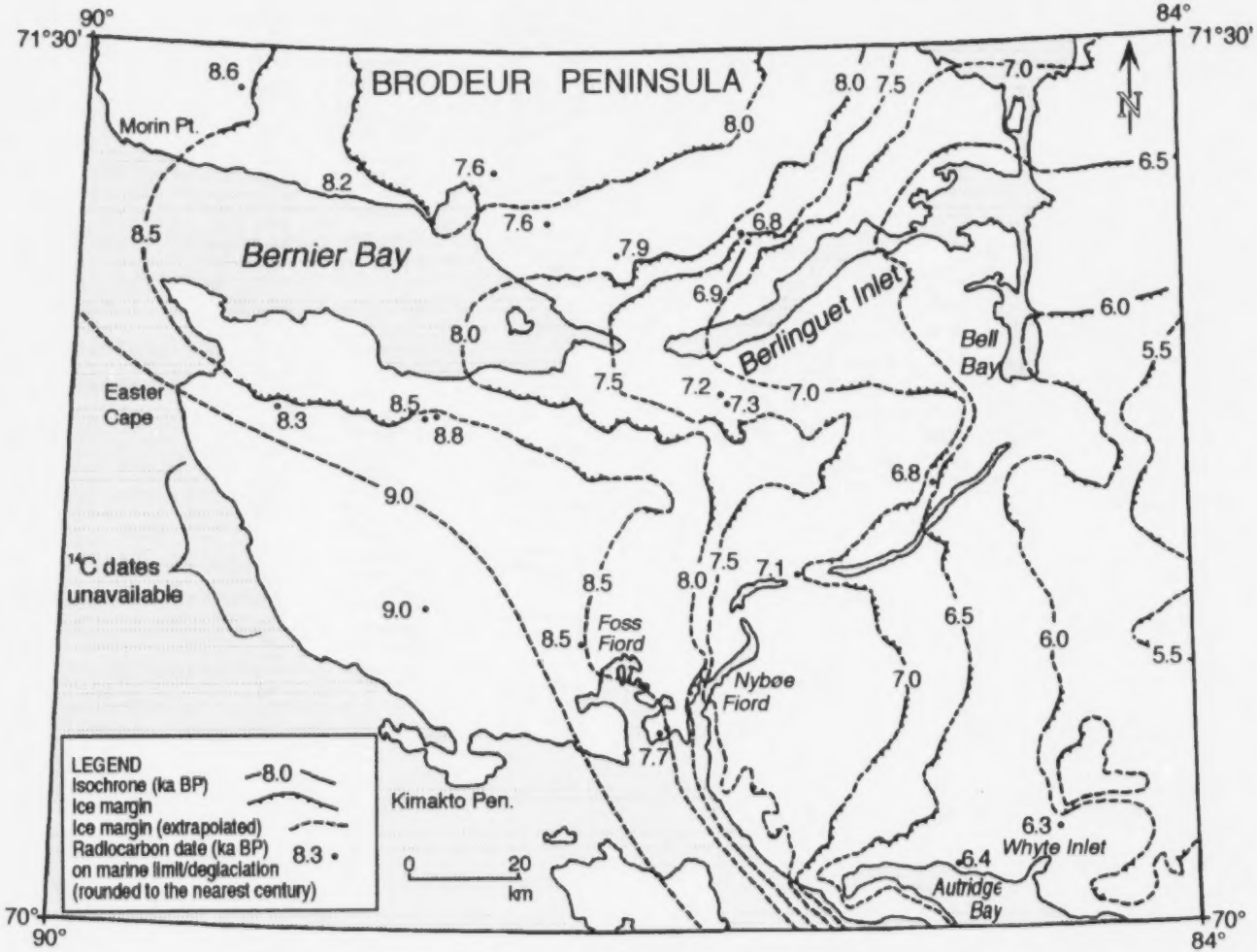

Figure 2-14. Deglaciation of the study area based on limiting radiocarbon dates and ice-marginal landforms.

Table 2-1. Radiocarbon dates on deglaciation

Lab Number	Taxa	Enclosing Material	Latitude Longitude	Elevation	Rel. Sea Level	Marine Limit	Age (yrs BP)	Location	Reference
GSC-5372	*M. truncata*	muddy sand	70°11' N 84°41' W	71.0 m	≤114 m	114 m	6310±80	Whyte Inlet	this paper
GSC-5331	*M. truncata*	sand	70°07' N 85°15' W	57.5 m	≥57.5 m	114 m	6350±100	Autridge Bay	this paper
GSC-4897	*M. truncata*	sand	70°45' N 85°18' W	69.5 m	≤92 m	134 m (?)	6780±90	Saputing Lake	this paper
GSC-5088*	*M. truncata* *H. arctica*	silt	71°11' N 86°25' W	68.5 m	≤111 m	111 m	6840±140	Berlinguet Inlet N	this paper
GSC-5089*	*H. arctica* *M. truncata*	pebbly silt	71°10' N 86°25' W	64.0 m	≤111 m	111 m	6860±100	Berlinguet Inlet N	this paper
GSC-307*	*H. arctica*	deltaic terrace	70°36' N 86°08' W	97 m	≥97 m	136† m	7120±140‡	Ivisarak Lake	Craig (1965)
GSC-4894*	*H. arctica*	sand	70°54' N 86°27' W	73.5 m	~ 76 m	130† m	7260±100	Berlinguet Inlet S	this paper
GSC-304*	*H. arctica*	sand terrace	70°55' N 86°27' W	89 m	≥89 m	130† m	7240±150‡	Berlinguet Inlet SW	Craig (1965)
I-1254			71°17' N 87°43' W	87 m	≥87 m	114† m	7576±500‡	Bernier Bay N	Craig (1965)
GSC-5091*	*M. truncata* *H. arctica*	stony silt	71°12' N 87°29' W	80.5 m	>80.5 m	112 m	7640±110	Bernier Bay NE	this paper
GSC-5327*	*H. arctica,* *M. truncata*	stony silt	70°20' N 86°48' W	95.5 m	≥95.5 m	138 m	7670±130‡	Agu Bay	this paper
GSC-306	*H. arctica*	frost boil	70°20' N 86°48' W	97 m	≥97 m	138 m	7690±140‡	Agu Bay	Craig (1965)
GSC-5090*	*M. truncata* *H. arctica*	stony silt	71°08' N 87°05' W	92.5 m	≤111 m	112 m	7910±120	Bernier Bay N	this paper
GSC-4695*	*M. truncata*	marine silt	71°18' N 88°28' W	92 m	~ 106	110 m	8240±110	Bernier Bay N	this paper
GSC-4703*	*M. truncata*	marine silt	70°53' N 88°54' W	91 m	> 91 m	116 m	8310±100	Bernier Bay S	this paper
GSC-4721*	*M. truncata*	glacio-marine silt	70°52' N 88°12' W	114 m	~ 125 m	125 m	8470±100	Bernier Bay SE	this paper
GSC-5086*	*M. truncata* *H. arctica*	stony silt	70°29' N 87°11' W	137.5 m	~ 138 m	138 m	8540±100	Foss Fiord	this paper
GSC-4742*	*M. truncata* *H. arctica*	marine silt	71°26' N 89°07' W	118 m	~ 118 m	118 m	8600±90‡	Bernier Bay NW	this paper
GSC-183*	*H. arctica* *M. truncata*	marine silt	70°53' N 88°06' W	119 m	≥119 m	125 m	8830±170‡	Bernier Bay SE	Craig (1965)
GSC-4898*	*M. truncata*	gravel	70°33' N 88°00' W	65 m	≥65 m	130† m	8950±120	Kimakto Peninsula	this paper

*Surface collections †Estimated local marine limit ‡date uncorrected for isotopic fractionation

PRINCE REGENT INLET

Deglaciation of the area began slightly before 9000 BP when a calving bay migrated south along Prince Regent Inlet and into the Gulf of Boothia effectively separating Foxe ice from McClintock ice to the west. The oldest date from the field area is 8950 ±120 BP (GSC-4898*) obtained on a surface sample (65 m asl) of *Mya truncata* collected north of Kimakto Peninsula (Fig. 2-14). The sample is well below marine limit, and hence gives a minimum age on the initial entry of the sea to the site, now 12 km inland. The date indicates that Prince Regent Inlet and the Gulf of Boothia were deglaciated by calving while adjacent ice on Baffin Island underwent slight areal retreat. The entire Gulf of Boothia coast of Agu Peninsula was probably deglaciated by about 9000 BP (Fig. 2-14) although dates are unavailable between Easter Cape and Kimakto Peninsula.

Dyke (pers. comm., 1994) obtained additional shell dates for northern Brodeur Peninsula, indicating that deglaciation occurred between 9780 ± 90 BP (GSC-4694) at the northern tip and 8050±90 BP (GSC-4886) in southern Admiralty Inlet north of the study area. The sea had reached Fitzgerald Bay, north of the mouth of Bernier Bay by 9260 ±150 BP (GSC-392, Dyck et al., 1966; Dyke, 1984). The dates show that deglaciation of the coastal fringe of northern Brodeur Peninsula proceeded from north to south beginning along the exposed coasts of Lancaster Sound, Prince Regent Inlet and northern Admiralty Inlet. The oldest date available from northern Melville Peninsula, on the mainland 50 km south of the study area, indicates that its west coast was deglaciated by 9110 ±100 BP (GSC-4324; Dredge, 1990). However the calving bay in Prince Regent Inlet had extended past the study area earlier than this as indicated by a date of 9430 ± 210 BP from Pelly Bay (GSC-2093; Dyke, 1984). Hence, marine-based ice in Prince Regent Inlet and the Gulf of Boothia calved into the sea whilst ice in Bernier Bay, Berlinguet Inlet, Admiralty Inlet and Fury and Hecla Strait remained largely intact.

---

* Corrected for isotopic fractionation and for marine reservoir effect.

BERNIER BAY

Dates on surface shell collections show that the outermost (i.e. farthest south) moraines south of Bernier Bay were abandoned by 8800 BP (Fig. 2-6). A younger date of 8600 ± 90 BP (GSC-4742, Table 2-1) was obtained on *Mya truncata* shells collected north of the mouth of Bernier Bay. This was the highest elevation shell collection from the north side of Bernier Bay (at 118 m asl) and records marine limit and the retreat of the southwestern margin of the Brodeur Peninsula Ice Cap while Bernier Bay was still occupied by a lobe of grounded ice.

A large moraine marks a former marginal position of the Brodeur Peninsula Ice Cap north of Bernier Bay. Surface *Mya truncata* fragments were collected from the flank of a large ice-contact delta which occupies a gap in the moraine (Figs. 2-14, 2-15). These provide a minimum age for the delta, and hence the moraine, of 8240 ± 110 BP (GSC-4695*). Distributary channels on the surface of this 110 m delta indicate a meltwater source to the north of the moraine. Retreat of the Brodeur Peninsula ice from this position is recorded by a date of 7576 ± 500 BP (I-1254; Craig, 1965) on shells collected north of the small, unnamed bay on the inner north side of Bernier Bay (Fig. 2-14). Farther east, a collection of *Mya truncata* from a col in the outermost moraine yielded a similar age of 7640 ± 100 BP (GSC-5091*).

Shells of *Mya truncata* collected from the surface 12 km north of the head of Bernier Bay (Fig. 2-14) dated 7910 ± 120 BP (GSC-5090*). The sample was collected at 93 m asl below a 111 m delta. Distributary channels on the delta surface (Fig. 2-16) indicate northward progradation of the delta with a meltwater source to the south. The channels and the presence of shells in the flanking silts indicate that an arm of the sea occupied the area north of this moraine, between the Bernier Bay Lobe and the Brodeur Peninsula Ice Cap, prior to deglaciation of the head of Bernier Bay.

---

* Corrected for isotopic fractionation.

Figure 2-15. Marine limit delta (outlined) at 110 m asl north of Bernier Bay showing its relation to the moraines marking the southern limit of the Brodeur Peninsula ice cap and the associated shell date (arrow) of 8240 ± 110 BP (GSC-4695).

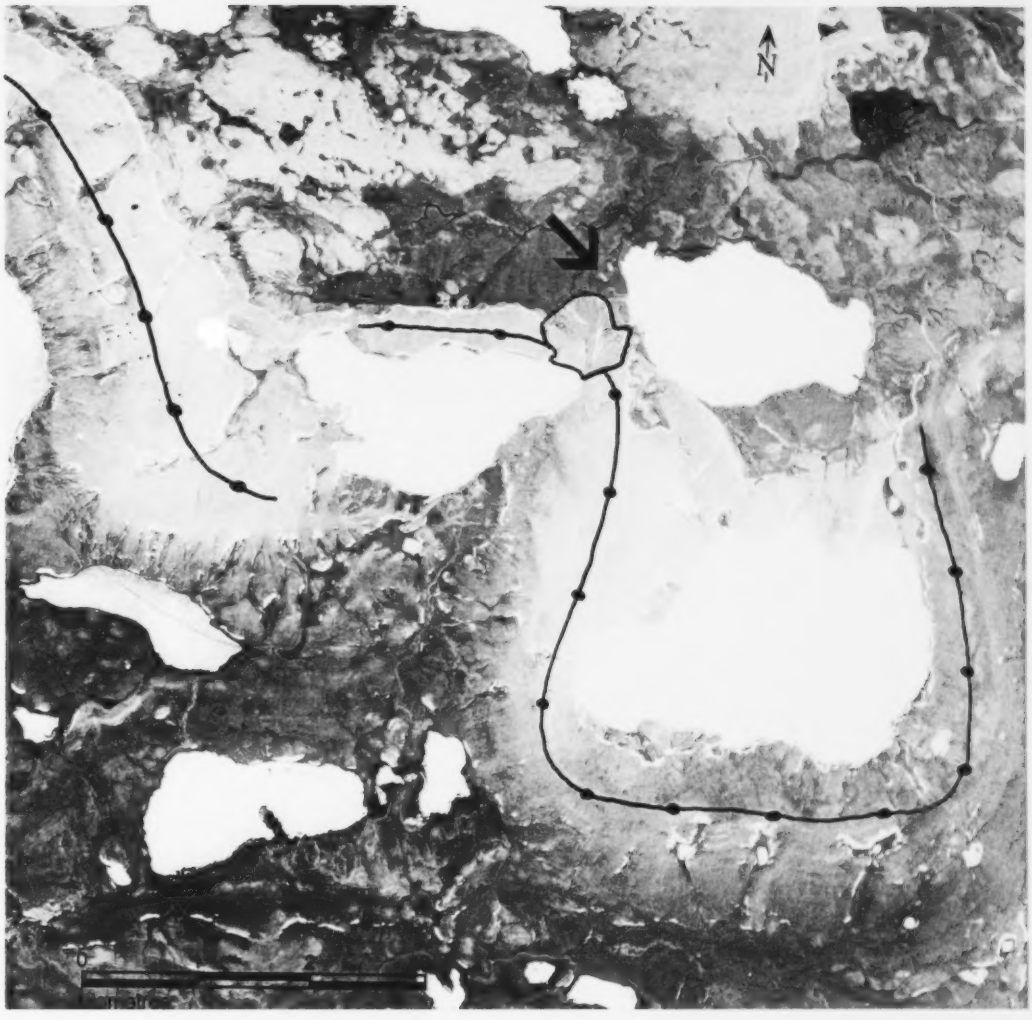

Figure 2-16. Marine limit delta (outlined) at 111 m asl north of the head of Bernier Bay. Shells collected from the surface of silts flanking the delta (arrow) dated 7910 ± 120 BP (GSC-5090). Flow in distributary channels was to the north. The Bernier Bay moraine is the light-toned sinuous ridge impounding ice-covered lakes.

On the south side of the bay, Craig (1965) collected shells dating 8830 ± 170 BP (GSC-183, Table 1, Fig. 2-6) on the distal side of the outermost moraine. This is the minimum age for entry of the sea along the south (ice-distal) side of the moraine. This event occurred about 600 years after deglaciation of Prince Regent Inlet as recorded by GSC-2093 (9430 ± 210 BP, Dyke, 1994) likely because of considerably deeper water in the inlet and because the study area was closer to the Foxe Dome. Thus, penetration of the sea to the area distal to the Bernier Bay Moraines occurred shortly after breakup of ice in Prince Regent Inlet.

A second collection made on the proximal side of the outermost moraine (Figs. 2-6, 2-14), dated 8470 ± 100 BP (GSC-4721*), and indicates that ice had retreated from the outermost moraine by this time. Both dates (GSC-183 and 4721) are significantly older than any within the Bernier Bay valley and hence predate entry of the sea into Bernier Bay itself. Consequently, these dates record a marine incursion between the south side of the Bernier Bay Lobe and higher terrain (above marine limit) on the plateau to the south. This incursion occurred about eight hundred years before deglaciation of the head of the bay (see below). The marine embayment thus formed was open to the Gulf of Boothia to the west and flanked on the north by persistent ice in Bernier Bay.

A date of 8310 ± 100 BP (GSC-4703*) was obtained on a sample of *Mya truncata* collected from a small gap in the outermost moraine ridge east of Thiboult Bay (Fig. 2-14). Older dates to the east (GSC-183 and 4721) suggest the site was deglaciated several hundred years earlier.

The radiocarbon dates and positions of moraines and deltas indicate that marine incursions occurred along both sides of the Bernier Bay Lobe, with an earlier and more prolonged incursion on the south side. That the ice lobe maintained stable, grounded margins in extensive shallow water along the sides of the trough and a calving margin in deeper water, at a point west of the mouth of Bernier Bay, is evidence for an abundant supply of ice from the Foxe Dome during Cockburn time. The possibility exists that moraine deposition extends back to the LGM (i.e. before 8830 BP).

---

* Corrected for isotopic fractionation.

BERLINGUET INLET

Four dates around Berlinguet Inlet record the continued eastward retreat of the Bernier Bay Lobe (Fig. 2-14). A mixed surface collection, of *Mya truncata* and *Hiatella arctica* was made on a silt plain alongside Berlinguet River and dated 6840 ± 140 BP (GSC-5088*). The sample is from the ice-distal (north) side of a large moraine which crosses the Berlinguet River valley where it was partially backfilled by ice of the Bernier Bay Lobe. A similar collection made nearby, on the proximal side of the same moraine, dated 6860 ± 100 BP (GSC-5089*). The older date records the retreat of the Bernier Bay Lobe from the moraine by 6860 BP. Since virtually identical ages were obtained on shells from the distal and proximal sides of the moraine, both dates are minimum ages for the retreat of ice from inside the moraine; the area outside the moraine must have been deglaciated earlier.

On the south side of the inlet, a surface sample of *Hiatella arctica* dated 7260 ± 100 BP (GSC-4894*, Table 2-1). The shells were collected at 74 m asl, immediately north of a 76 m delta. This is nearly identical in age to the date (7240 ± 150; GSC-304) reported by Craig (1965) from a nearby site (Fig. 2-14). The delta, which is one of three near this elevation on the south side of Berlinguet Inlet, records a pulse of meltwater entering the inlet from the plateau to the south.

BELL BAY/IVISARAK LAKE

Three shell dates record the progressive eastward deglaciation of Bell Bay and the valley connecting it, via Saputing and Ivisarak lakes to the head of Nybøe Fiord. Craig (1965) reports a date of 7120 ± 140 (GSC-307) for the east end of Ivisarak Lake. A second date was obtained on a sample of *in situ Mya truncata* valves from a stream-cut section at 70 m asl on the north side of Saputing lake (Fig. 2-14). These dated 6780 ± 90 BP (GSC-4897*) and provide a minimum age estimate for deglaciation and the formation of a nearby marine limit delta at 92 m asl. This agrees closely with a date obtained by Dyke (pers. comm., 1992) on *Mya truncata* from the upper sands (66 m asl) of an ice-contact, marine-limit delta (marine limit at 72 m asl) at Jungerson Bay adjacent to the northeast

* Corrected for isotopic fractionation.

corner of the study area. The shells dated 6620 ± 90 BP (GSC-5073) indicating that Laurentide ice was still reaching tidewater at that time but was no longer flowing from the centre near Foxe Basin because the sea had already penetrated there (Craig, 1965). Deglaciation of Bell Bay and southern Admiralty Inlet marks the demise of marine-based ice on the western flank of the Foxe Dome. From then on, steady eastward retreat across the uplands was recorded by numerous ice marginal channels.

AGU BAY

A date of 8540 ± 100 BP (GSC-5086*) was obtained on surface shells from a hilltop at or near marine limit (138 m asl, Table 2-1) northwest of the head of Foss Fiord (Fig. 2-14) and is a good indication that the deglaciation of Foss Fiord (i.e. inner Agu Bay) was complete by that time.

FURY AND HECLA STRAIT/FOXE BASIN

Dredge (1990) obtained a series of dates from the north end of Melville Peninsula. The oldest date from the Fury and Hecla Strait coast (south of the area of Fig. 2-14) is on shells from a beach section at 121 m asl which dated 6520 ± 70 BP (GSC-4378). Older dates from the west side of the peninsula pertain to the earlier deglaciation of the Gulf of Boothia and Committee Bay (Dredge, 1990).

The youngest deglacial dates in the present study area are from Autridge Bay and Whyte Inlet (Fig. 2-14), north of the west end of Fury and Hecla Strait. *Mya truncata* valves collected from a stream cut yielded an age of 6350 ± 100 (GSC-5331*, Table 2-1). The true age of deglaciation is probably older since the sample site is well below a marine limit delta (114 m asl). The moraines north of the head of Autridge Bay indicate that it was occupied for a time by an ice lobe buttressed by the rugged peninsula forming its southern shore. North of the head of Whyte Inlet (Fig. 2-15), a date on *Mya truncata* from a slump at the foot of a 114 m delta had an age of 6310 ± 80 BP (GSC-5372*, Table 2-1). The age of the sample, and the fact that the associated delta is lower than deltas along the outer coast (at 130 m asl), suggest that the delta formed after ice had

---

* Corrected for isotopic fractionation.

retreated from Autridge Bay but remained on the interior highlands to the northeast.

On the Foxe Basin coast of Melville Peninsula, Craig (1965) obtained shells dating 6880 ± 180 (GSC-291) and Sim (1964) obtained a date of 6725 ± 250 BP on shells from the east side of Foxe Basin (Ikpik Bay; I-406). Thus, deglaciation of Foxe Basin occurred shortly after 7000 BP whereas Fury and Hecla Strait was open by 6500 BP when ice over Baffin Island and Melville Peninsula separated.

SUMMARY

Deglaciation of the study area began with the migration of a calving bay down Prince Regent Inlet and into the Gulf of Boothia about 9400 BP with the outer coasts becoming ice free by about 9000 BP. The ice margin stabilized as it retreated into shallow water or above marine limit, except in Bernier Bay where a calving margin was maintained offshore possibly by a still-vigorous flow of Foxe ice down the Bernier Bay/Berlinguet Inlet valley. By 8000 BP, the Bernier Bay Lobe retreated almost to the east end of Bernier Bay and was flanked on three sides by the sea. After 8000 BP, the ice in Bernier Bay calved away; the calving front migrated eastward, reaching Bell Bay and allowing the sea to isolate Brodeur Peninsula, forming an island, by about 6500 BP. Meltwater from melting ice on the plateau south of Berlinguet Inlet deposited a series of deltas in the 70-80 m asl range at about 6800 BP. By 6200 BP, all of the marine channels and bays were ice-free and the remaining Early Barnes ice was undergoing steady retreat on uplands in the southeast. It retreated beyond the eastern margin of the study area soon thereafter.

The Bernier Bay Lobe was grounded below sea level in the Bernier Bay/Berlinguet Inlet trough and was sufficiently dynamic, due to massive inputs of ice from the Foxe Dome, to construct numerous large moraines and delay entry of the sea until long after other marine-based ice in Prince Regent Inlet and the Gulf of Boothia had calved away. Consequently, the earliest penetration of the sea to the interior was in areas along the margins of the lobe where the land surface was slightly below marine limit and plateau ice was thin or absent. Ice retreat to the head of Bernier Bay occurred during the Cockburn Substage as defined

by Andrews and Ives (1978) chronostratigraphy. However the ice remained at or near the moraines around Berlinguet Inlet considerably longer, until about 6500 BP. Hence, the upper boundary of the Cockburn Substage as originally defined does not appear to mark a significant change in either moraine construction or ice retreat rate in the study area. It is clear that the ice had retreated from the most distal parts of the system soon after 9000 BP, when the earliest penetration of the sea occurred but the distal parts of the system could have been deposited earlier, prior to the entry of the sea, during the last glacial maximum. Hence, the interval 8000-9000 BP in the study area was one of protracted retreat that continued until ice left the area, rather than one of readvance to maximum Wisconsinan positions.

Till Characteristics and Dispersal

Tills in the study area are typically massive, compact, stony silts, 0.5-50 m thick, deposited in subglacial and supraglacial settings. Deposition is inferred to have been primarily by meltout, but lodgement may have occurred in warm-based zones. In permafrost areas, meltout can only occur from the top down and ceases when the thickness of material accumulating on the ice surface is the same as the depth of the active layer, after which cores of buried glacier ice survive. The formation of such cores also requires a sufficiently high concentration of englacial debris to form a protective surface accumulation, so ice cores are not expected to form from the melting of clean ice. Waterlaid sediments, such as sand partings (Shaw, 1985), which would allow more conclusive recognition of meltout tills, were not observed. From the landforms, particularly the extensive end moraines and drumlins, it is clear that parts of the ice sheet were warm-based, hence the processes of till deposition are thought to have been similar to those in temperate regions.

The till in areas covered by cold-based ice during the last glaciation, where the effects of the last glaciation are restricted to the extensive series of ice-marginal channels, could not have been deposited by lodgement, neither does it consist solely of preglacial residuum or colluvium (which can resemble till), because Precambrian erratics were always present, although often at trace levels.[1] This material could be produced if sparse debris melted out of the ice during deglaciation, and was later mixed into the surface sediment by cryoturbation. Another possibility, which does not require a debris entrainment mechanism at the bed of a cold-based ice sheet, is that this material consists of preexisting residuum which was partially reworked during a previous regional glaciation.

Figure 2-17. Locally-derived sandstone felsenmeer containing Precambrian erratics on hilltop north of Whyte Inlet.

[1] This includes sites where no Precambrian erratics were found in the till granule fractions.

The composition of till is closely related to the underlying bedrock. This finding is supported by laboratory results and the fact that the till is usually the same colour as local outcrops. Due to the original coarse texture of gneiss and sandstone, tills derived from them tend to be much coarser than carbonate-derived tills. Such tills contain numerous boulders over 1 m across, and more closely resemble felsenmeer (Fig. 2-17). Although they often appeared to be solely derived from the local bedrock, glacial erratics were commonly found within the blockfields.

Lithology of Granule Fractions

Following Dyke et al., (1992), tills were divided into ten lithic facies defined by the dominant constituents of the granule (2-5 mm) fraction (Table 2-2, Appendix A). The majority of the tills (55%) are of carbonate-rich (lithic facies C, >90% carbonate) and 75% of the tills have between 70 and 100% carbonate clasts due to the prevalence of carbonate bedrock in the field area and the relatively short distance of glacial transport.

Table 2-2. Till Lithic Facies Definitions

Lithic Facies	Percent carbonate granules	Percent sandstone granules	Percent gneiss/granite granules	Number of samples
C	90-100			132
MCC	80-89			33
MC	70-79			15
S		90-100		2
MSS		80-89		10
MS		70-79		11
P			90-100	3
MPP			80-89	0
MP			70-79	2
M	0-69	0-69	0-69	31
Total				239

Shield Clasts

Contours drawn on the distribution of shield clasts show an internally complex plume of westward transport (Fig. 2-18) along the Bernier Bay/Berlinguet Inlet valley and a broad zone of westward dispersal on Agu Peninsula. The axis of the northern plume roughly parallels, but lies within, the main moraines north and south of the

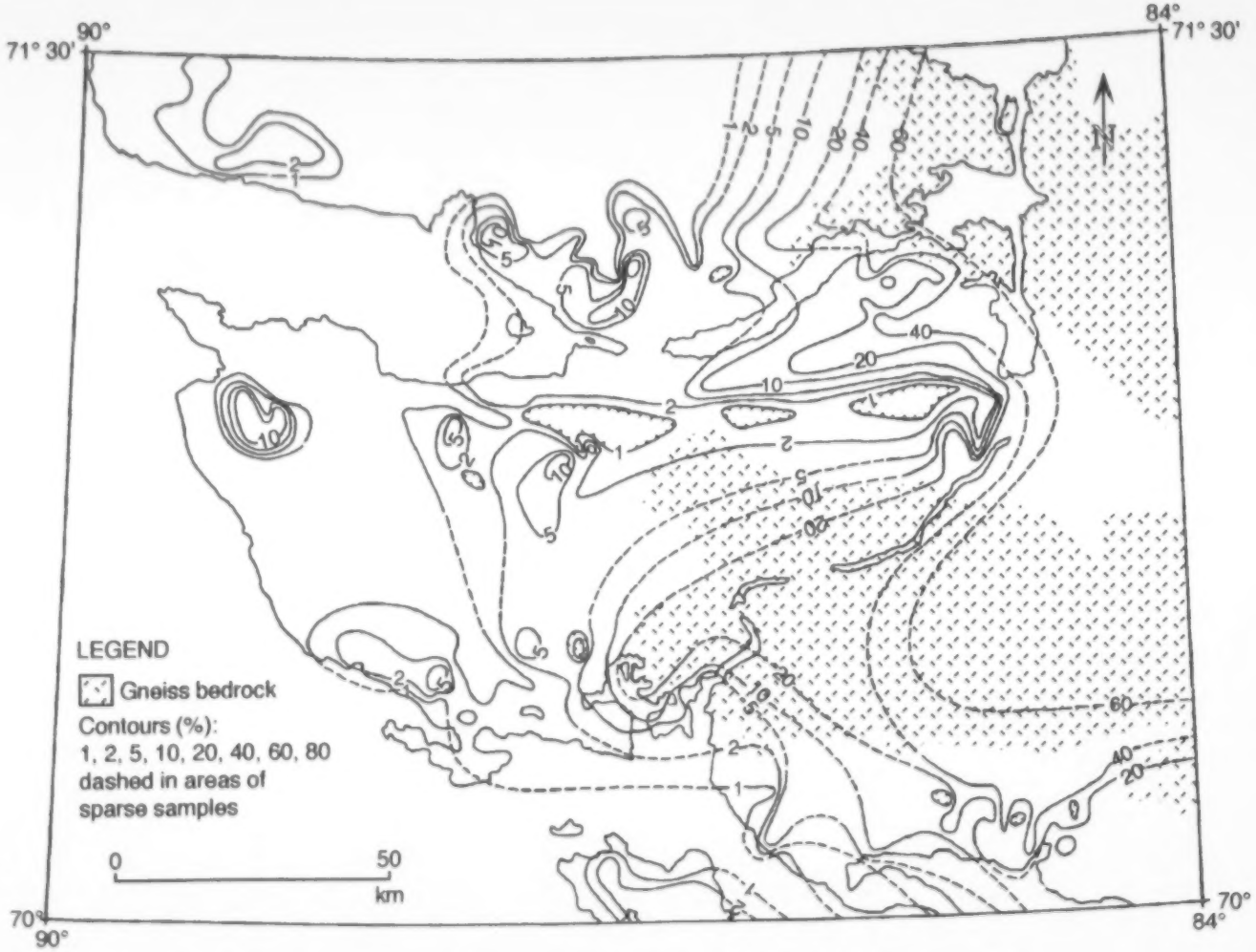

Figure 2-18. Distribution of Precambrian (gneiss) clasts in the granule

inlet. On the north side of the inlet, shield clast concentrations fall to less than 10%, 20-30 km west of the source outcrops but two zones of higher (above 10%) shield clast concentrations occur farther downice, north of the head of Bernier Bay. The furthest of these is about 60 km from the source outcrop. None of the samples had 100% shield clasts because only one was collected from the area of gneiss bedrock due to difficulty of access.

On the south side of the inlet, shield clasts were dispersed farther west with the concentration falling steadily to below 10% about 60 km west of the source outcrops on the east side of Bell Bay (Fig. 2-18). The highest concentrations of shield-derived material occur along the sides of the trough and are separated by slightly depressed shield clast concentrations in till from the Berlinguet Inlet valley floor. The concentration of shield-derived material within the moraine belt itself is very low and forms series of closed depressions where it is below 1%.

Particularly apparent in this dispersal pattern is the effect of a prominent carbonate knoll which rises to over 180 m asl on the south side of Berlinguet Inlet (Fig. 2-18). The highest part of the trough floor to the south is at about 90 m asl. The Bernier Bay Ice Stream flowed over and around this obstacle through the adjoining lowlands where bands of Precambrian-rich till occur. Lower concentrations of shield clasts separate these bands directly downice (west) of this obstacle and indicate enhanced erosion on the upland, which diluted the amount of shield-derived material in tills deposited downice (Fig. 2-18). Diversion of ice around the obstacle could produce a similar effect; however, this particular upland has been well scoured by overriding ice.

The Agu dispersal zone lies west of the Saputing Lake valley and records the dispersal of shield erratics westward across Agu Peninsula between inner Bernier Bay and Kimakto Peninsula. The large westward deflection of the contours toward the head of Foss Fiord is partly a result of the location of the contact between gneiss and carbonate bedrock, which reaches its greatest westward extent in this area (Fig. 2-18). Except for small outliers, shield clast concentrations drop rapidly to below 5% within 30 km of the source rocks. The dispersal pattern is consistent with westward flow of ice over a broad area, although here the

ice was a less effective agent of transport than in the Bernier Bay dispersal train, discussed above.

Around Nyebøe Fiord, the concentrations reach a maximum of 20% along a sinuous axis at the centre of the Precambrian rocks. The few till samples in this area, however, make it difficult to tell whether the dispersal pattern necessarily records a corresponding ice tongue flowing down the fiord versus increasing availability of Precambrian rocks. Samples collected on sandstone terrain around Cape Appel have very low concentrations of shield clasts. In this area, warm-based conditions along the fringe of the ice sheet led to incorporation of quantities of local rock while little, if any, shield clasts were being transported from the area covered by cold-based ice to the northeast. Shield erratics on Crown Prince Frederick Island are scarce, below 4% for all samples, due to its greater distance from source outcrops.

Higher concentrations of shield clasts occur around Autridge Bay and Whyte Inlet, which are also in the area of sandstone bedrock. These areas were within the warm-based marginal fringe which extended well into the area of shield rocks to the north. Hence, shield clasts were readily eroded and dispersed southwest across the sandstone terrain.

The dispersal pattern around Autridge Bay (Fig. 2-18) reflects a positive correlation between increasing shield clast concentrations and increasing elevation. Ice in the valleys may have been eroding more of the local sandstone, diluting the concentration of entrained shield clasts. Protective, cold-based ice did not erode preexisting sediments (containing shield clasts) from the uplands. Typically, the concentration of gneiss erratics in till on the sandstone highlands approaches 50% whereas in valleys and coastal lowlands they decline to 10-20%. An anomalously high content of erratics in one sample from the northwest side of Whyte Inlet is interpreted as a result of ice rafting because the site is below marine limit.

Some inferences about debris transport and comminution of material by Foxe ice can be drawn from the pattern of shield clast dispersal along Berlinguet Inlet and Bernier Bay. Till around Bernier Bay typically has low concentrations of shield erratics. Inland from Easter Cape, however, three samples had high concentrations of shield clasts (up to 18%). Since the sites are below marine limit, ice-rafting is the

most likely explanation. The sample sites are also close to the location of the former grounding line proposed in Fig. 2-8). A few samples from the north side of the bay also had elevated shield clast contents. If these outliers are taken as the western limits of the dispersal train (Fig. 2-18), then the maximum transport distance downice of source outcrops for the is 150 km.

An alternative explanation for the higher concentrations of shield clasts on the south side of the bay is the westward deflection of the Precambrian contact on the southern plateau (Fig. 2-18). However, this source is unlikely because it requires westward flow along the entire distal side of the southern moraine belt and erosion/entrainment of material by cold-based ice.

The western limit of continuous shield clast dispersal along the south side of the Bernier Bay trough can be used to gauge the rate of comminution of material by the ice stream. If the ice moving over the source outcrop was carrying only shield rocks, then shield clast content beneath the south side of the Bernier Bay Ice Stream, declined from 100% to less than 5% over a distance of 70 km after it crossed onto the carbonate terrain. This may mean that 95% of the granules were lost to comminution over this distance. However, shield granules in the basal ice could also have been lost to deposition and their concentration lowered due to dilution by newly eroded carbonate. The effects of comminution and dilution cannot be resolved and many granules could have been transported much farther before being comminuted to sand. Carbonate contents, discussed below, do not provide a clear indication of the dispersal and comminution of shield clasts because the carbonate bedrock contains variable amounts of siliceous impurities.

Low concentrations of shield clasts in tills from the central part of the trough could have been caused by more vigorous, i.e. erosive, flow along the centre of the ice stream which caused granules to be comminuted to sand over shorter distances, and/or increased dilution by locally eroded carbonates. The Bernier Bay Ice stream was clearly diverted around the carbonate upland on the south side of Berlinguet Inlet. Although it is on the south side of the inlet, this upland lies close to the axis of the main trough and was a significant obstacle to flow. The resulting diversion of ice would have had two effects. Firstly, it divided

the main flow of basal ice (and consequently its entrained debris) into two streams. Secondly, erosion of the obstacle would have diluted the concentration of shield clasts creating a tail of lowered shield clast concentrations downice, along the axis of the main trough to the west. Low concentrations of shield clasts in tills from the moraine crests are likely the result of enhanced erosion of carbonates as ice flowed upslope toward the moraines. It is also possible that this ice reworked preexisting calcareous sediment from the valleysides which was then incorporated in the moraines.

Carbonate Content of Granule Fraction

Because the amounts of different lithologies in the granule fraction are expressed as percentages, and because there are only two major source rocks, the abundance of carbonate clasts in till is, in large part, the inverse of the distribution of shield clast contents (Fig. 2-19). In most samples, the proportion of carbonate clasts is above 70%. East of the contact with gneiss and sandstone bedrock, carbonate drops abruptly reflecting no eastward dispersal of carbonates. In the south, parts of the sandstone terrain have elevated carbonate contents which reflect transport from Paleozoic limestone along the northern shore of Foxe Basin (Andrews and Sim, 1964).

Relative amounts of carbonate increase westward from the shield. Southwest of Bell Bay is an area of high carbonate contents downice of a prominent dolostone escarpment along the west side of Saputing Lake. This resistant upland of carbonate rock likely acted as a source of clasts as well as diverting ice carrying shield clasts around it. Generally, carbonate contents increase to over 90% within a 10 km downice (west) of the contact but the shift to high carbonate contents is less rapid in the areas where shield clasts were dispersed westward along Berlinguet Inlet by active ice.

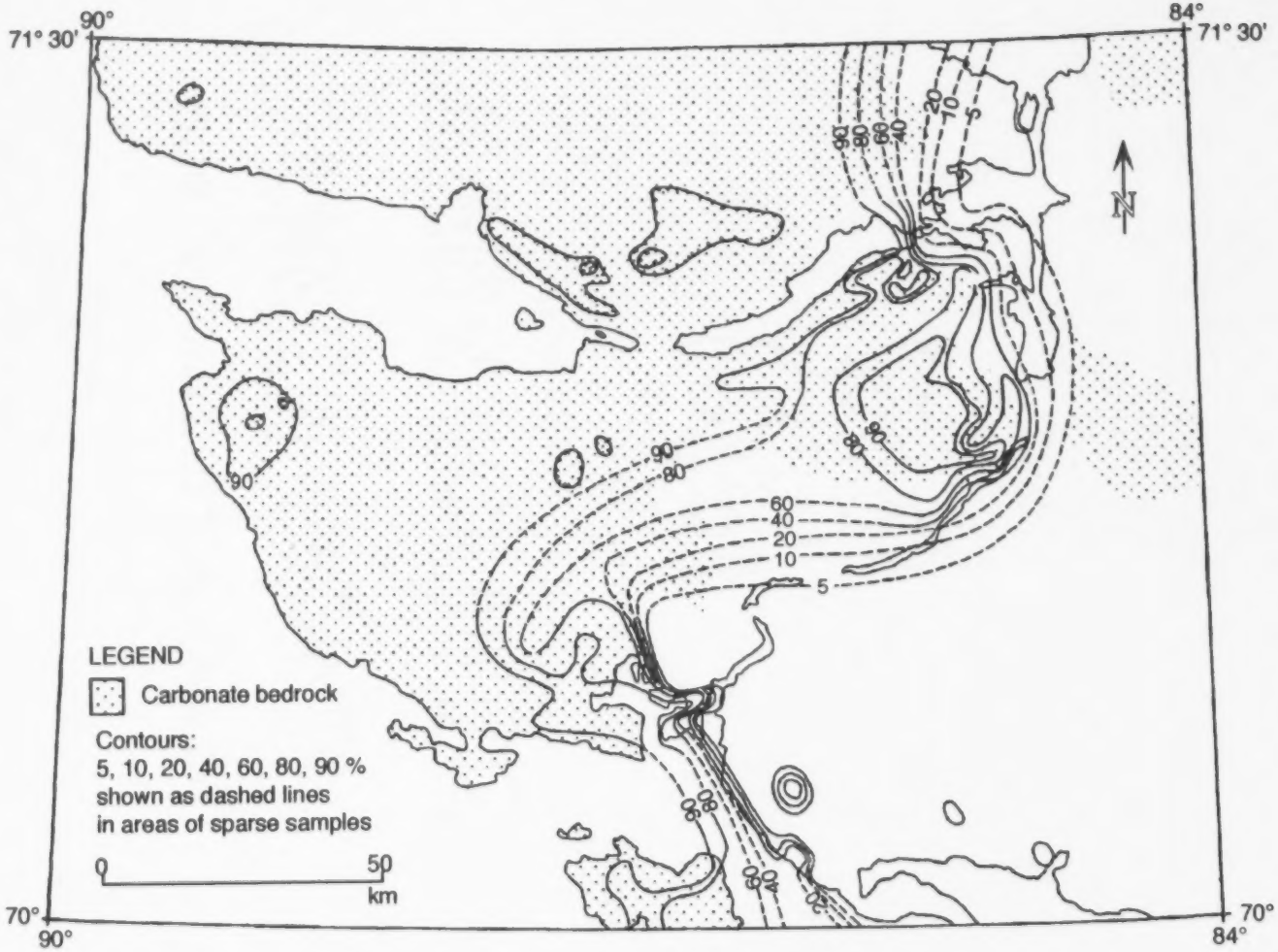

Figure 2-19. Distribution of carbonate clasts in the granule

Along the Bernier Bay/Berlinguet Inlet valley, carbonate contents are generally above 80%, except near the Precambrian contact at the east end of Berlinguet Inlet. However, samples collected from the tops of the moraines typically had slightly higher carbonate contents than samples from the valley floor (not apparent in Fig. 2-19 due to the coarse contour interval). Although crossing carbonate bedrock, ice flowing down the axis of the trough contained more shield clasts (Fig. 2-18). As the ice flowed toward the lateral moraines, it would have moved upslope entraining more carbonate rock. The trend is more pronounced in the distribution of matrix carbonate discussed below. Beyond the lateral moraines south of the trough, carbonate contents drop slightly. On the north side of Bernier Bay and Berlinguet Inlet, in the area formerly covered by the Brodeur Peninsula Ice Cap, carbonate contents are uniformly high indicating a lack of shield outcrops and Precambrian erratics left by older glaciations.

CARBONATE CONTENT OF MATRIX (CHITTICK ANALYSIS)

Carbonate content of the till matrix (silt and clay, Appendix B) reflects both the carbonate content of local bedrock and dilution or enrichment by transported silts and clays. Carbonate rocks are seldom free of insoluble siliceous impurities so the carbonate content always undermeasures the proportion of the matrix derived from carbonate rock (Dyke et al., 1992). The distribution of matrix carbonate in the tills is a result of till dispersal superimposed on "background" levels of non-carbonate matrix due to fine grained impurities in the local rock (Fig. 2-20).

Carbonate in the granule fraction increases more rapidly than matrix carbonate west of the contact with Precambrian rocks. This is expected if greater distances are required before transported material is comminuted to carbonaceous silt and clay. However, the same effect results if the tills contain insoluble fines from erosion of local carbonate rock. The latter explanation is supported by the fact that matrix carbonate content was lower than granule carbonate throughout the area.

Mean carbonate content of tills derived from sandstone bedrock in the southeastern part of the study area, lithic facies S, MSS and MS (>70% sandstone granules) was low, between 1.2% and 2.8%. Since the measured carbonate content of the source sandstones is less than 1% (Blackadar, 1970), these tills probably contain some transported carbonate. Likely source areas for this material are outcrops of Paleozoic rocks on the north side of Foxe Basin (Andrews and Sim, 1964).

Calcite/dolomite ratios vary from 7.21 to 0.001 with a mean of 0.77 (Fig. 2-21, Table 2-2). Because most of the tills are locally-derived, bedrock composition is the main control on the relative amounts of calcite and dolomite in the sample; extreme values reflect nearly pure limestone (high) or dolostone (low). Prevalence of dolostone over limestone in the study area accounts for the large number of samples with ratios less than 1.

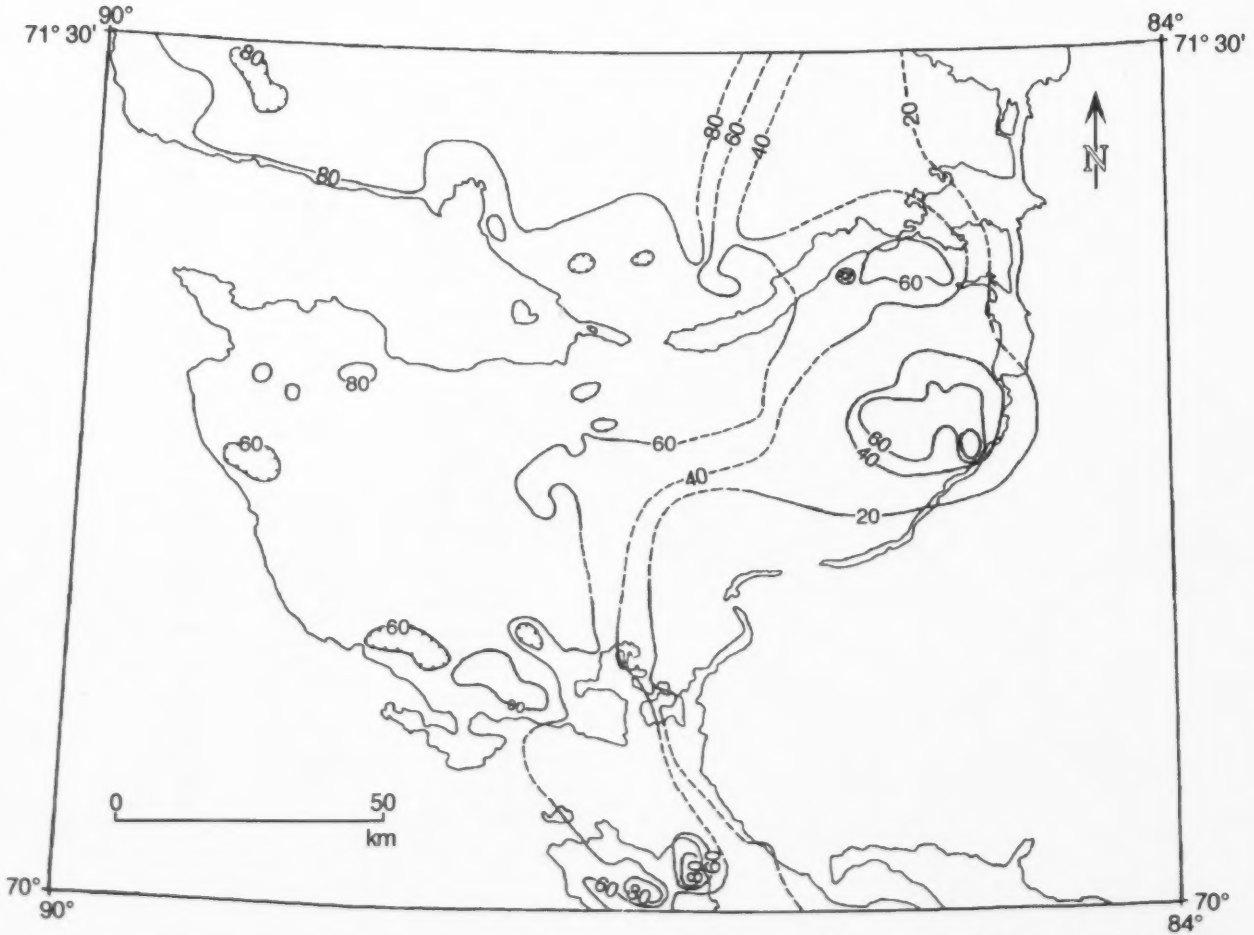

Figure 2-20. Distribution of carbonate (acid soluble) minerals (%) in the matrix fraction.

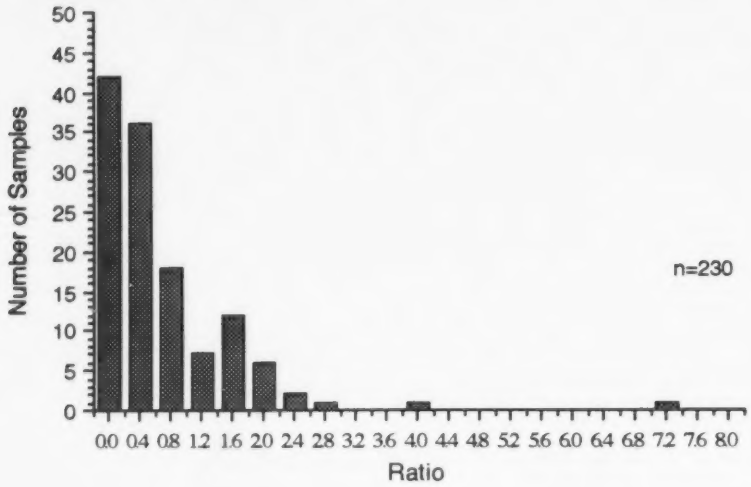

Figure 2-21. Calcite/dolomite ratios for tills.

As expected, the matrix carbonate content of tills derived from sandstone and gneiss (lithic facies S, MS, MSS and P) is much lower than that of tills derived from carbonate rocks (lithic facies C, MC, MCC; Fig. 2-22). An even stronger relationship is apparent in the granule fraction of the tills (Fig. 2-23) included for comparison. However, this is expected since the lithic facies classification is based on the percentages of different granules in the tills. Both graphs show the same general distribution but the matrix of tills derived from carbonate bedrock have lower and more variable matrix carbonate contents than suggested by the composition of the granule fraction. Thus, the lithic composition of the granule fraction is a better indicator of till dispersal than the carbonate content of the matrix because the local bedrock contains variable quantities of insoluble siliceous impurities. It is also possible that carbonate is crushed to granule size more rapidly than to matrix size.

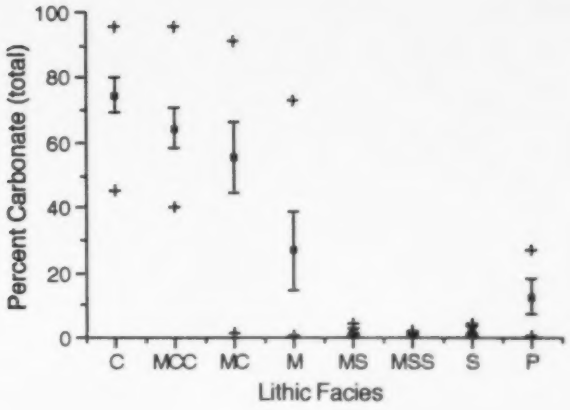

Figure 2-22. Percent carbonate content of till matrix. Solid bars are the standard deviation for each class. Crosses are maximum and minimum values.

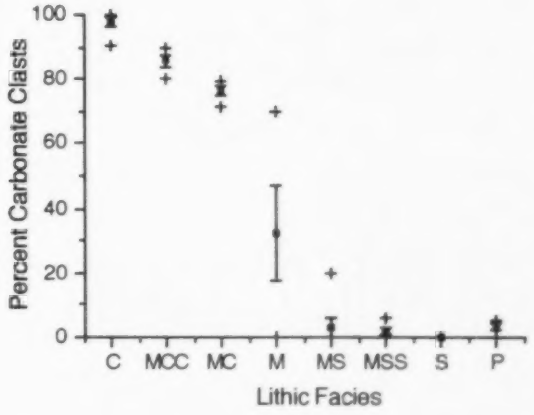

Figure 2-23. Percent carbonate clasts in till granule fractions. Solid bars are the standard deviation for each class. Crosses are maximum and minimum values.

The highest matrix carbonate contents (above 80%) occur on southern Brodeur Peninsula (Fig. 2-20), because of the exclusion of Laurentide ice from this area during the last glaciation by the Brodeur Peninsula Ice Cap. This is more likely the result of till dispersal than of variation in the amounts of bedrock impurities because rocks north and south of Bernier Bay are of similar composition (Trettin, 1964).

A pronounced eastward deflection of the contours marks an area of higher than normal carbonate concentrations around the head of Berlinguet Inlet (Fig. 2-20). Erosion and rapid comminution at the head of the Bernier Bay Ice Stream where it crossed onto carbonate terrain resulted in a more rapid westward increase in matrix carbonate than in adjoining areas. This is expected if the ice stream was warm-based and fast flowing. The area is also downice of the carbonate knoll discussed above which provided a source of erodable carbonate at the base of the ice stream.

A northward deflection of the 80% contour occurs on the north side of Bernier Bay (Fig. 2-20) and corresponds with the field of drumlins that record late glacial flow from the Brodeur Peninsula Ice Cap into Bernier Bay. On either side, matrix carbonate is high reflecting the dominance of the Brodeur Peninsula Ice Cap which lacked a source of shield material. The drumlins occupy a shallow valley which extends into the interior of Brodeur Peninsula. The valley previously was partly backfilled by Foxe ice of the Bernier Bay Ice Stream impinging on the north coast of Bernier Bay. Sediments deposited by Foxe ice were then reworked by the drumlin-forming flow after removal of buttressing ice in Bernier Bay. On Landsat imagery (Fig. 1-4) the drumlin field appears as a southward extension of light-toned tills crosscutting a fringe of dark-toned (better vegetated because of more shield-derived material) till along the north side of Bernier Bay.

Pockets of high carbonate concentrations in the till matrix occur near dolostone cliffs northwest of Bell Bay, west of Saputing Lake and at the east end of Crown Prince Frederick Island (Fig. 2-20). The cliffs acted as obstacles to flow and were sites of high local erosion.

SANDSTONE

The location of sandstone outcrops is the main control on the distribution of sandstone granules in tills (Fig. 2-24). The dispersal of sandstone is less distinct than shield clasts for two reasons. Firstly, the sandstone, usually brown, is less resistant and hence is comminuted to sand within a short distance. Secondly, chert and sandstone bands are common in carbonate bedrock. This accounts for widespread low levels of sandstone granules in till. North and south of Bernier Bay, sandstone is generally low, whereas west of the head of Bell Bay it increases to 48% (Fig. 2-24). Elevated sandstone contents occur west of the escarpment on the west side of the Saputing Lake valley and indicate the existence of an (unmapped) outcrop in this area. Sandstone contents are high throughout the area of sandstone bedrock in the southeast part of the study area and drop rapidly within a few kilometers of the source. Variability in the amount of sandstone granules in the Cape Appel and Autridge Bay areas is the result of fluctuating contents of shale and volcanic granules derived from a complex of local shale outcrops and gabbro sills. The drop in sandstone concentrations (from 20% to 80%) across the sandstone outcrop north of Autridge Bay is caused by increasing amounts of ice-rafted material below marine limit.

The sandstone content of tills on Crown Prince Frederick Island is highest on the eastern part of the island, reaching a maximum of 13% on one hilltop. The sample represents southwestward dispersal of sandstone from outcrops north of the head of Autridge Bay, a distance of about 30 km.

GRAIN SIZE

Due to the nature of the source material, tills derived from carbonate rock typically contain more silt and clay than tills derived from sandstone (Table 2-2, Figs. 2-25A, B and C, Appendix C). Carbonates are less resistant to comminution than sandstone, which is reduced to highly resistant quartz sand. High clay contents occurred in the four samples with more than 70% shield clasts in the granule fraction (lithic facies P, Table 2-2). These and a few other instances of localized high clay content in material collected below marine limit probably reflects marine deposition of clays after deglaciation.

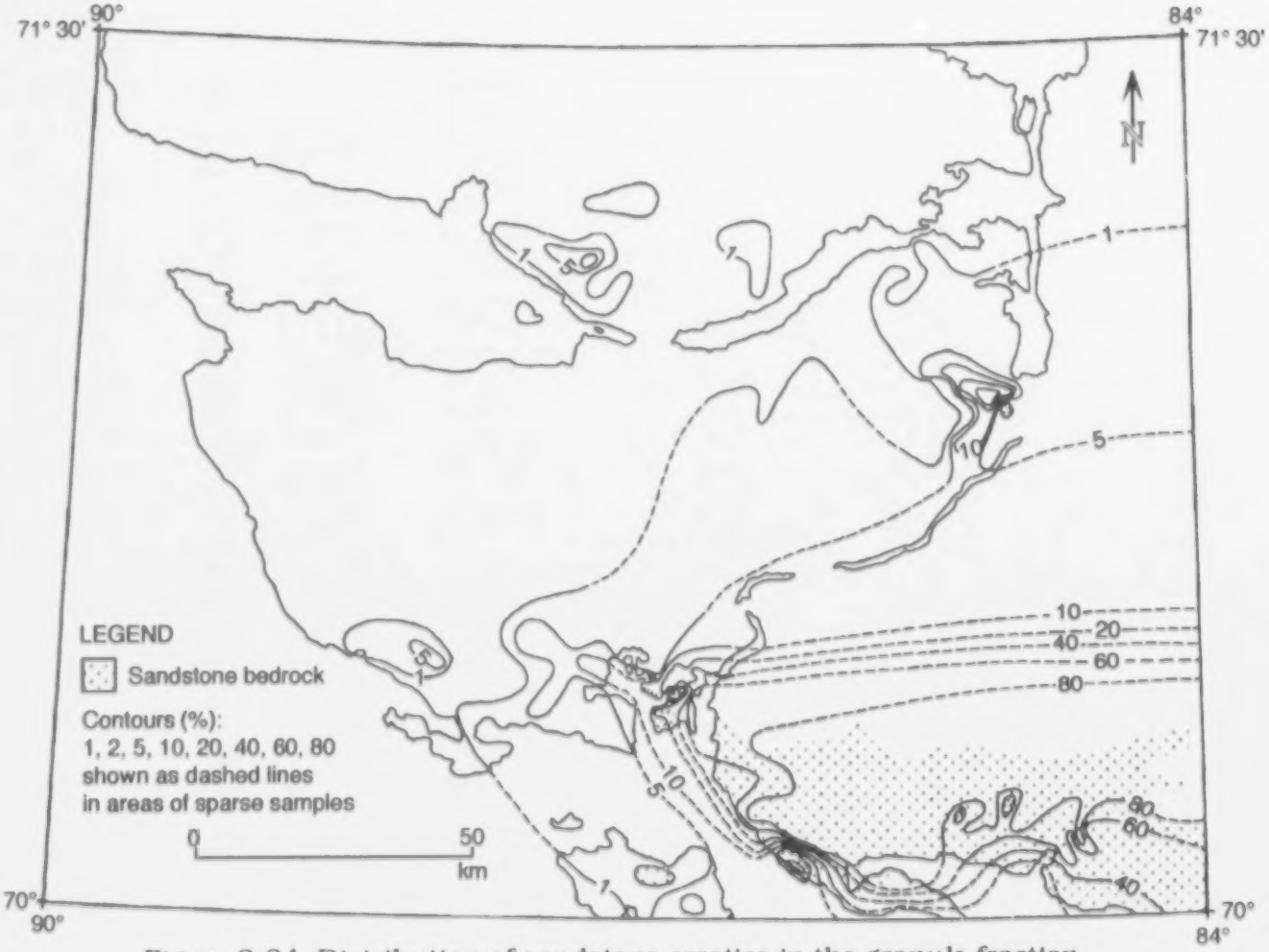

Figure 2-24. Distribution of sandstone erratics in the granule fraction.

Grain size data reinforce the local origin of the tills. Transport distances seem to have been short and had little effect on grain size distribution because new material was continually being eroded and comminuted. However, matrix carbonate analysis suggests that many of the tills contain some far-travelled material. The influence of this material on the grain size distributions appears to have been effectively masked by inputs of local sand and silt. Erratics in the granule fraction of tills (discussed above) provide the best estimate of the direction and distance of glacial transport.

The highest percentages of sand occur in sandstone facies, S, MS and MSS (>70% sandstone granules, Fig. 2-25A) which contain 82 to 85% sand whereas the matrix of the carbonate dominated facies contained 45 to 56% sand. Average values of sand are higher than those of silt, and average values of silt higher than those of clay, for all lithic facies.

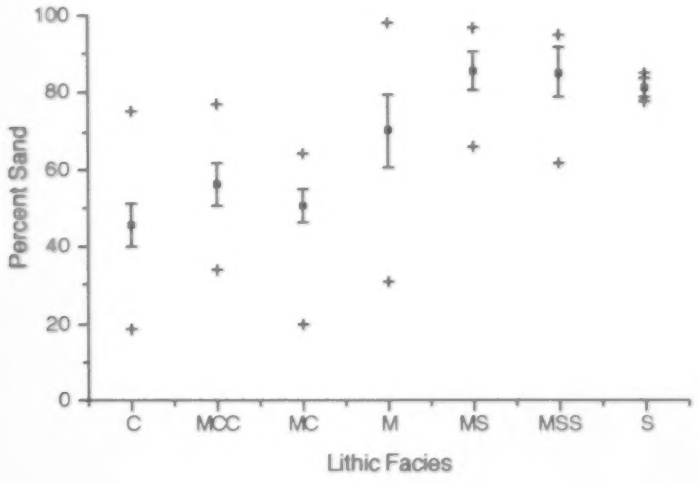

Figure 2-25A. Sand content of tills. The solid bar is the standard deviation for each class. Crosses indicate range of values.

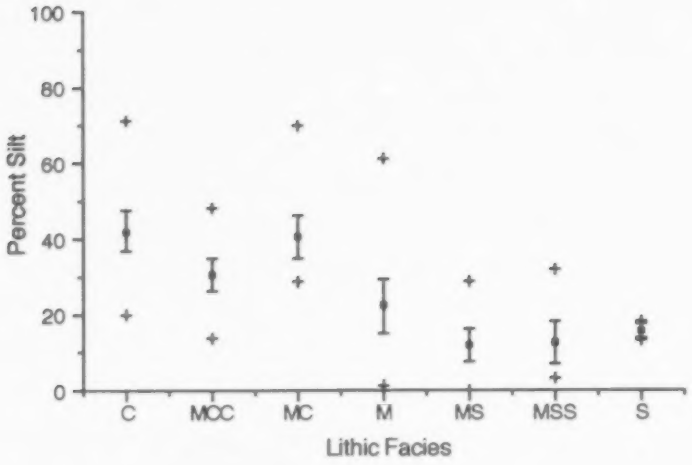

Figure 2-25B. Silt content of tills. The solid bar is the standard deviation for each class. Crosses indicate range of values.

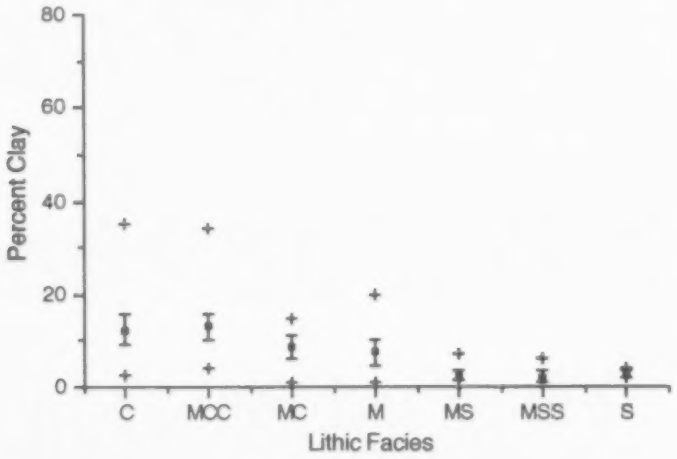

Figure 2-25C. Clay content of tills. The solid bar is the standard deviation for each class. Crosses indicate range of values.

Discussion

Glacial Events

During the LGM, the area was completely ice covered but the thickness, flow rate and basal thermal regime were not uniform. The Bernier Bay Ice Stream was a major topographically-controlled conduit connecting the Foxe Dome with an ice shelf in Prince Regent Inlet. The ice stream was buttressed by slower flowing, largely cold-based ice on the adjoining plateaux. Flow within the ice stream was sufficiently fast to maintain basal temperatures above pressure melting point, through frictional heating at the bed and strain heating in the overlying ice.

The elevation of the highest moraines and the bathymetry of Bernier Bay indicate that ice in the bay remained grounded during the period of moraine deposition. At the LGM, the profile of the tributary ice stream in Bernier Bay was controlled by surface profile of the ice in the Gulf of Boothia and Prince Regent Inlet. Assuming that the Bernier Bay ice was only slightly thicker then than during the Cockburn Substage, and considering the depth of the inlet, ice in Prince Regent Inlet had to be floating. This answers the question raised in Dyke and Prest (1987) as to whether Prince Regent Inlet was occupied by grounded ice or an ice shelf. The Bernier Bay Ice Stream was probably not a great deal thicker at the last glacial maximum because there is little evidence that it spread laterally to overwhelm ice on the adjoining plateaux and because local ice caps in the central Arctic, most notably the Brodeur Peninsula Ice Cap, were not the final vestiges of retreating ice but lasted for 10-20,000 years (Dyke, 1993).

The confluences of the ice stream with inert and thinner ice on the plateaux to the north and south is marked by interlobate moraines and tills of different composition. These confluences were zones of lateral shearing between the ice stream and slower flowing, plateau ice and were saddles on the ice surface, farthest from ice divides. Hence, early marine incursions along these zones were favoured by a thin ice cover.

To the north, the Brodeur Peninsula Ice Cap was cold-based in its accumulation area but had a warm-based marginal fringe (Dyke, 1993). The interior of Agu Peninsula, underwent little modification during the

last glaciation. However, there is abundant evidence, in the form of drumlins and scoured rock surfaces, for warm-based conditions along the southern and western margins of this plateau. Thus, Foxe ice cover on the southern plateau also had a warm-based marginal fringe and cold-based interior. Glacial modification within the cold-based zone was limited to the formation of numerous marginal channels and small moulins during retreat. Small moraines formed in a few valleys and isolated moulin kames suggest that, during retreat, only slight heating was capable of triggering a shift to warm-based conditions.

Following disintegration of the ice shelf in Prince Regent Inlet, about 9000 BP, the early Holocene sea entered the area along the shear zone between the Bernier Bay Ice Stream and plateau ice to the south, forming a moat. This marine incursion displaced thin plateau ice grounded below marine limit. By 8000 BP, the Bernier Bay lobe had retreated to the head of Bernier Bay and an arm of the sea occupied the area between Foxe and Brodeur ice (Fig. 2-14). Calving of buttressing ice in the bay initiated drawdown flow from the south flank of the Brodeur Peninsula Ice Cap into the bay forming a small field of drumlins and Rogen moraines on southern Brodeur Peninsula and depositing the large moraine to the west. The thickness of the Bernier Bay Lobe, particularly its extent above marine limit, allowed it to remain grounded while thinner ice grounded slightly below marine limit to the south, and later the north, calved.

The loops and embayments in the moraines attest to the dynamic nature of the Bernier Bay Lobe which continued to be well supplied by ice from the east during the Cockburn Substage. The buoyancy of the ice would have reduced basal yield stress, and increased the flow rate, for some distance behind the calving front, by lowering the effective weight of the ice on the bed. Deforming sediments at the bed may also have lowered basal shear stress. However, the floor of the trough appears to have been an area of net erosion and the present cover of unconsolidated sediment is thin. This does not exclude the possibility that ice initially rested on deformable sediments, probably pre-Foxe marine deposits of unknown age, which were subsequently eroded.

The period of moraine deposition in the study area is partly correlative with the deposition of the Cockburn Moraines on

northeastern Baffin Island. The multiple nested ridges of the Bernier Bay Moraines suggest the margin of Foxe ice underwent slight fluctuations during a period of overall stability between 9000 and 6500 BP. This included periods of stability, during the deposition of individual moraines, punctuated by periods of retreat and possibly slight readvances. Minor readvances that occurred during this interval are recorded by drumlinized till on the proximal side of the moraines. However, the number of nested ridges suggests that the depositional episode was primarily one of protracted retreat where a stable ice margin was reestablished in sequentially more restricted positions.

The position of the moraines in relation to marine limit is unusual. A more typical retreat sequence might include rapid retreat of marine-based portions of an ice sheet by calving, followed by the establishment of a stable tidewater margin along the coast, and ending with slow terrestrial retreat toward the centre of the former accumulation area, usually on an upland. In this case, an equilibrium condition occurred where the destabilizing influence of the sea was balanced by continuous resupply of ice from the Foxe Dome. This is the only explanation for the persistence of marine-based ice in Bernier Bay and implies very large throughputs of ice to the calving front west of the bay mouth. Deglaciation of Foxe Basin soon after 7000 BP (Dredge, 1990, 1991) probably contributed to the rapid retreat of the Bernier Bay lobe at that time by cutting off or greatly reducing the supply of ice from the east.

The regional correlation of the Bernier Bay Moraines and others of Cockburn age suggests a change in climate. Increased precipitation caused a period of positive mass balance on the Foxe Dome, despite the fact that the arctic climate was probably warmer than present. The apparent contradiction posed by ice sheet growth at a time of climatic warming, is explained by the earlier development of a vast expanse of open water to the west of the study area (Dyke and Morris, 1990) which acted as a moisture source to the atmosphere. These authors reported large number of bowhead whales occupying in the inter-island channels around Prince of Wales Island during the interval 11,000-8500 BP which proves there was seasonally open water in the central Arctic during Cockburn time (see discussion in Chapter 4). The deposition of the Bernier Bay Moraines at this time adds additional weight to the climatic

interpretation because more strongly positive mass balance conditions are required to stabilize the position of the ice margin in a marine setting.

Ice Dynamics and Drift Dispersal

During the last glaciation, the southern part of the field area was inundated by ice flowing westward from the Foxe Dome and, after 7000 BP, from the Early Barnes Ice Cap. This Laurentide ice was excluded from the southern part of Brodeur Peninsula by the Brodeur Peninsula Ice Cap. Westward flow took the form of a major ice stream in the Bernier Bay/Berlinguet Inlet valley. The ice stream fed into an extensive ice shelf in Prince Regent Inlet and the Gulf of Boothia.

The study area contains three recognizable zones of till dispersal, recorded by their granule lithologies. The Brodeur Peninsula Ice Cap had a radial flow pattern (Dyke and Prest, 1987; Dyke, 1993) and lacked a source of Precambrian material. Hence, at least for the last glaciation, dispersal of Precambrian erratics onto southern Brodeur Peninsula was very limited. This interpretation is supported by Landsat imagery which shows a clear tonal contrast between dark, Precambrian-rich tills along the Bernier Bay/Berlinguet Inlet trough and light-toned tills on the plateau to the north (Fig. 1-4). This marked tonal contrast is not as apparent south of the trough where Precambrian erratics were transported from source areas to the east (Fig. 2-18) probably during a pre-Foxe glaciation.

The second zone of dispersal is characterized by medium to low levels of Precambrian erratics in the Bernier Bay/Berlinguet Inlet valley and on the large unnamed plateau to the south. Within this zone, the quantities of Precambrian erratics decrease rapidly westward from the source areas. With some exceptions, the quantity of Precambrian erratics is higher in the valley, supporting the interpretation that it served as a conduit for an ice stream during the last glaciation. Flow within the ice stream was faster and erratics were more plentiful and dispersed farther west than on the uplands to the south. Flow over the plateau to the south was also westward, but was slower and less erosive than flow

within the valley. Since ice on these uplands was cold-based, erratics on this surface likely predate the last glaciation.

Ice rafted debris caused increased amounts of Precambrian clasts in a few samples collected below marine limit. In other instances, reworking of preexisting till may also have increased the observed contents of Precambrian erratics. This possibility is raised by the ubiquity of the erratics, although the pre-Late Wisconsinan history of the area is largely speculative.

The third zone comprises areas of sandstone- and Precambrian-rich tills in the Agu Bay area. Southwestward ice flow in this area resulted in Precambrian erratics being transported into the area of sandstone bedrock whereas both Precambrian and sandstone erratics were transported into the area of limestone bedrock. It is likely that the rapid evacuation of ice into the Gulf of Boothia and/or the arrival of a calving margin at the west end of Fury and Hecla Strait resulted in a shift from westward to southwestward flow, as a consequence of deglaciation of the Gulf of Boothia at about 9000 BP. Patterns of till dispersal observed did not contradict what was generally expected, i.e. in most cases it was westward, with little evidence of eastward dispersal. The presence of carbonate erratics around Whyte Inlet records drift dispersal nearly due west from source rocks on the north side of Foxe Basin, beyond the eastern margin of the study area.

Summary and Conclusions

Ice flow in the study area comprised three regimes during the last glaciation. The Brodeur Peninsula Ice Cap and Foxe ice on the southern plateau were separated by an ice stream in Bernier Bay. Warm-based conditions prevailed beneath the ice stream but the adjoining ice was warm-based only along its margins. Glacial landforms, with the exception of marginal channels, are absent in the areas formerly under cold-based ice, but common in areas of former warm-based ice cover. Surfaces formerly covered by cold-based ice are mantled by preexisting residuum and felsenmeer which was little-altered despite complete ice cover during the last glaciation. Spatial variations in basal thermal

regime were caused by differences in the flow rate of the overlying ice which controlled the amount of strain heating (Dyke, 1993).

Deglaciation of the area began about 9000 BP with the breakup of an extensive ice shelf in Prince Regent Inlet. Shortly thereafter, a stable margin developed along the Bernier Bay/Berlinguet Inlet valley which persisted during the Cockburn Substage when large moraines were deposited. This marginal position persisted despite incursions of shallow seas alongside the lobe where its margins were below marine limit and when the central part of the lobe was grounded well below sea level. The main moraine-building episode around Bernier Bay ended about 8000 BP, the end of the Cockburn Substage (Andrews and Ives, 1978), but ice remained at or near eastern parts of the moraine system until 6500 BP. Subsequently, ice in Berlinguet Inlet, Admiralty Inlet, and Bell Bay disintegrated by calving, with the marine channels in the area becoming ice-free by approximately 6000 BP.

The gradient of the southern moraine belt reveals that grounded ice occupied Bernier Bay during the Cockburn Substage, terminating at a calving front near the mouth of the bay. During the last glacial maximum, the ice stream in Bernier Bay was not a great deal thicker than during the Cockburn Substage. From the thickness of this tributary ice in Bernier Bay, it is suggested that an ice shelf, rather than grounded ice, occupied Prince Regent Inlet during the last glaciation. A likely location of the former grounding line of this ice shelf is marked by a large ridge of gravelly sand descending to modern sea level at Van Koenig Point.

Deglaciation by calving in interior valleys below marine limit proceeded rapidly thereafter and was followed by gradual eastward retreat of Foxe ice on interior uplands. The steady eastward retreat of Foxe ice and northward retreat of the Brodeur Peninsula Ice Cap was recorded by abundant ice marginal channels on uplands. Although the early Holocene climate was warmer than present, a period of marginal stability occurred during the moraine-building episode. This stability was caused by increased precipitation on the Foxe Dome that resulted from extensive open water to the west in the area formerly occupied by the McClintock Ice Divide.

References

Andrews, J.T. and Sim, V.W., 1964. Examination of carbonate content of drift in the area of Foxe Basin, N.W.T. *Geog. Bull.* 21:44-53.

Andrews, J.T. and Ives, J.D., 1978. "Cockburn" nomenclature and the Late Quaternary history of the eastern Canadian Arctic. *Arct. Alp. Res.* 10:617-633.

Blackadar, R.G., 1970. Precambrian geology, northwestern Baffin Island, District of Franklin. *Geol. Surv. Can. Bull.* 191. 89 p.

Blake, W., Jr., 1966. End moraines and deglaciation chronology in northern Canada with special reference to southern Baffin Island. *Geol. Surv. Can. Pap.* 66-26, 31 p.

Bryson, R.A., Wendland, W.M., Ives, J.D. and Andrews, J.T., 1969. Radiocarbon isochrones on the disintegration of the Laurentide Ice Sheet, *Arct. Alp. Res.* 1:1-14.

Canadian Hydrographic Service, 1976. Chart 7503, *Cape Crauford to Cornwallis Island*, Surveys and Mapping Branch, Energy, Mines and Resources Canada.

Craig, B.G., 1965. Notes on moraines and radiocarbon dates in northwest Baffin Island, Melville Peninsula and northeast District of Keewatin. *Geol. Surv. Can. Pap.* 65 20, 7 p.

Dredge, L.A., 1990. The Melville Moraine: sea-level change and respnse of the western margin of the Foxe Ice Dome, Melville Peninsula, Nothwest Territories. *Can. J. Earth. Sci.* 27: 1215-1224.

Dredge, L.A., 1991. Raised marine features, radiocarbon dates, and sea level changes, eastern Melville Peninsula, Arctic Canada. *Arctic* 44(1):63-73.

Dredge, L.A. and Cowan, W.R., 1989. Quaternary geology of the southwestern Canadian Shield. In R.J. Fulton (ed.) *Quaternary Geology of Canada and Greenland*, Geological Survey of Canada, Geology of Canada, no. 1 , Chapter 3 pp. 214-235. (also Geological Society of America, The Geology of North America, v. K-1)

Dyck, W., Fyles, J.G. and Blake, W., Jr., 1965. Geological Survey of Canada Radiocarbon Dates V. *Radiocarbon* 7:24-46.

Dyck, W., Lowdon, J.A., Fyles, J.G. and Blake, W., Jr., 1966. Geological Survey of Canada Radiocarbon Dates V. *Geol. Surv. Can. Pap.* 66-48, 32 p.

Dyke, A.S., 1974. *Deglacial Chronology and Uplift History: Northeastern Sector, Laurentide Ice Sheet.* Colorado University Institute of Arctic and Alpine Research, Occasional Paper No. 12, 113 p.

Dyke, A.S., 1983. Quaternary geology of Somerset Island, District of Franklin. *Geol. Surv. Can. Mem.* 404, 32 pp.

Dyke A.S., 1984. Quaternary geology of Boothia Peninsula and northern District of Keewatin, central Canadian Arctic. *Geol. Surv. Can. Mem.* 407, 27 p.

Dyke, A.S. 1993. Landscapes of cold-centred Late Wisconsinan ice caps, Arctic Canada. *Progress in Physical Geography* 17(2):223-247.

Dyke, A.S., Dredge, L.A. and Vincent, J-S., 1982. Configuration and dynamics of the Laurentide Ice Sheet during the Late Wisconsin Maximum. *Geographie physique et Quaternaire* 36:5-14.

Dyke, A.S. and Morris, T.F., 1990. Postglacial history of the bowhead whale and of driftwood penetration: implications for paleoclimate, central Canadian Arctic. *Geol. Surv. Can. Pap.* 89-24, 17 p.

Dyke, A.S. and Prest, V.K., 1987. Late Wisconsinan and Holocene history of the Laurentide Ice Sheet. *Geographie physique et Quaternaire* 41(2):237-263.

Dyke, A.S., Morris, T.F., Green, D.E.C. and England, J., 1992. Quaternary Geology of Prince of Wales Island, N.W.T. *Geol. Surv. Can. Mem.* 433, 142 p.

Falconer, G., Ives, J.D., Løken, O.H. and Andrews, J.T., 1965. Major end moraines in eastern and central Arctic Canada. *Can. Dept. Mines Tech. Surv., Geog. Bull.* 7:137-153.

Hooper, J.M., 1990. *Late Quaternary Glacial and Sea Level History of the Bernier Bay Area, Northwest Baffin Island, N.W.T.*, unpublished M.Sc. thesis, Memorial University of Newfoundland, 98 p.

Ives, J.D. and Andrews, J.T., 1963. Studies in the physical geography of north-central Baffin Island, N.W.T., *Geog. Bull.* 19:5-48.

McNeely, R. and Jorgensen, P.K., 1992. Geological Survey of Canada Radiocarbon Dates XXX. *Geol. Surv. Can. Pap.* 90-7, 84 p.

Miller, G.H. and Dyke, A.S., 1974. Proposed extent of Late Wisconsin Laurentide ice on Baffin Island. *Geology* 2:125-130.

Peltier, W.R., 1982. Dynamics of the ice age earth. *Advances in Geophysics* 24:1-146.

Peltier, W.R., 1984. The thickness of the continental lithosphere. *Journal of Geophysical Research* 89:11303-11306.

Quinlan, G., 1985. A numerical model of postglacial relative sea level change near Baffin Island. In: *Quaternary Environments: Eastern Canadian Arctic, Baffin Bay, and West Greenland*, J.T. Andrews (ed.), Allen and Unwin, London.

Sim, V.W., 1960. A preliminary account of late Wisconsin glaciation in Melville Peninsula, N.W.T. *Canadian Geographer* 17:21-34.

Sim, V.W., 1964. Terrain Analysis of west-central Baffin Island, N.W.T. *Geog. Bull.* 21:66-92.

Shaw, J., 1985. Subglacial and ice marginal environments. In G.M. Ashley, J. Shaw and N.C. Smith (eds.) Glacial Sedimentary Environments. *Soc. Econ., Paleontol., Mineral., Short Course*, 16:7-84.

Chapter 3: Holocene Sea Level History

Introduction

Ninety-four radiocarbon dates were obtained to measure the rate and amount of Holocene emergence in the study area. Of these dates, 28 were obtained on marine mollusc shells, 56 on bowhead whalebones, five on walrus tusks, four on driftwood, and one on a narwal tusk. The dates contribute to a regional database for the central Arctic currently being developed (e.g. Dredge, 1990, 1991; Dyke, 1979; Dyke et al., 1991) and are used to construct a series of 10 emergence curves and two partial curves for different parts of the coast. The emergence history provides an indirect record of the events during the last glaciation and is an important adjunct to the geomorphic evidence. However, the emergence history of an area cannot be used to reconstruct the glacial history because non-glacioisostatic tectonic movements may be occurring simultaneously. Accordingly, Dyke et al., (1991) cautioned that "paleoice-sheet reconstructions should proceed independently of the sea level reconstructions to avoid an automatic and potentially meaningless correlation."

Mathematical modelling has allowed prediction of sea level changes caused by rearrangement of ice and water loads on a viscoelastic earth (Clark et al., 1978). These authors divided the earth's oceans into six zones each of which has a characteristic emergence history. The study area has been undergoing continuous emergence since deglaciation. Hence, its history is typical of those from recently deglaciated areas (Zone I of Clark et al., 1978).

Previous Research

The pattern of isostatic recovery in Arctic Canada has long been a subject of interest because of its potential to yield information about the magnitude and location of former ice loads. The pattern of isostatic recovery also yields important geophysical information on the viscosity and behavior of the upper mantle (e.g. Cathles, 1975). Early isobase maps (Andrews, 1970a) and Walcott's (1970) smoothed free-air gravity

anomaly map generated further interest in elucidating the pattern of crustal recovery especially since free-air gravity anomalies can be measured over water bodies as well. On northwestern Baffin Island, the first radiocarbon dates from the study area were obtained in the early 1960s (Craig, 1965; Dyck et al., 1965, 1966). The area has since received little attention but the early Bernier Bay emergence curve based on these few scattered dates has long been used as a control point in geophysical models (Peltier, 1982, 1984; Quinlan, 1985). Continuing research in adjoining areas, summarized below, has emphasized the construction of emergence curves and the defining of the isobase surfaces.

An early emergence curve for was published for Steensby Inlet, on the north side of Foxe Basin (Ives, 1963). A shell date established the minimum age of the 88 m asl marine limit at 6725 ± 250 BP (I-406;Ives, 1963). The lower height of marine limit in this area, which is closer to the location of the Foxe Dome, is due to late deglaciation. On the east side of Foxe Basin, Andrews (1970b) published an equidistant shoreline diagram for the Flint Lake area based on surveys of raised shorelines. The highest marine limit in the area is at 107 m asl. Shorelines were assigned ages from an emergence curve based on twelve radiocarbon dates. Isobases on the 6700 BP shoreline extend northwest-southeast, parallel to the Isortoq Moraines, which delimit the margin of the late-glacial Barnes Ice Cap. Shorelines rise away from the Isortoq Moraines reflecting a centre of maximum uplift in Foxe Basin located north of Southampton Island and the measured rate of uplift declined exponentially from an immediate postglacial maximum (Andrews, 1970b).

Four emergence curves were drawn for the west coast of Melville Peninsula (Dredge, 1990). The oldest date from northern Melville Peninsula is 9110 ± 100 BP (GSC-4324) where marine limit reaches 235 m asl. The regional isobases likely parallel the west coast of the peninsula (north-south), because little differential emergence was detected along the west coast (Dredge, 1990). Hence, the crustal deformation appears to have been dominated by the Foxe Dome to the east. Two curves are available for eastern Melville Peninsula (Dredge, 1991) where marine limit is lower (between 100 - 144 m asl). Although the east side is closer to the former centre of loading, the lower emergence is due to later deglaciation.

Dredge (1990) also suggests that a halt in emergence occurred while the ice stood at the Melville Moraine. This apparent halt in emergence is based on four shell dates which define the upper part of the emergence curves. Since the molluscs could all have grown in some depth of water, they may all be older than expected from their elevations (i.e. plotting below and to the right of the emergence curve). This tendency of shells to date older than their associated shorelines is well illustrated by the scatter of dates in the lower part of the northern Melville Peninsula curves. Because the half-response time of glacioisostatic recovery is about 2000 years, (Dyke and Morris, 1990), it is unlikely that a short-lived cessation of ice retreat (at the Melville Moraine) would cause a simultaneous and complete halt in glacioisostatic recovery. If such rapid adjustments did occur, emergence of coasts in formerly glaciated areas would have ceased within a few hundred years following deglaciation. Only a temporary balance between the rate of uplift and the rate of eustatic sea level rise would cause a halt in emergence.

Dyke (1979) presents a set of four radiocarbon dated emergence curves and one partial curve for Somerset Island, northwest of the study area. The curves show an exponential decline in sea level following deglaciation at 9200 BP. The 9200 BP shoreline on Somerset Island is strongly tilted, rising from 80 m asl in the northeast to 160 m asl in the southwest. This tilting is a result of crustal loading dominated by the McClintock Ice Divide, a Late Wisconsinan Laurentide dispersal centre located southwest of Somerset Island over McClintock Channel (Fig. 1-1). Farther south, on northeastern Boothia Peninsula, the highest marine limit lies at 215 m asl and has an age of 9230 ± 130 BP (GSC-2720; Dyke, 1984).

Dyke et al. (1991) published 14 emergence curves for Prince of Wales Island and an updated set of isobase maps for the central Arctic. This emergence history, amongst the best documented in Canada, reveals both glacioisostatic and tectonic influences. Isobases on the 9300 BP shoreline form a conspicuous north-south trending ridge over Boothia Peninsula inconsistent with loading by the McClintock Ice Divide. This pattern of shoreline deformation indicates that the Boothia Arch (Kerr, 1980) was briefly reactivated following deglaciation, producing 60-120 m of relief on the 9300 BP shoreline (Dyke et al., 1991).

After 8500 BP, all of Prince of Wales Island rebounded as a single block, i.e. shorelines at the same elevation are the same age across the entire island. This glacioisostatically abnormal pattern is not adequately explained by the history of former ice loads on the island (Dyke and Morris, 1990; Dyke et al., 1991) and demonstrates that load changes produced by deglaciation can interact with regional geologic structures. Hence, the islands of the central Arctic acted as a mosaic of blocks which underwent varying degrees of tilting during isostatic rebound (Dyke et al., 1991). Tectonism may also have influenced the emergence of Lowther and Griffith Islands in Barrow Strait (Dyke, 1993) where raised shorelines dip southward, opposite to the tilt predicted by the former ice load configuration.

Given the geologic history and continuing seismicity of the central Arctic (Basham et al., 1977; Kerr, 1980), the considerable isostatic adjustment of the postglacial period probably interacted with the structural geology. However, because of the difficulty of separating the glacioisostatic and tectonic components of rebound, tectonic effects are hard to recognize unless they produce emergence patterns which are clearly inconsistent with the glacial history as reconstructed from geomorphic evidence (Dyke et al., 1991).

Methods

The major research objective was to obtain independently-controlled emergence curves for different coastal areas. Emergence curves from small geographical areas are preferable to those which combine dates from widely scattered localities since the latter incorporate differential emergence (tilt) in a single curve (Dyke et al., 1991). Over four field seasons (1988-91), considerable time was spent searching for samples of shells, whalebone and wood to date raised shorelines. When dates were scarce, the available dates were combined to construct a single curve. In a few cases, due to the difficulty of finding samples that could be reliably tied to known relative sea levels, only minimum curves could be drawn.

Raised beaches are the most common geomorphic evidence for falling sea levels (Fig. 3-1). These are best developed over broad coastal lowlands within the limestone terrain where large areas lie below marine

limit. Most of the whalebone and all the wood samples were found on raised beaches. Whale bones were often found in well-vegetated swales between widely spaced beaches or on boggy coastal plains. Most of the shells were collected from silt plains below marine limit deltas. In the Precambrian terrain, coastal lowlands are restricted to narrow plains adjacent to the modern shoreline; raised marine sediments and dateable materials are correspondingly scarce.

Elevations of all samples were measured using a Wallace and Tiernan surveying altimeter with 2 m graduations read to the nearest half metre. Appendix D discusses the range and sources of errors expected with this type of altimetry. Sample preparation is described in Appendix E.

Figure 3-1. Flights of raised beaches near Easter Cape.

Radiocarbon dating of whale and walrus bones was conducted at the Saskatchewan Research Council laboratory, Saskatoon. Shells and driftwood were dated by the GSC Radiocarbon Laboratory in Ottawa. Shell dates (uncorrected ages in Table 3-1) were normalized to -25‰ $\partial^{13}C$, the wood activity standard, then corrected to 0‰ $\partial^{13}C$, the PDB standard for marine carbonate. This results in a date about 400 years younger, partially correcting for the reservoir effect which causes marine shells to date 400 to 700 years too old (Mangerud and Gulliksen, 1975). The reservoir effect is due to the decay of ^{14}C in seawater over time and varies spatially, being greatest in areas of upwelling old water. Measurement of the reservoir effect by dating modern samples from different parts of the world is today hampered by the higher ^{14}C content of the atmosphere brought about by atmospheric atomic bomb testing in the 1950s and 1960s. Since measurement of the reservoir effect relies on dating shells, whose age is already known by other means, nothing is known about temporal changes in the reservoir effect which might be caused by changes in oceanic circulation. Finally, due the difficulty of finding suitable samples, the best available measurement of the reservoir effect in Arctic Canada is based on only three dates, all from Ellesmere Island (Mangerud and Gulliksen, 1975).

Corrected dates in Table 3-1, below, refer to shell and wood dates corrected for isotopic fractionation using the measured $\partial^{13}C$ value of the sample (if available). The fractionation correction usually adds a few decades to the age of the sample. No corrections for isotopic fractionation or reservoir effects were applied to whalebone dates because $\partial^{13}C$ values were only measured for a few samples.

The uncorrected radiocarbon ages were used for plotting emergence curves. For comparison purposes, an uncorrected whalebone date is likely about 250 years older than an equivalent (adjusted to the 0‰ $\partial^{13}C$ standard) shell date (Dyke, pers. comm., 1995). This is based on the measured $\partial^{13}C$ of whale bone which is typically about -15‰, and a 400 year reservoir correction (see Appendix F for a list of $\partial^{13}C$ values and corrected bone dates, where available). The 400 year reservoir correction for shells is the only available estimate for the reservoir effect in whale bones since there are no dated whale bones of known age collected before the period of bomb testing.

Bowhead Whalebone and Driftwood

The research technique relies on the assumption that driftwood and whalebones were stranded at, or close to, ancient high tide. Because of their size and low buoyancy, carcasses of the bowhead whale (*Balaena mysticetus*) probably stranded in shallow water, where they decomposed, and the skeletons were incorporated in the beach primarily by ice-push. Thus it was expected that radiocarbon dates on whalebone would seldom plot more than 2-3 m below the emergence curve, the keel-depth of a floating whale carcass. Sea ice could push the bones above the high tide line. The maximum positive elevation error resulting from ice-push would be similar to the maximum height of ice-pushed ridges on raised beaches today which are up to 2 m high along the most exposed parts of the coast (Fig. 3-2). Hence, most whale bone should have stranded within 2 m above and 3 m below the former high tide line.

Figure 3-2. Ice-pushed ridges on the north side of Bernier Bay.

Over most of the coast, however, ice-pushed ridges are less than 1 m high. Ice-push is the dominant beach forming process in the area. Sandy beaches are rare and coarse beach gravel is largely immune to displacement by small waves. Small, level beach berms, produced by wave action, were observed to form by late summer in a few localities.

Most of the whalebone finds were large cranial bases, the thick plate of bone that forms the back of the skull (Fig. 3-3). No articulated skeletons were found, most were scattered along tens of metres of beach and many of the finds consisted of isolated cranial bases. Fortunately, the cranial bases frequently contained the earbones, the best part of the entire skeleton for dating (Barr, 1971). These bones, the otic capsule and periotic bones, are extremely dense and hence resist infiltration by dirt and penetration by plant rootlets. Most cranial bases (skulls) were found in association with a few other bones such as ribs or vertebrae (Fig. 3-4). Others were found in isolation. Skeletons which appeared complete, although disarticulated and partly buried, are less common. Several of the whale bone dates discussed below are older than suggested by their elevations, indicating that the carcasses sank offshore. These dates provide reliable ages for the bones but are not particularly useful for constructing emergence curves as they provide only maximum ages for their associated shorelines.

Driftwood is the best material for dating raised shorelines because it reliably strands very close to sea level, and is easier to sample and clean than whalebone. However, due to erosion, the most common problem is redeposition of wood from higher elevations. Furthermore, because of the shortage of wood in the Arctic, some driftwood pieces may have been moved by humans (Dyke et al., 1991). Small pieces may be moved by wind. Driftwood is extremely scarce in the study area, much scarcer than in areas to the north and west; only four pieces were found despite considerable searching.

Usually, the internal consistency of a set of radiocarbon dates is such that those which are older than expected are easily recognized. For example, where whalebone dates plot below well-controlled emergence curves, it is possible to estimate the depth of water in which the carcass sank.

Figure 3-3. Collecting bone fragments from bowhead skull. Note the oasis of vegetation around the skull.

Figure 3-4. Scatter of whalebone on raised beach. The very long bone in the foreground is the right-hand side of the mandible. Part of the skull base protrudes from the beach just behind the mandible.

Shell Samples

Dates on marine molluscs can be much older than suggested by site elevations if deepwater communities were sampled. For instance, *Mya truncata* can grow in water depths of up to 100 m (Andrews, 1986). Surface shell collections are also prone to contamination and downslope displacement. Hence, shells found in growth position are preferable to surface samples, particularly where they can be related to a former sea level marked by the topset beds of raised deltas. Surface collections were dated only where shells enclosed in sediment could not be found (15 of the 27 dated shell samples were surface collections).

In this study, the oldest limiting dates on marine limit, and hence deglaciation, were obtained on shells (cf. Chapter 2). Penetration of bowhead whales into the marine channels bordering the field area did not occur until several thousand years after deglaciation (cf. Chapter 4). This differs markedly from other parts of the central Arctic where whales lived in close proximity to the retreating ice margin (Dyke and Morris, 1990).

Emergence Curves

The emergence curves were drawn subjectively but conservatively. The reliability of the curves depends on the number of accordant dates constraining a particular curve segment. Accordant dates are defined as groups of three or more dates which plot along an internally self-consistent curve. The amount of emergence accomplished by a given time should be considered a minimum when the curve is not constrained by at least three accordant dates or by dates on surface shell collections. Such curves, or portions thereof, are termed minimum curves below, and shown as dashed lines or envelopes. Statistical routines were not used to fit curves to the radiocarbon dates (cf. Dyke et al., 1991) because it is more likely that points will plot below, rather than above, the curve (i.e. errors are not randomly distributed). Hence, curves plotted with regression techniques overemphasize the importance of dates which fall below the curve, plot dates in unlikely positions above the curve and intersect the elevation axis several metres above modern sea level. The fit

of such a curve could be improved by leaving out obviously erroneous points but this reintroduces a subjective element in curve plotting.

Deglaciation and Marine Limit

The first seven radiocarbon dates from the study area (Table 3-1) were reported in Craig (1965), Dyck et al., (1965) and Dyck et al., (1966). All but two of these dates were on surface shell collections which provide minimum ages for deglaciation and marine limit. The dates also suggested that the Bernier Bay moraines were correlatives of the Cockburn moraines of northeastern Baffin Island. The new dates from the area (see below) corroborate the accuracy of the original dates. For example, Craig's date of 8830 ± 170BP (GSC-183) remains the oldest available date for deglaciation of the area south of Bernier Bay.

Marine limit constitutes the upper points on emergence curves, and ranges between 92 and 138 m asl in the field area. It is marked in places by raised deltas, washing limits and the lower limit of ice-marginal meltwater channels. Where ice retreat occurred in contact with the sea, marine limits become progressively younger in age and lower in elevation to the east. Restrained (i.e. deglacial) rebound in response to thinning of the ice sheet prior to deglaciation accounts for lower marine limits in areas closer to the centre of loading.

Minimum ages for deglaciation and establishment of marine limit are provided by sixteen radiocarbon dates on shells (Table 2-2). Deglaciation of the area, discussed in Chapter 2, was mapped from ice-contact landforms and marine sediments containing the oldest dated shells (Fig. 2-14). Unequivocal measurements of marine limit were obtained on ice contact deltas, the largest of which is 6 km^2 in extent, where meltwater streams deposited abundant sediment into the late glacial sea (Fig. 3-5).

Beaches and washing limits are rare at elevations approaching marine limit due to rapid initial emergence, which limited the time available for their formation. Also, relatively long exposure to periglacial processes and subaerial weathering have degraded shorelines at higher elevations. Thus, the upper limit of raised beaches is often tens of metres below the marine limit.

Figure 3-5. Large ice-contact delta north of Bernier Bay (see Fig. 2-15 for a vertical air photo of this feature).

Table 3-1. Radiocarbon dates on marine limit and raised shorelines. Bone elements listed under Material/Taxa are those of the bowhead whale (*Balaena mysticetus*). See Fig. 3-6 for locations.

MORIN POINT:

Lab Number	Material/ Taxa	Enclosing Material	Latitude Longitude	Elevation	Related Sea Level	C14 Age (corrected)
GSC-4742†	*M.truncata* *H. arctica*	marine silt*	71°26' N 89°07' W	118 m	~118 m	8600±90
GSC-4695†	*M. truncata*	marine silt*	71°18' N 88°28' W	92 m	~106 m	8210±110 (8240±110)
GSC-4754†	*H. arctica*	marine silt*	71°23' N 89°18' W	95 m	>95 m, ≤118 m	8120±110 (8140±80)
GSC-4777	*M. truncata*	marine silt	71°19' N 88°50' W	15 m	~50 m	6580±80 (6600±80)
S-3042	earbone	raised beach	71°28' N 89°52' W	33 m	≥33 m	5600±90
S-3100	earbone	raised beach	71°23' N 89°42' W	30 m	≥30 m	5220±80
S-3074	earbone	raised beach	71°22' N 89°41' W	24 m	≥24 m	4350±70
S-3043	earbone	raised beach	71°21' N 89°52' W	21 m	≥21 m	3950±70
S-3041	vertebra	raised beach	71°19' N 89°31' W	5 m	≥5 m	2175±130

VAN KOENIG POINT:

GSC-4703†	*M. truncata*	marine silt*	70°53' N 88°54' W	91 m	>91 m	8290±100 (8310±100)
S-3093	walrus skull	raised beach	70°58' N 89°07' W	38 m	≥38 m	6200±80
S-3098	earbone	raised beach	71°03' N 89°22' W	27 m	≥27 m	5520±70
S-3095	walrus tusk	raised beach	70°44' N 89°06' W	30 m	≥30 m	4810±90
S-3045	earbone	raised beach	70°58' N 89°07' W	28 m	≥28 m	4500±80
S-3094	walrus tusk	raised beach	71°03' N 89°22' W	26 m	≥26 m	4440±70
S-3101	walrus tusk	raised beach	71°03' N 89°02' W	23 m	≥23 m	4320±90
GSC-4776	*H. arctica*	muddy gravel	70°57' N 89°02' W	24 m	~ 25 m	4310±70 (4330±70)
S-3096	earbone	raised beach	70°55' N 89°03' W	23 m	≥23 m	4250±70
TO-5017	*Monodon monocerus*	raised beach	71°02' N 89°24' W	20 m	≥20 m	2880±60
S-3044	earbone	raised beach	71°01' N 89°20' W	11 m	≥11 m	2570±60
S-3099	earbone	raised beach	71°02' N 89°22' W	4 m	≥4 m	1110±60
GSC-239‡	wood (*Picea*)	partly embedded	70°55;N 89°11;W	3 m	≥3 m	940±130

Table 3-1 (cont.)

Sample Number	Material /*Taxa*	Enclosing Material	Latitude Longitude	Elevation	Related Sea Level	C14 Age (corrected)
BERNIER BAY NORTHEAST:						
GSC-189‡	shells	till*	71°07' N 87°24' W	101 m	≥ 101 m	> 30,580
GSC-5090†	*M. truncata* *H. arctica*	marine silt*	71°08' N 87°05' W	93 m	≤111 m	7880±120 (7910±180)
GSC-5091†	*M. truncata* *H. arctica*	stony silt*	71°12' N 87°29' W	81 m	>81 m, ≤110 m	7620±110 (7640±110)
I-1254‡	shells	surface	71°17' N 87°43' W	87 m	≥87 m	7576±500
S-3359	earbone	raised beach	71°03' N 87°17' W	47 m	≥47 m	6150±90
S-3360	earbone	raised beach	71°03' N 87°17' W	37 m	≥37 m	5200±90
S-3358	earbone	raised beach	71°08' N 87°37' W	30 m	≥30 m	4860±80
S-3355	earbone	raised beach	71°09' N 87°42' W	28 m	≥28 m	4530±80
S-3353	earbone	raised beach	71°07' N 87°40' W	19 m	≥19 m	3880±80
S-3357	earbone	raised beach	71°07' N 87°36' W	19 m	≥19 m	3780±80
S-3354	earbone	raised beach	71°09' N 87°45' W	21 m	≥21 m	3740±80
S-3356	earbone	raised beach	71°07' N 87°36' W	17 m	≥17 m	3330±100
S-3352	earbone	raised beach	71°02' N 87°17' W	9 m	≥9 m	2290±70
BERNIER BAY SOUTHEAST:						
GSC-183†‡	*H. arctica* *M. truncata*	marine silt*	70°53' N 88°06' W	119 m	~125 m	8830±170
GSC-4721†	*M. truncata*	glacioma-rine silt*	70°52' N 88°12' W	114 m	~ 125 m	8440±100 (8470±110)
GSC-4775	*H. arctica*	marine silty clay	70°55' N 87°23' W	63 m	~ 64 m	7130±90
S-3013	earbone	raised beach	70°56' N 87°42' W	49 m	≥49 m	6585±105
S-3014	earbone	raised beach	70°56' N 87°47' W	37 m	≥37 m	5670±100
S-3040	earbone	raised beach	70°56' N 87°56' W	28 m	≥28 m	5050±165
S-3015	earbone	raised beach	70°56' N 87°45' W	20 m	≥20 m	4115±85
S-3097	skull fragments	raised beach	70°57' N 87°19' W	22 m	≥22 m	4010±70
S-3075	skull fragments	raised beach	70°56' N 87°14' W	22 m	≥22 m	3930±80
S-3016	earbone	raised beach	70°56' N 87°30' W	7 m	≥7 m	2220±75

Table 3-1 (cont.)

Lab Number	Material /*Taxa*	Enclosing Material	Latitude Longitude	Elevation	Related Sea Level	Age (yrs BP) (corrected)
BERLINGUET RIVER:						
GSC-5089†	*M. truncata* *H. arctica*	pebbly silt*	71°10' N 86°25' W	64 m	~111 m	6840±100 (6860±100)
GSC-5088†	*M. truncata* *H. arctica*	marine silt *	71°11' N 86°25' W	69 m	≥69 m	6820±140 (6840±140)
S-3349	earbone	raised beach	71°02' N 86°41' W	21 m	≥21 m	4090±80
S-3351	earbone	raised beach	71°01' N 86°46' W	23 m	≥23 m	4010±80
S-3350	earbone	raised beach	71°04' N 86°20' W	21 m	≥21 m	3700±80
S-3347	earbone	raised beach	71°05' N 86°14' W	19 m	≥19 m	3340±80
S-3348	earbone	raised beach	71°03' N 86°21' W	18 m	≥18 m	3280±80
BERLINGUET INLET WEST						
GSC-304†‡	*H. arctica*	sand terrace*	70°55' N 86°27' W	89 m	>89, ≤139 m	7240±150
GSC-4894†	*H. arctica*	deltaic sand*	70°54' N 86°27' W	74 m	>76, ≤130 m	7240±100 (7260±100)
S-3128	earbone	raised beach	70°57' N 86°39' W	30 m	≥30 m	5080±80
S-3134	earbone	raised beach	70°58' N 86°41' W	20 m	≥20 m	3940±90
S-3263	earbone	raised beach	70°58' N 86°41' W	20 m	≥20 m	3250±80
S-3262	earbone	raised beach	70°58' N 86°40' W	15 m	≥15 m	2700±90
S-3261	earbone	raised beach	70°59' N 86°26' W	16 m	≥16 m	2650±80
BERLINGUET INLET EAST:						
S-3125	earbone	raised beach	71°07' N 85°37' W	33 m	≥33 m	4520±100
S-3124	earbone	raised beach	71°08' N 85°40' W	27 m	≥27 m	4300±110
S-3181	earbone	raised beach	71°08' N 85°40' W	19 m	≥19 m	4220±80
S-3183	earbone	raised beach	71°07' N 85°51' W	16 m	≥16 m	3990±80
S-3182	earbone	raised beach	71°08' N 85°40' W	21 m	≥21 m	3870±80
S-3258	earbone	raised beach	71°08' N 85°44' W	18 m	≥18 m	3320±80
S-3259	earbone	raised beach	71°08' N 85°40' W	17 m	≥17 m	2800±70
S-3260	earbone	raised beach	71°07' N 85°51' W	12 m	≥12 m	2310±80

Table 3-1 (cont.)

Lab Number	Material /*Taxa*	Enclosing material	Latitude Longitude	Elevation	Related Sea Level	C14 Age (corrected)
BELL BAY:						
GSC-4897†	*M. truncata*	deltaic sand	70°45' N 85°18' W	70 m	≤92 m	6770±90 (6780±90)
S-3180	earbone	raised beach	70°57' N 85°05' W	44 m	≥44 m	6070±90
S-3098	earbone	raised beach	70°57' N 85°00' W	31 m	≥31 m	4930±80
S-3176	earbone	raised beach	70°55' N 85°01' W	28 m	≥28 m	4500±100
S-3179	earbone	raised beach	70°56' N 85°00' W	21 m	≥21 m	3790±80
S-3256	earbone	raised beach	70°53' N 84°54' W	23 m	≥23 m	3230±80
S-3257	earbone	raised beach	70°53' N 84°54' W	23 m	≥23 m	3190±90
S-3177	earbone	raised beach	70°56' N 84°58' W	9 m	≥9 m	2060±100
FOSS FIORD/KIMAKTO PENINSULA:						
GSC-4898†	*M. truncata*	gravel*	70°33' N 88°00' W	65 m	>65 m, ≤130 m	8910±120 (8950±120)
GSC-5086†	*M. truncata* *H. arctica*	stony silt*	70°29' N 87°11' W	138 m	~138 m	8520±100 (8540±100)
S-3345	earbone	raised beach	70°24' N 87°15' W	38 m	≥38 m	5110±90
GSC-5077	wood (*Picea*)	raised beach	70°22' N 87°42' W	37 m	≥37 m	4660±80 (4680±80)
S-3346	earbone	raised beach	70°25' N 87°10' W	31 m	≥31 m	4610±60
GSC-5076	wood (*Picea*)	raised beach	70°22' N 87°16' W	3 m	≥3 m	1140±80 (1140±80)
NYBØE FIORD:						
GSC-306†‡	*H. arctica*	frost boil	70°20' N 86°48' W	97 m	>97 m, ≤138 m	7690±140
GSC-5327†	*H. arctica* *M. truncata*	stony silt*	70°20' N 86°48' W	96 m	>96 m, ≤138 m	7670±130
GSC-307‡	*H. arctica*	delta terrace*	70°36' N 86°08' W	97 m	≥97 m, <138 m	7120±140
GSC-5373	*M. truncata* *M.calcaria*	marine mud	70°25' N 86°52' W	8 m	≥8 m	3150±90 (3200±90)

Table 3-1 (cont.)

CROWN PRINCE FREDERICK ISLAND:

S-3433	earbone	raised beach	70°04' N 86°40' W	72 m	≥72 m	6350±130
GSC-5295	wood (*Picea*)	raised beach	70°02' N 86°37' W	68 m	≥68 m	5870±70
S-3432	earbone	raised beach	70°05' N 86°43' W	50 m	>50 m	5700±120
S-3431	earbone	raised beach	70°00' N 86°40' W	50 m	≥50 m	5310±120
S-3434	earbone	raised beach	70°00' N 86°40' W	47 m	≥47 m	5120±120
TO-5016	walrus tusk	raised beach	70°02' N 86°35' W	41 m	≥41	4940±70
GSC-5294	wood (*Picea*)	raised beach	70°04' N 86°46' W	35 m	≥35 m	4210±70

AUTRIDGE BAY/WHYTE INLET:

Lab Number	Material/ Taxa	Enclosing Material	Latitude Longitude	Elevation	Related Sea Level	Age (yrs BP)
GSC-5331†	*M. truncata*	deltaic sand	70°07' N 85°15' W	58 m	>58 m	6300±100 (6350±100)
GSC-5372†	*M. truncata*	deltaic sand	70°11' N 84°41' W	71 m	>71 m, ≤114 m	6260±80 (6310±80)
GSC-5087	*H. arctica*	silty clay*	70°07' N 86°07' W	66 m	≥66 m	5900±100 (5930±100)
GSC-5395	*M. truncata* *H. arctica*	deltaic sand	70°08' N 85°16' W	65 m	≥65 m	5810±100 (5850±100)
GSC-5345	*M. truncata* *H. arctica*	marine silt*	70°07' N 85°12' W	45 m	≥45 m	5530±100 (5560±100)
GSC-5311	*M. truncata* *H. arctica*	deltaic sand	70°07' N 84°46' W	11 m	≥11 m	3790±90 (3830±90)
GSC-5374	*M. truncata* *H. arctica*	sandy mud	70°07' N 84°47' W	24 m	≥24 m	3790±90 (3820±90)
GSC-5364	*M. truncata*	deltaic sand	70°07' N 85°17' W	16 m	≥16 m	3360±60 (3390±60)
GSC-5316	*M. truncata* *Portlandia*	deltaic sand	70°07' N 84°48' W	4 m	≥4 m	2420±100 (2460±100)

*Surface shell collections

†Marine limit dates

‡Dates by B.G. Craig (1965)

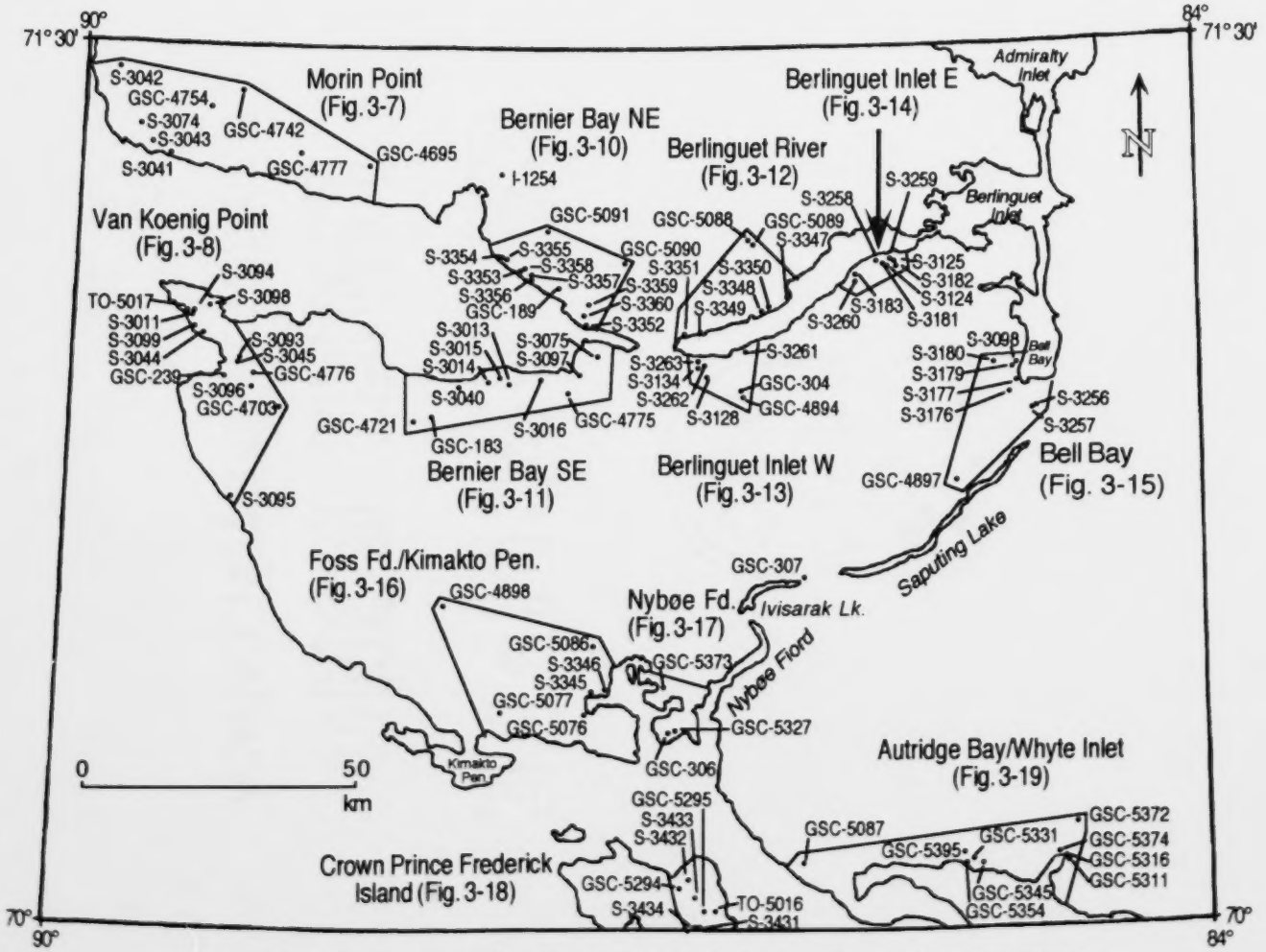

Figure 3-6. Locations of radiocarbon dated samples and curve areas.

Emergence Curves

Radiocarbon dates pertaining to raised shorelines have been grouped into curve areas (Fig. 3-6, Table 3-1). All the dates on whale bones, skull fragments and earbones are on bones of the bowhead whale, *Balaena mysticetus*. The dates on walrus, *Odebenus rosmarus*, are on walrus tusks and bones. Ten emergence curves (Figs. 3-7, 3-8, 3-10, 3-11, 3-12, 3-13, 3-14, 3-15, 3-18 and 3-19) and two partial curves (Figs. 3-16 and 3-17) were drawn using uncorrected bone and wood dates; shell dates incorporate a correction for reservoir effects but not isotopic fractionation. Solid lines on these curves indicate well-controlled curves or curve segments. Dashed lines indicate minimum curves or poorly controlled curve segments. Letters beside points denote the material dated: (B) whalebone, (S) shells, (Wa) walrus and (W) driftwood.

Morin Point

The Morin Point emergence curve (Fig. 3-7) is based on four shell dates and four whalebone dates. The oldest shell date (8600 ± 90 BP, GSC-4742) is on a mixed sample of *Mya truncata* and *Hiatella arctica* containing numerous whole valves collected from the surface of marine silts at 118 m asl. This was the highest occurrence of shells in the vicinity and is at nearly the same elevation as the observed upper limit of silt near the sample site, estimated at 120 m asl. In the absence of other geomorphic indicators, these two elevation measurements constitute the best available estimate of marine limit along the outer coast.

A date of 8210 ± 110 BP was obtained on a collection of *Mya truncata* fragments (GSC-4695) from the surface of deflating silt (92 m asl) adjacent to an ice-contact delta at 110 m asl. The date provides a minimum age for marine limit and deglaciation of the eastern Morin Point area. The delta is associated with a large moraine marking the position of the Brodeur Peninsula Ice Cap at the culmination of a readvance around 8210 BP. Hence, during deglaciation of Morin Point, sea level fell by at least 10 m between 8600 and 8210 BP.

A slightly younger sample of *Hiatella arctica* shells (8120 ± 110, GSC-4754) was collected at 95 m asl and plots on the curve indicating

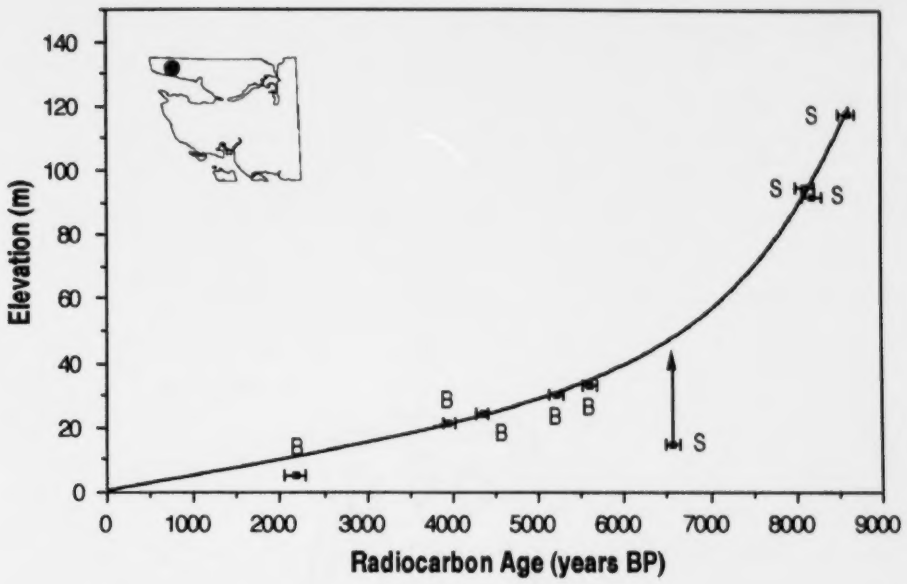

Figure 3-7. Emergence curve for Morin Point. Letters denote whale bones (B), walrus tusks and bones (Wa), narwal tusks (N) and shells (S).

the shells grew in shallow water. Paired valves (*Mya truncata*, GSC-4777) were excavated from laminar sands at 15 m asl but yielded an age of 6580 ± 80 BP, about 3500 years older than expected for their elevation. Interpolating from the curve, it is estimated that shells grew in about 40 m of water. This maximum age for the 15 m shoreline proves the laminar sands are deepwater (i.e. from suspension), as opposed to littoral, sediments.

Four accordant dates on bowhead earbones constrain the middle part of the curve. The first was collected from a skull at 33 m asl which dated 5600 ± 90 BP (S-3042), plotting on or slightly below, the curve. This could be due to the skull sinking in shallow water, or to slight differential emergence as the sample is the furthest west of the Morin Point dates. The second was collected from a skull found in barren beach gravel at 30 m asl and dated 5220 ± 80 BP (S-3100). The third dated 4350 ± 70 BP (S-3074) and was embedded in a beach at 24 m asl. The fourth earbone was collected from a skull partly embedded in a boggy, well vegetated beach at 21 m asl and dated 3950 ± 70 BP (S-3043). The lowest dated sample was a small bowhead vertebra excavated from beach

gravel at 5 m asl. Its excellent preservation was due to its young age and the sterility of the enclosing gravel. This sample dated at 2176 ± 130 BP (S-3041) and plots slightly below the curve.

Van Koenig Point

Twelve dates were obtained on shells (2), whalebone (5), walrus tusks (4), and one narwal (*Monodon monocerus*) tusk to plot the Van Koenig Point emergence curve (Fig. 3-8). An additional date was obtained earlier on a piece of driftwood by B.G. Craig (Dyck et al., 1965). A minimum age (8290 ± 100 BP, GSC-4703) for the marine limit is provided by surface fragments and whole valves of *Mya truncata* from stony glaciomarine clay at 91 m asl on the south (distal) flank of the outermost ridge of the Bernier Bay Moraines. Thirteen kilometres east of this site, a large marine limit delta occurs at 118 m asl. Although shells were not found in silts flanking the delta, it remains the best available estimate of marine limit at Van Koenig Point. A better constraint on the age of marine limit here is a date of 8830 ± 170 BP (GSC-183, discussed below) on shells collected east of this site. The transgression must have passed through the Van Koenig Point area by that time.

The skull of an immature walrus (Fig. 3-9) was found on a sandy raised beach at 38 m asl and one of its tusks dated 6200 ± 80 BP (S-3093). A second tusk, found a short distance away, was clearly from the same animal because it fitted the skull perfectly. This skull is slightly too old for its elevation, falling about 7 m below the curve (Fig. 3-8) suggesting that the animal sank after death or was subsequently redeposited downslope. The date is noteworthy because it records the earliest documented penetration of walrus into the study area.

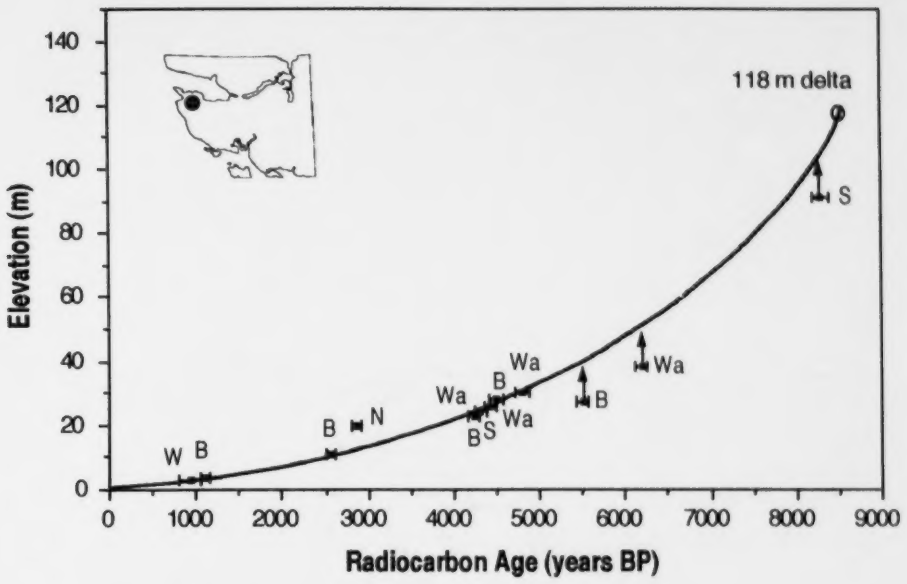

Figure 3-8. Emergence curve for Van Koenig Point.

Figure 3-9. Walrus skull found on raised beach southeast of Van Koenig Point.

The oldest whalebone date was obtained on an earbone subaerially exposed on top of a large bowhead skull embedded in a raised beach at 27 m asl. The sample dated 5520 ± 70 BP (S-3098), about 1000 years older than suggested by its elevation. The date plots below the curve by about 12 m and may represent a bowhead carcass which sank a short distance offshore.

The middle part of the Van Koenig Point curve is constrained by accordant dates on three walrus tusks, two bowhead earbones, a narwal tusk and a shell sample. A large walrus tusk was collected 20 km southeast of Easter Cape (Fig. 3-6) on the surface of a beach at 30 m asl. The 45 cm long skull found nearby was entirely embedded in gravel. The second tusk, judging by its well worn, blunted end, likely broke at the gumline while the animal was still alive. The tusk yielded an age of 4810 ± 90 BP (S-3095) for this shoreline. The second whalebone date at Van Koenig Point pertains to a periotic bone collected from a large bowhead skull embedded in gravelly sand at 28 m asl. This was the highest whalebone observed in the Van Koenig Point area and dated 4500 ± 80 BP (S-3045). The sample reliably dates the 28 m shoreline and confirms that S-3098 relates to a higher relative sea level.

The walrus tusk dates (S-3101 and S-3094) are from an area of prolific walrus bones at 23 and 26 m asl, and dated 4320 ± 90 and 4440 ± 70 BP, respectively. The two dates plot on or slightly below the emergence curve. Many walrus bones were found scattered along a beach about 200 m to the east (2 m below this site) and appear to comprise several complete skeletons. No evidence of Paleo-Eskimos (pre-Thule) was found in the area. Also at 23 m asl, a bowhead earbone was collected from part of a large skull found on a raised beach. The earbone closely approximates the ages of the walrus samples dating 4250 ± 70 BP (S-3096). Most of the skeleton of this large bowhead appears to be present, much of it shallowly embedded. At 20 m asl, a single unerupted narwal tusk was found in a small skull. The tusk yielded an age of 2880 ± 60 BP (TO-5017) and plots above the curve, likely due to contamination by humic acids.

At the same elevation, shells were excavated from gravelly mud at 24 m and dated 4310 ± 70 BP (GSC-4776). The sample consisted of whole valves of *Hiatella arctica* found in growth position. The section is cut in

the side of an extensive level surface of gravelly marine sediment, similar to that on modern tidal flats in the area. The shells correctly date the 24 m raised shoreline, indicating that the shells grew in shallow water when the dated whale and walrus skeletons were stranded. The internal consistency of the dates from the Van Koenig Point area is noteworthy. The age of the 23 m bowhead earbone (S-3096, 4250 BP) is within one standard deviation of the date on the 23 m walrus tusk (4320 BP, S-3011). Furthermore, shells collected nearby at 24 m asl were dated by a different laboratory at 4310 BP (GSC-4776). The close agreement between these dates on different materials supports the assumption, discussed earlier, that carcasses of marine mammals tend to strand at the contemporaneous sea level, or in shallow water. The close agreement between the whalebone, walrus and shell dates also suggests that only a minimal reservoir correction is required for marine mammal bones.

Two more accordant (i.e. plotting on or only slightly below the curve) dates on earbones constrain the lower part of the curve. The first pertains to a pair of well preserved periotic bones collected from a skull embedded in gravelly sand at 11 m asl, about 12 km southeast of Van Koenig Point. The earbones yielded a date of 2570 ± 60 BP (S-3044). The second date is on an earbone removed from a fragmented skull found partly embedded in a beach at 4 m asl. The sample yielded a date of 1110 ± 60 BP (S-3099). Decomposing ribs and vertebrae were found nearby, scattered along the length of the beach and partly covered by clumps of moss and *Dryas*. This is the youngest whalebone date from the study area. A piece of driftwood (*Picea* sp.), collected at 3 m asl dated 940 ± 130 (Dyck et al., 1965), the youngest date from the study area. This pair of dates provides an important constraint on the reservoir correction for bowheads (discussed below).

Bernier Bay Northeast

Nine dates on bowhead earbones and two shell dates have been used to plot an emergence curve for the eastern north shore of Bernier Bay, the best-controlled curve from the field area (Fig. 3-10). The upper part of the curve is based on two shell dates associated with a delta at 111 m asl marking marine limit. Surface fragments and a few whole valves of *Mya truncata* and *Hiatella arctica* were collected from stony silt at 92 m asl immediately below the delta. The resulting date of 7880 ± 120 BP (GSC-5090) provides a maximum age for the 92 m shoreline and a minimum age for the 111 m delta which appears to have prograded over the bottomset silt. The true age of marine limit is likely older as indicated by the date of 8210 ± 110 BP from Morin Point (GSC-4695). A younger date was obtained on shell fragments from the surface of a diamict occupying a gap in a large moraine at 81 m asl, 3.5 km northwest of the 111 m delta. The collection included a few whole valves (*Mya truncata* and *Hiatella arctica*) and yielded an age of 7620 ± 110 BP (GSC-5091). This provides a maximum age for the 81 m sea level and plots on the emergence curve.

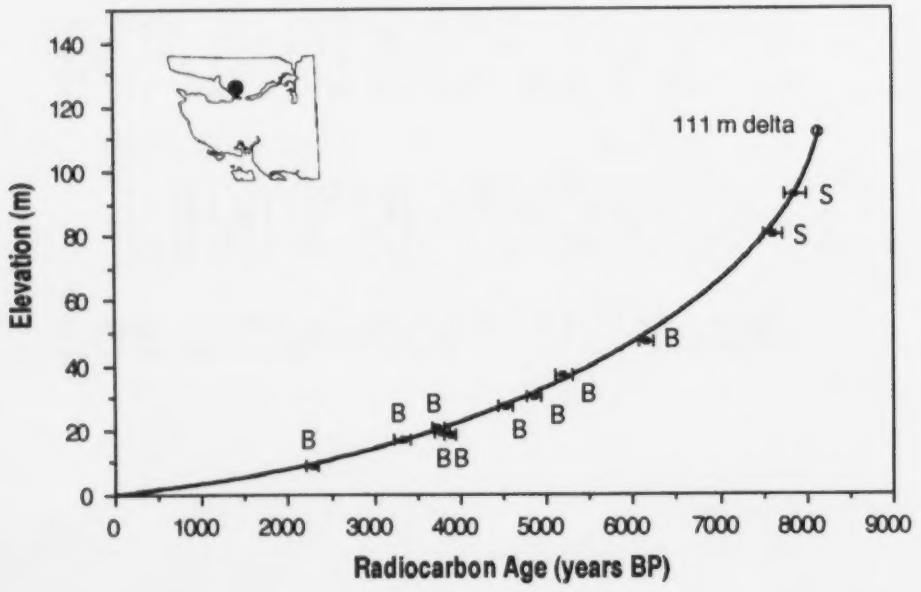

Figure 3-10. Emergence curve for Bernier Bay northeast.

Good control on the middle of the emergence curve is provided by four earbone dates. The highest sample was a single periotic bone retrieved from fragments of a skull found embedded in beach gravels at 47 m asl, which dated 6150 ± 90 BP (S-3359). The date plots on or slightly below the emergence curve and is the second oldest whalebone date from the field area. A second pair of periotic bones were collected at 37 m asl. The bones were retrieved from their sockets in the skull and were well preserved. The bones had an accordant radiocarbon age of 5200 ± 90 (S-3360). A third pair of periotic bones collected at 30 m asl dated 4860 ± 80 BP (S-3358) which plots slightly below the curve. The fourth date is on earbone fragments collected from a beach at 28 m asl and dated 4530 ± 80 BP (S-3355).

The next three earbone dates are tightly grouped in the 19 to 21 m range. A set of periotic bones was found in association with the cranial base, partly buried in damp grass and moss between beach ridges. The sample, from 21 m asl, yielded an age of 3740 ± 80 BP (S-3354). A second date pertains to a complete set of earbones collected at 19 m asl which dated 3780 ± 80 BP (S-3357). The third whalebone date is on a periotic bone collected at 19 m asl. The sample was partly exposed at the surface and dated 3880 ± 80 BP (S-3353). The date is plotted slightly below the emergence curve because two other dates, discussed above, have slightly younger ages but slightly higher elevations. These dates plot on or slightly below the curve. This "small-scale noise" is expected given: 1) sea-ice push and 2) the keel depth of a floating whale. Two earbone dates provide good control on the lower part of the curve. A single periotic bone excavated from beach gravels at 17 m asl, about 26 km northwest of the head of Bernier Bay, yielded an age of 3330 ± 100 BP (S-3356). The lowest date is on a bowhead earbone found in beach gravels at 9 m asl which dated 2290 ± 70 BP (S-3352). The curve (Fig. 3-10) demonstrates that the correct curve form is a simple exponential function rather than one involving minor transgressions.

Bernier Bay Southeast

Three high elevation shell dates and seven accordant whale bone dates define the emergence curve for southeastern Bernier Bay (Fig. 3-11). This curve is essentially identical to the curve from the inner north shore (Fig. 3-10) however its marine limit is slightly higher and older. Five of the dates are on bowhead earbones; two are on fragments of dense bone chipped from skulls. The age of marine limit is provided by thick *Mya truncata* fragments collected from the deflating surface of marine silts that dated 8440 ± 100 BP (GSC-4721). This sample was collected at 114 m asl, 11 m below the adjacent delta surface at 125 m, for which it provides a minimum age. A more closely limiting age for the delta and local deglaciation is provided by a date of 8830 ± 170 BP (GSC-183; Craig, 1965) obtained on shells collected at 119 m asl from the surface of the same silt plain.

Control on the middle of the curve is provided by a date on whole valves of *Hiatella arctica* excavated from a section of laminated marine silts at 63 m asl which dated 7130 ± 90 BP (GSC-4775). The top of the section is a level silt plain at 65 m asl. The date plots on or just below the curve connecting marine limit and the highest bone date.

The highest whalebone date (on earbone) was obtained on a sample collected at 49 m asl on a sandy raised beach about 7 m away from a large bowhead skull. This otic capsule was the only earbone not found attached or adjacent to a skull and dated 6585 ± 105 BP (S-3013). The date is a good control point for the age of the 49 m shoreline and is the oldest whalebone date from the entire field area.

Another earbone sample was collected from a skull embedded in beach gravel about 30 km southwest of the head of Bernier Bay. The sample is from 37 m asl and dated 5670 ± 100 BP (S-3014). A sample of periotic bone, collected from a skull embedded in a beach at 28 m asl, dated 5050 ± 165 BP (S-3040). The date plots on, or slightly below the emergence curve. Two bone fragments were collected at 22 m asl. The first was embedded in sandy beach gravel and dated 4010 ± 80 BP (S-3097). The second skull fragment was collected from a boulder-strewn raised beach (22 m) and dated 3930 ± 80 BP (S-3075). The next younger date is on a piece of periotic bone collected from a fragmented bowhead skull

embedded in a beach at 20 m asl. This sample dated 4115 ± 85 BP (S-3015), more than 100 years older than the two dates from 22 m asl. However, errors (1 σ) on the dates overlap. The consistent ages of these three dates give confidence in the use of bone to date raised shorelines and suggest that no contaminants were present in the bone collagen. Therefore, these minor differences are best explained by ice-push and the keel depth of a floating whale. The youngest bone sample for this area is an earbone collected from a small skull embedded in beach gravels at 7 m asl. The sample dated 2220 ± 75 BP (S-3016) and plots slightly below the curve but probably by no more than the keel-depth of the animal when floating.

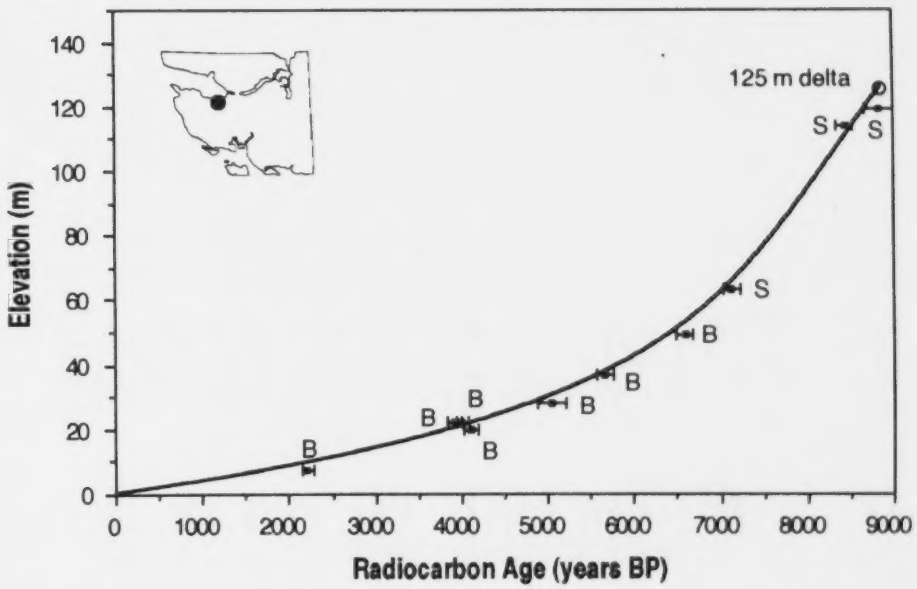

Figure 3-11. Emergence curve for southeast Bernier Bay.

Berlinguet River

Two shell dates and five whalebone dates are used to draw an emergence curve for the area west of Berlinguet River and north of the head of Berlinguet Inlet (Fig. 3-12). However, the lack of a marine limit date means the upper part is based solely on two shell collections. It was hoped that, because they were collected on the distal and proximal sides of a moraine, their ages would bracket its formation, but both dates are similar. On the ice-proximal (south) side of the moraine a sample of *Hiatella arctica* and *Mya truncata* fragments from 64 m asl yielded an age of 6840 ± 100 BP (GSC-5089). The collection site is about 200 m north of a marine limit delta at 111 m asl. The second date, from the ice-distal side of the moraine at 69 m asl has a similar age of 6820 ± 140 BP (GSC-5088). These concordant dates indicate that the shells grew after the ice had retreated when the sea occupied both sides of the moraine. This implies that the dates do not relate to the 111 m marine limit delta which required meltwater issuing from an ice front at the moraine for its formation. Consequently, the age of the delta is estimated at 8000 BP and the two shell dates, from 69 and 64 m asl, are plotted on and slightly below the curve.

The tight grouping of five whalebone dates at 18-23 m asl provides good control for the lower part of the curve. The highest whalebone date is on a single, broken periotic bone found in a skull at 23 m asl. The sample was well preserved, deeply buried in beach gravel, and yielded an accordant date of 4010 ± 90 BP (S-3351). A slightly older date was obtained on a set of periotic bones collected from a raised beach at 21 m asl which dated 4090 ± 80 BP (S-3349). Judging by the younger age of S-3351 (23 m asl) above, it is likely that sample S-3349 (21 m asl) stranded in shallow water, hence the date is plotted slightly below the emergence curve. This interpretation is verified by a second earbone date on the 21 m beach which is about 400 years younger (3700 ± 80 BP, S-3380).

Two dates were obtained on samples from 18-19 m asl. The first is on a set of periotic bones collected from a small skull in a raised beach at 19 m asl. The earbones were partly exposed with the end of one periotic bone being sunbleached. The earbone had an age of 3340 ± 80 BP

(S-3347). The second date is on a collection of periotic bone fragments from 18 m asl. The earbone pieces were excavated from the skull and dated 3280 ± 80 BP (S-3348). The two dates are accordant and reliably date the 18 and 19 m shorelines.

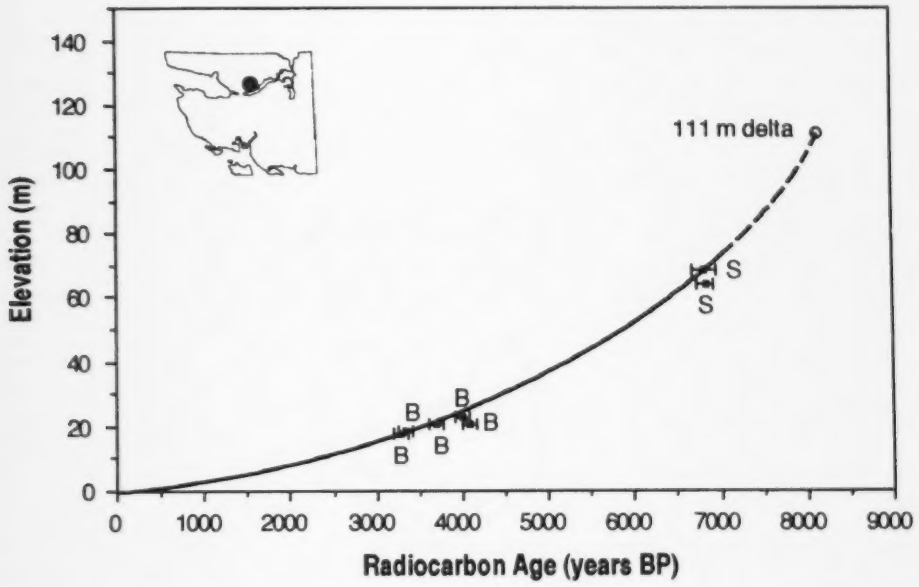

Figure 3-12. Emergence curve for Berlinguet River.

Berlinguet Inlet West

A shell date and five whalebone dates are used to draw an emergence curve for a small area south of the head of Berlinguet Inlet (Fig. 3-13). The uppermost date is on a sample of fragments and whole valves of *Hiatella arctica* collected from the surface of colluviated deltaic sands. The sample, from 74 m asl, yielded an age of 7240 ± 100 BP (GSC-4894). The collection site is on the flank of a perched delta (76 m asl) and the date is considered a maximum age for this shoreline because surface shells of identical age were collected nearby at 89 m asl, 13 m *above* the delta (Craig, 1965; 7240 ± 150, GSC-304). This indicates that marine limit is higher still (Table 2-1), perhaps as high as a delta measured on the north side of the inlet (Berlinguet River) at 111 m asl. If so, the age of marine limit here is about 7500 BP.

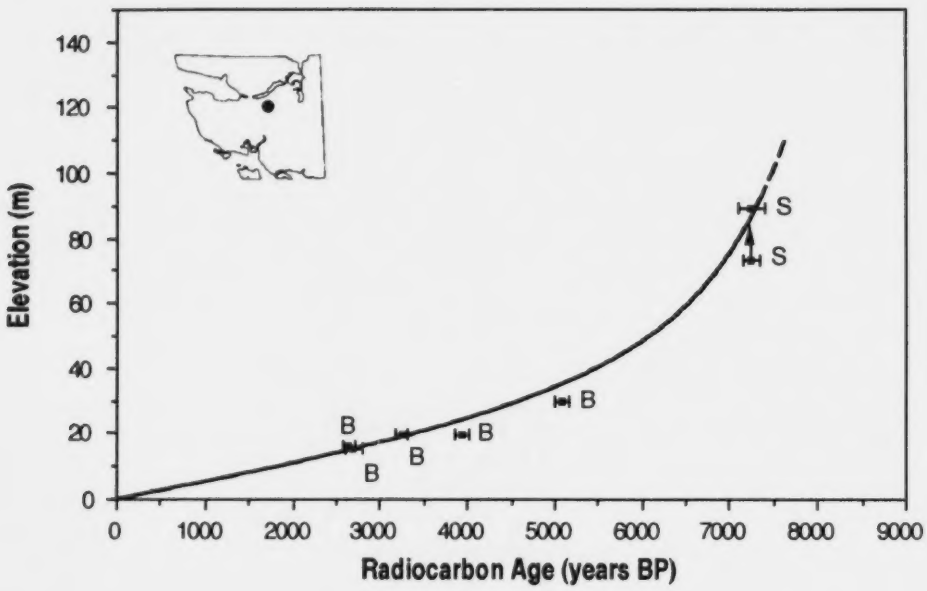

Figure 3-13. Emergence curve for Berlinguet Inlet west.

The oldest whalebone date (5080 ± 80 BP, S-3128) was obtained on periotic bone fragments and an otic capsule found buried alongside a skull in a beach at 30 m asl. The sample is probably older than suggested by its elevation due to the material sinking in an unknown depth of water. The scarcity of points between this sample and the upper shell sample makes it difficult to estimate how far the date plots below the true height of the 5080 BP shoreline.

Two earbone samples were submitted from sites at 20 m asl. The first consisted of fragments of periotic bone attached to a skull embedded in a raised beach at 20 m asl, which yielded an age of 3250 ± BP (S-3263). The second was also a collection of periotic bones recovered from a skull embedded in frozen beach sand. This sample dated 3940 ± 90 BP (S-3134), almost 700 years older than S-3263, hence it is considered too old for its elevation and is plotted 8 m below the emergence curve (Fig. 3-13).

The lower part of the curve is constrained by two dates on periotic bones. The first was retrieved from a skull embedded in a raised beach at 16 m asl and yielded an age of 2650 ± 80 BP (S-3261). The second was collected from a skull embedded in a raised beach at 15 m asl and dated

2700 ± 90 BP (S-3262). Given the elevation errors and the standard errors of the radiocarbon dates, the two ages are essentially equivalent for the purpose of dating the 16 m asl raised shoreline.

Berlinguet Inlet East

Eight dates on bowhead earbones were used to draw an emergence curve for eastern Berlinguet Inlet (Fig. 3-14). Four of the dates are accordant and define a smooth curve; the rest are older than expected for their elevations. This curve had the greatest number of unexpectedly old earbone dates in the field area. The restricted channel (Berlinguet Inlet) in this vicinity may have acted as a trap for melting pack ice, which prevented some bowhead carcasses from stranding on beaches, forcing the remains to sink offshore.

The minimum elevation of marine limit marked by a raised delta at 78 m asl. The delta is one of three between 76 and 78 m asl along the south side of Berlinguet Inlet. The deltas are likely below the true height of marine limit because Craig (1965) reports shells at 89 m asl south of the head of the inlet (cf. previous section). Hence the deltas must have formed after deglaciation of the inlet due to melting of ice on the plateau to the south slightly after 7200 BP. Furthermore, marine limit east of Bell Bay (discussed below) is also higher.

The oldest date was obtained on an earbone sample from a raised beach at 33 m asl. The earbone yielded an age of 4520 ± 100 BP (S-3125), reliably dating the 33 m shoreline. The first of several unexpectedly old dates was obtained on earbone fragments found embedded in a beach at 27 m asl. The sample dated 4300 ± 110 BP (S-3124), indicating that the carcass sank in about 5 m of water. A second date (3870 ± 80 BP, S-3182) was obtained on a fragmented otic capsule and periotic bone found embedded in frozen gravels at 21 m asl. This suggests that the carcass sank in about 7 m of water. The third date is on a collection of earbones found embedded in a raised beach at 19 m asl which dated 4220 ± 80 BP (S-3181). The material is about 900 years older than expected for its elevation indicating the carcass sank in about 12 m of water. The fourth date is on an earbone collected from a beach at 16 m asl that dated 3990 ± 80 BP (S-3183), about 1000 years older than expected for its elevation.

Hence, this carcass likely sank in about 13 m of water. The dates demonstrate that it is not necessary for the carcasses to strand on the contemporaneous shoreline in order for the bones to be incorporated in beach sediment. These occurrences are are thought to represent cases where the bones were incorporated in the beach as the shoreline regressed across skeletons deposited offshore.

Three dates on bowhead earbones constrain the curve below 18 m asl. The first was found in poorly drained beach gravels at 18 m asl and dated 3320 ± 80 BP (S-3258). The departure from the expected age could be due either to the whale sinking in shallow water or to slight downslope displacement of the skull by solifluction. The second is on an otic capsule found on a well vegetated raised beach at 17 m asl that dated 2800 ± 70 BP (S-3259). The lowest point on this curve is a date on a periotic bone collected from a raised beach at 12 m asl (2310 ± 80 BP, S-3260).

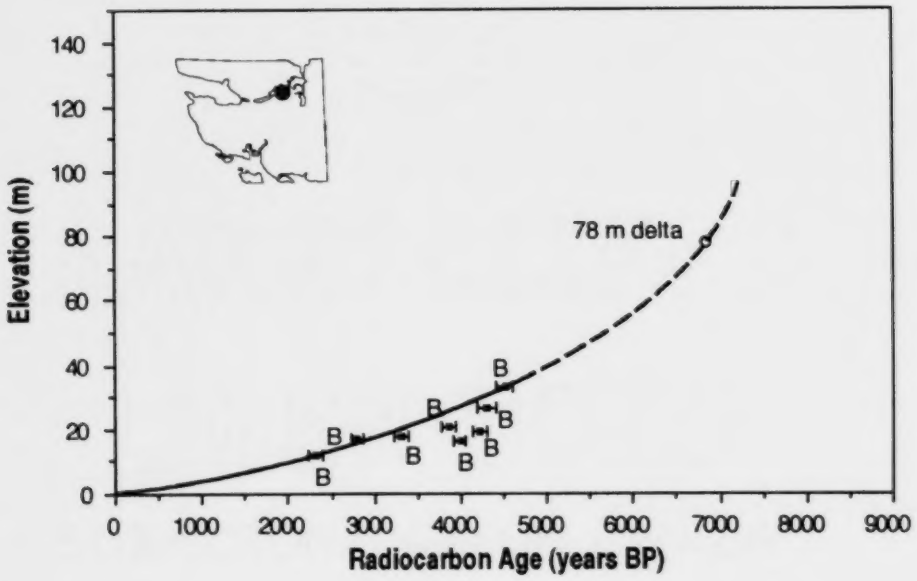

Figure 3-14. Emergence curve for Berlinguet Inlet east.

Bell Bay

A shell date and seven dates on bowhead earbones are used to draw an emergence curve for the area west of Bell Bay (Fig. 3-15). The slope of coastal lowlands south and west of the bay is very low and the area is noticeably warmer than other parts of the field area. As a consequence, beach ridges are barely discernable and the near saturated active layer supports a dense cover of grass and moss. Bowhead skulls in the area often act as nuclei for the development of raised peaty mounds, and most bones, except earbones, were unsuitable for dating. Dark brown to black humic staining of the exterior surface of the earbones was common. Contamination by humic acids, which leached into microscopic pores in the earbones, is possible for two of the dates which plot slightly above the curve, defining the top of the envelope in Fig. 3-15.

The uppermost point on the curve is a date on shells excavated from laminar deltaic sands exposed in a stream cut at 70 m asl. Most of the sample consisted of paired whole valves of *Mya truncata* and it dated 6770 ± 90 BP (GSC-4897). The sample site occurs below a nearby raised delta at 92 m asl for which it provides a minimum age. It is not clear whether the sample relates to the 92 m delta or to one of several nested delta surfaces between the 92 m surface and the sample site. A large raised delta was measured west of Bell Bay at 134 m asl, but shells were not found in silts nearby. The height of the delta, the apparent lack of shells, and the setting of the site suggest that it formed in a large proglacial lake impounded between the south side of an ice lobe in Berlinguet Inlet and higher ground to the south. Several other graded surfaces of outwash gravels in the vicinity were measured up to 179 m asl, and record fluctuating lake levels. Consequently, the date of 6770 ± 90 BP is considered the best minimum age for the 92 m marine limit. This relatively low and young marine limit is corroborated by a shell date of 6620 ± 90 (GSC-5073; Dyke, pers. comm., 1995). The shells were collected from a sand section at 60 to 66 m asl and date a 72 m marine limit delta at Jungerson Bay, north of Bell Bay (Fig. 1-1).

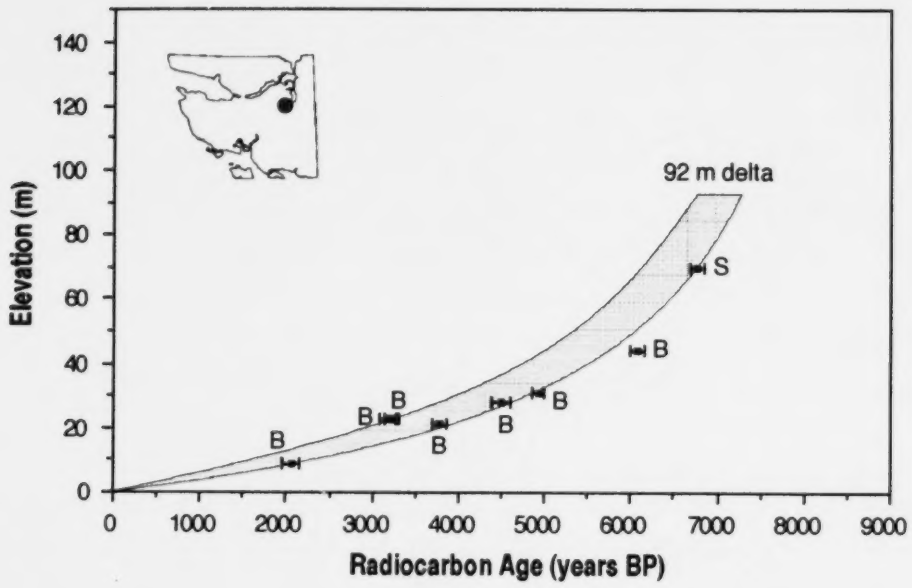

Figure 3-15. Emergence curve for Bell Bay.The curve is shown as an envelope because five of the whalebone dates are accordant but plot below the curve as defined by the two dates from 22.5 m.

The oldest whalebone date (6070 ± 90 BP, S-3180) was obtained on a periotic bone found on a beach at 44 m asl and is slightly older than expected for its elevation. Another date (4930 ± 80 BP, S-3098) was obtained on a collection of earbone fragments found embedded in a boggy raised beach at 31 m asl and plots slightly below the curve. Another date was provided by a sample of periotic bone recovered from a skull at 28 m asl that dated 4500 ± 100 BP (S-3176).

Two dates were obtained on samples from 23 m asl. The first is on a collection of earbone fragments from a beach on the west side of Saputing River that dated 3190 ± 90 BP (S-3257). The date is considered slightly too young for its elevation. More periotic bone fragments were collected at the same elevation from another skull nearby. The skull was protruding above the surface of well vegetated beach sands and dated 3230 ± 80 BP (S-3256). This date is also slightly younger than expected from its elevation. Two periotic bones and an otic capsule were collected at 21 m asl. The bones were shallowly buried in beach gravels in or alongside the skull and dated 3790 ± 80 BP (S-3179). This may be slightly

older than the 21 m raised shoreline and is plotted immediately below the curve. The lowest point on the curve is from a periotic bone collected from a beach at 9 m asl which dated 2060 ± 100 BP (S-3177). The curve is shown as an envelope in Fig. 3-15 because five of the whalebone dates are accordant but plot below the curve as defined by the two dates from 22.5 m.

Foss Fiord/Kimakto Peninsula

Radiocarbon dates from two camp areas were combined to draw a minimum emergence curve for the Foss Fiord/Kimakto Peninsula area (Fig. 3-16). The curve is based on two shell dates, two whalebone dates and two driftwood dates.

A collection of fragments and whole valves of *Mya truncata* and *Hiatella arctica* from 65 m asl, dated 8910 ± 120 BP (GSC-4898). The sample was collected from the surface of stony silts and the date plots well below the emergence curve. Although it does not reveal the elevation of the 8900 BP shoreline, the date provides a minimum age for marine limit (deglaciation) in the southwestern part of the study area.

The uppermost date was obtained on a collection of fragments and whole valves of *Mya truncata* and *Hiatella arctica* found at 138 m asl northwest of the head of Foss Fiord. The sample has an age of 8520 ± 100 BP (GSC-5086). The date is a minimum age for deglaciation and marine limit at its site but it is at least 400 years younger than the highest marine limit feature in the area. No marine limit delta was measured in the area but several small deltas on the opposite valley side occur at approximately 140 m asl.

Two earbone dates and one wood date constrain the middle part of the curve. The highest of these was a periotic bone collected from a beach at 38 m asl. The earbone dated 5110 ± 90 BP (S-3345); the date plots slightly below the curve. A date obtained on a sample of driftwood collected from beach gravels at 37 m asl, only 1 m below the earbone described above yielded an accordant (i.e. plotted on the emergence curve) age of 4660 ± 80 BP (GSC-5077). The next lowest date was obtained on a pair of periotic bones embedded in a raised beach at 31 m asl. This date

(4610 ± 60 BP, S-3346) plots on, or slightly below the curve. The lowest date is on a small piece of driftwood found resting on a raised beach at 3 m asl which yielded an age of 1140 ± 80 BP (GSC-5076). The date is slightly older than expected for the 3 m raised shoreline.

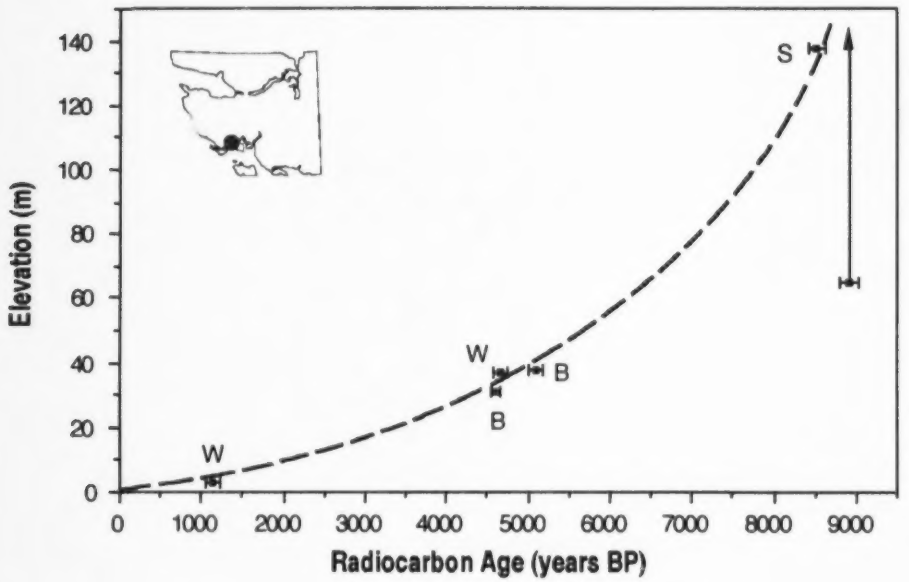

Figure 3-16. Emergence curve for Foss Fiord and Kimakto Peninsula.

Nybøe Fiord

Three shell dates and the elevation of a marine limit delta form a tentative minimum emergence curve for the west side of Nybøe Fiord (Fig. 3-17). The area is very close to Foss Fiord (Fig. 3-7) and probably experienced a similar emergence history. The first date (7120 ± 140, GSC-307), pertaining to deglaciation of the Nybøe Fiord Valley (not shown on curve because it is too far from the other samples), was obtained on surface shells collected at 97 m asl by B.G. Craig (1965).

The upper date (7670 ± 130 BP, GSC-5327) is on a sample of *Hiatella arctica* fragments with a few whole valves from the surface of stony silt at 96 m asl. Craig (1965) dated shells from a nearby site (97 m asl) at 7690 ± 140 (GSC-306). These dates are *both* minimum ages for the local marine limit marked by a raised delta at 138 m asl. The true age of the

marine limit is likely older as indicated by the date of 8520 ± 100 BP (GSC-5086) to the west, discussed in the preceding section. The lower part of the emergence curve is poorly constrained by a date obtained on a collection of paired whole valves of Mya truncata excavated from a stream cut in laminated mud at 8 m asl. The collection dated 3150 ± 90 BP (GSC-5373) and relates to a former sea level an unknown height above the site.

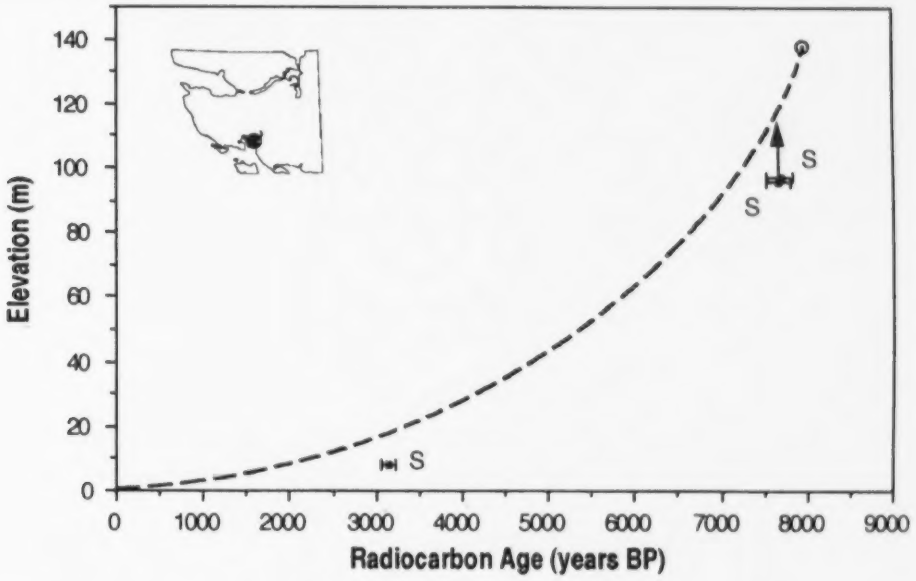

Figure 3-17. Emergence curve for Nybøe Fiord.

Crown Prince Frederick Island

Two wood dates, four earbone dates and one walrus tusk date were used to plot an emergence curve for Crown Prince Frederick Island (Fig. 3-18). The highest point on the island is slightly over 92 m asl (map) which is below marine limit. The oldest date from the island was obtained on a pair of periotic bones collected from a raised beach at 72 m asl. The sample dated 6350 ± 130 BP (S-3433). This is the second oldest bone date in the study area and the age plots slightly below the emergence curve. The date also records the earliest known penetration of bowheads into the eastern part of the Gulf of Boothia, west of Fury and Hecla Strait.

A small driftwood log was found in the interior of the island embedded in gravels at 68 m asl. The entire log was removed and shipped to the laboratory. A subsample of this material dated 5870 ± 70 BP (GSC-5295). This was the oldest driftwood collected in the field area and reliably dates the 68 m shoreline. It also provides a minimum age for the earliest penetration of driftwood into the Gulf of Boothia.

Two earbone dates are available for the 50 m asl shoreline (Fig. 3-18). The first was obtained on a periotic bone that had an accordant age of 5310 ± 120 BP (S-3431). The second was obtained on a pair of periotic bones and an otic capsule that dated 5700 ± 120 BP (S-3432). The younger date is likely closer to the true age of the 50 m raised shoreline. Periotic bone fragments from a skull found on a raised beach at 47 m asl dated 5120 ± 120 BP (S-3434). The date plots on or slightly below the curve. At 41 m asl, a walrus tusk dated 4940 ± 70 BP (TO-5016), and plots slightly below the curve. The lowest point on the emergence curve is a date of 4210 ± 70 BP (GSC-5294) obtained on a sample of driftwood from a log found embedded in beach gravel at 34.5 m asl.

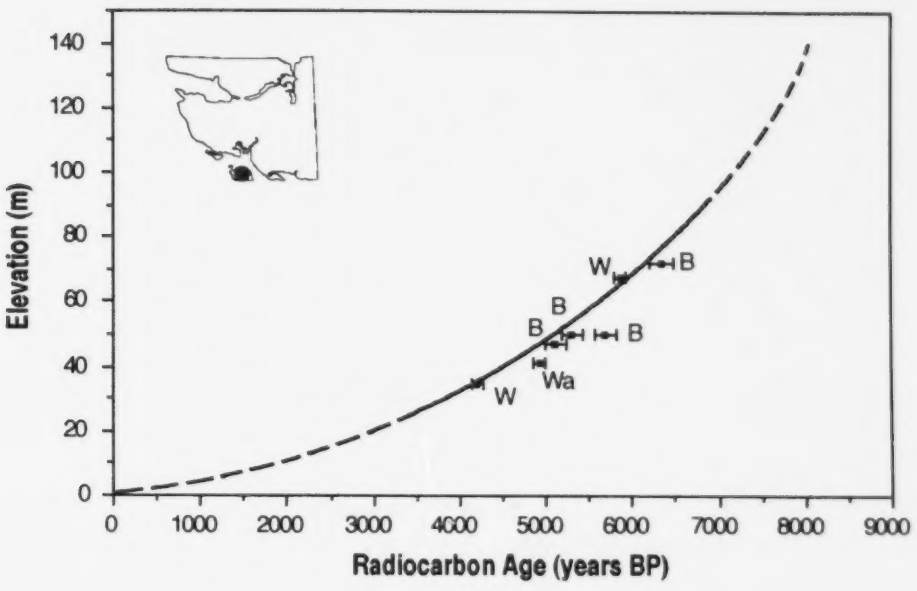

Figure 3-18. Emergence curve for Crown Prince Frederick Island.

Autridge Bay/Whyte Inlet

A minimum emergence curve for Autridge Bay and Whyte Inlet (Fig. 3-19) is based on nine shell dates. Whale bones and driftwood were not found east of Kimakto Peninsula despite considerable searching. The Holocene marine limit is recorded by large deltas along the north side north of Autridge Bay. Altimeter measurements of these deltas and outwash terraces span the range 94-144 m asl. The clearest marine limit indicator is a delta lip at 122 m asl. Higher measurements are on apices of deltas or gravel terraces grading to marine limit which now exist as remnants following dissection by modern streams.

A sample of *Mya truncata* excavated from colluviated muddy sand at 71 m asl from the foot of a 114 m delta north of the head of Whyte Inlet yielded an age of 6260 ± 80 BP (GSC-5372). The date provides a minimum age for marine limit.

Two shell dates are available from 65 m asl. The first is on a collection of fragments of *Hiatella arctica* found on the surface of marine silt at 66 m asl that dated 5900 ± 100 BP (GSC-5087). A second date for the 65 m shoreline (5810 ± 100 BP, GSC-5395) is provided by a collection

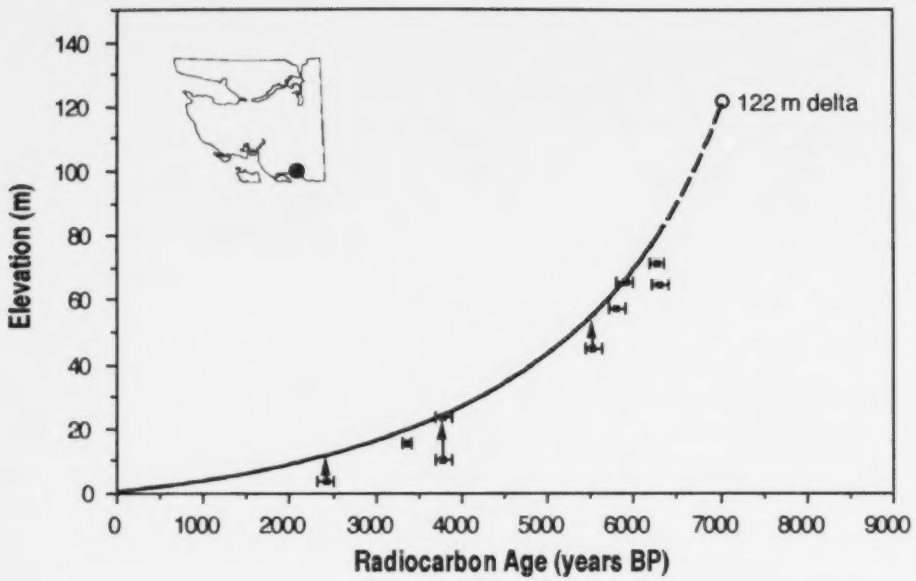

Figure 3-19. Emergence curve for Autridge Bay and Whyte Inlet.

of paired valves of *Mya truncata* excavated from deltaic sands at 65 m asl. The dates are considered reasonable maximum ages for the 65 m raised shoreline and plotted slightly below the curve. A collection of paired valves of *Mya truncata*, from a section in deltaic sands at 57.5 m asl, yielded an age of 6300 ± 100 BP (GSC-5331). This date is clearly older than expected from its elevation because it is slightly older than GSC-5372 from 71 m asl (above). Hence, it provides a minimum age for deglaciation.

Five dates on marine shells provide maximum ages for their associated elevations, and partially constrain the lower part of the curve. Fragments and whole valves of *Mya truncata* collected from the surface of marine silt at 45 m asl yielded a date of 5530 ± 100 BP (GSC-5345). The date is also older than expected from its elevation. The next lower date is on a sample of *Mya truncata* valves from a stream cut in deltaic sands at 24 m asl north of the head of Whyte Inlet. The shells dated 3790 ± 90 BP (GSC-5374) which is a maximum age for the 24 m raised shoreline. The age of the sample is very close to that of GSC-5311 (discussed below) but the sample site is 13 m higher. At 16 m asl, a sample of paired whole valves of *Mya truncata* was collected from a small section in laminated

sands and mud. The sample, from prolittoral sediment, dated 3360 ± 60 BP (GSC-5364). At 11 m asl, a collection of paired whole valves of *Mya truncata* was excavated from a section in poorly stratified sands and muds. The sample yielded an age of 3790 ± 90 BP (GSC-5311) and is clearly older than suggested by its elevation. The lowest point on the curve is a date obtained on whole valves of *Mya truncata* excavated from massive deltaic sand just above modern high tide line at 4 m asl. Landward of the sample site is an extensive delta terrace at 5.5 m asl. The sample yielded an age of 2420 ± 100 BP (GSC-5316). The date plots slightly below the curve.

Summary

All the curves have a similar exponential form indicating that the different parts of the coast underwent similar, although not identical, emergence histories. Generally, the lower and middle portions of the curves have the best control. The best available marine limit dates are limiting dates on shells collected from the surface of bottomset silts close to a measured feature, usually a delta. The maximum rate of initial emergence (the steepness of the upper part of the curve) is obtained by assuming that the shells accurately date delta formation whereas a minimum estimate is obtained by assuming the shells grew when sea level was only slightly above the shell site. Thus, assigning minimum ages to the deltas based on the age of the associated shells potentially overestimates the gradient of the upper curve. This is significant when comparing individual curves when the age differences, if any, between the marine limit feature and the highest shell dates are unknown.

The lower parts of the emergence curves are well controlled except in the southeast part of the area where whalebone is scarce or absent. The internal consistency of the dataset is due to the small errors associated with the dates (altimetry and counter errors) and shows that errors from ice push and downslope displacement by solifluction were also small. It also demonstrates the correctness of the assumption that dead bowheads strand at or very close to sea level. The same is true of radiocarbon-dated walrus in this study, although cases of walrus wandering far inland before dying have been reported (Dyke, 1979).

Only the Nybøe Fiord and Autridge Bay/Whyte Inlet curves are unconstrained by bone or wood dates. The dates provide accurate ages for the shells, but many more dates are required to achieve the same level of reliability as a comparable wood- or bone-based curve.

Emergence in Adjoining Areas

Additional data are available from adjoining areas. South of the study area, there are four emergence curves from the west side of Melville Peninsula (Dredge;1990) and two from the east side (Dredge, 1991). The radiocarbon dates for the three northernmost curves, Brevoort River, Baker Bay and Purfur Cove/Fury and Hecla Strait (Appendix G) are replotted here as a composite emergence curve (Fig. 3-20). The data can be accommodated by a smooth curve, although some dates fall farther below the curve than they do if a stepped curve is used as proposed by Dredge (1990). Marine limit for the Baker Bay area is at 230 m asl, much higher than on the adjacent Baffin Island coast.

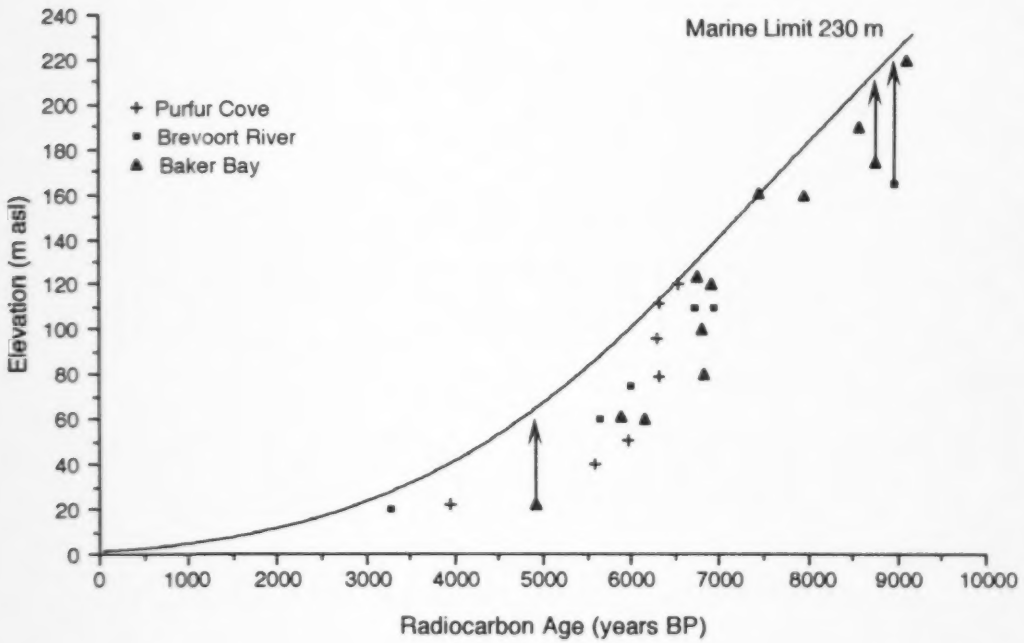

Figure 3-20. Emergence curve for northern Melville Peninsula (data from Dredge, 1990).

Raised shoreline elevations (from radiocarbon-dated emergence curves) are available for several sites on Brodeur Peninsula and the coast of Admiralty Inlet (Dyke, pers. comm., 1995). Data are available for Fitzgerald Bay, on the west side of Admiralty Inlet, 90 km north of Morin Point, Tikiraq River, on the east side of the peninsula 85 km north northeast of the head of Berlinguet Inlet and Jungersen Bay on the east side of the head of Admiralty Inlet (Table 3-2). Missing values in the table indicate that these sites were still covered by glacial ice.

Table 3-2. Shoreline elevations (m asl) for southern Brodeur Peninsula sites near the present study area (see Fig. 1-1 for locations).

Age (yrs BP)	Fitzgerald Bay	Tikiraq R.	Jungersen Bay
8500	80		
8000	67	93	
7500	57	73	
7000	50	58	82
6500	36	47	68
6.0	31	40	53
5.5	27	34	42

Pattern of Shoreline Delevelling

The emergence curves were used to draw an equidistant diagram showing the delevelling of shorelines dated 8500, 8000, 7500, 7000 and 6000 BP (Fig. 3-21). Shoreline heights are based on interpolations from local emergence curves (cf. Fig. 3-6). The gradient of a segment of the 8500 BP shoreline (shaded zone in Fig. 3-21) was estimated by comparing the elevations of dated shells (with overlapping error terms) from Bernier Bay Southeast and Foss Fiord. Choice of transect made based on the good control provided by upper shell dates in these two areas, so that the transect would cross, rather than parallel the isobases.

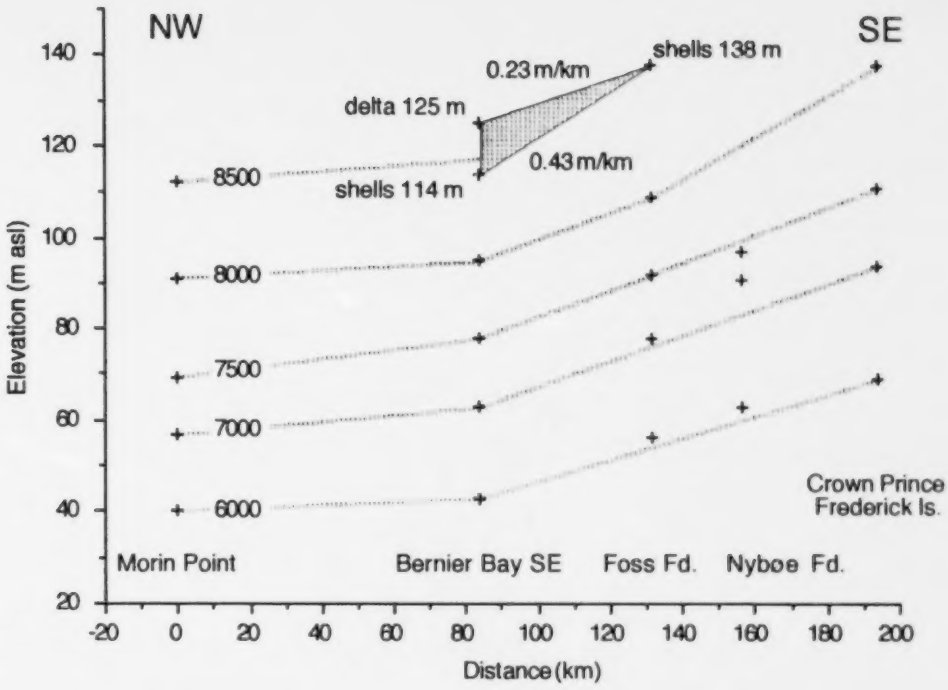

Figure 3-21. Equidistant diagram showing the gradient of the 8500, 8000, 7500, 7000 and 6000 BP shorelines between Morin Point and Crown Prince Frederick Island (see Fig. 3-22 for line of transect).

At Bernier Bay southeast, shells from 114 m asl provided a minimum age of 8440 ± 100 BP (GSC-4721) for a 125 m asl marine limit delta. A similar date was obtained on shells collected at 138 m asl near the head of Foss Fiord, 56 km to the southeast. These dated 8520 ± 100 BP (GSC-5086). Hence, the 8500 BP shoreline lies between 114 and 125 m asl at Bernier Bay southeast and at 138 m asl in the Foss Fiord area. Applying the minimum age to the delta yields a gradient of 0.23 m/km. Using the sample heights as minimum estimates of the height of the 8500 BP shoreline yields a gradient of 0.43 m/km (Fig. 3-21). The latter figure is considered more realistic because an older minimum age is available for the 125 m delta (8830 ± 170, GSC-183; Craig, 1965). The gradient might be somewhat steeper if the shells from Foss Fiord grew in some depth of water. However, no deltas were found in the Foss Fiord area above 138 m asl.

The gradients of younger shorelines decline systematically (cf. Andrews and Dugdale, 1970) and the gradient across Bernier Bay (Morin Point to Bernier Bay southeast) is significantly flatter than shoreline gradients to the southeast. Between Morin Point and Crown Prince Frederick Island the 7500 BP shoreline has a gradient of 0.57 m/km. Over the same transect, the 6000 BP shoreline has a gradient of 0.40 m/km. Between Morin Point and Bernier Bay southeast the 7500 BP and 6000 BP shorelines have gradients of 0.11 m/km and 0.04 m/km, respectively.

ISOBASE MAPS

Interpolations from local emergence curves were used to construct a set of isobase maps showing the height of the 8500, 8000, 7500, 7000 and 6000 BP shorelines (Figs. 3-22 to 3-26). Elevations followed by a plus sign (+) were estimated from minimum curve segments; elevations followed by a plus/minus sign (±) were estimated from extrapolated or weakly controlled curve segments. Where appropriate, elevations of additional isolated dates were used. Ice marginal positions, mapped earlier from moraines and meltwater channels (cf. Fig. 2-14), are also shown. In drawing the isobases, uniform shoreline gradients were assumed between curve areas, and data from adjoining areas, discussed above, were used to control the orientation of isobases around the margin of the study area.

At 8500 BP only the western and southwestern part of the area was ice-free (Fig. 3-22). The 8500 BP shoreline rises toward the southeast from 118 m asl in the northwest to 138 m in the southeast. The height of this shoreline on Crown Prince Frederick Island is uncertain, as the entire island lies below marine limit.

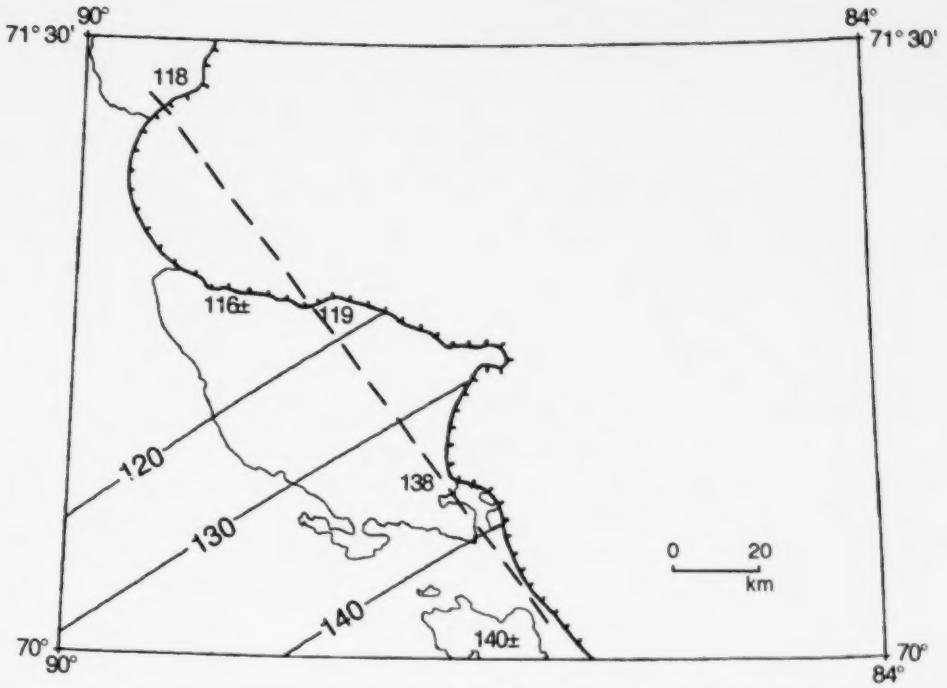

Figure 3-22. Isobases on the 8500 BP shoreline. The dashed line shows the line of transect used in Fig. 3-21.

By 8000 BP, the ice sheet had undergone eastward retreat and the Brodeur Peninsula Ice Cap had separated from the ice lobe in the head of Bernier Bay. The placement of the 8000 BP margin north of Berlinguet Inlet (Fig. 3-23) is based on the height of the marine limit delta at Berlinguet River. This 111 m delta is probably only slightly younger than the 110 m delta north of Bernier Bay which had an age of 8210 ± 110 BP (GSC-4695). If the delta is as young as implied by its minimum age of 6840 ± 100 BP (GSC-5089), then there was zero emergence between 8200 and 6800 BP, which is unlikely. The 8000 BP shoreline rises about 43 m, from 91 m asl in the northwest to approximately 134 m asl in the southeast (Fig. 3-23) but with minimal gradient across the Bernier Bay area.

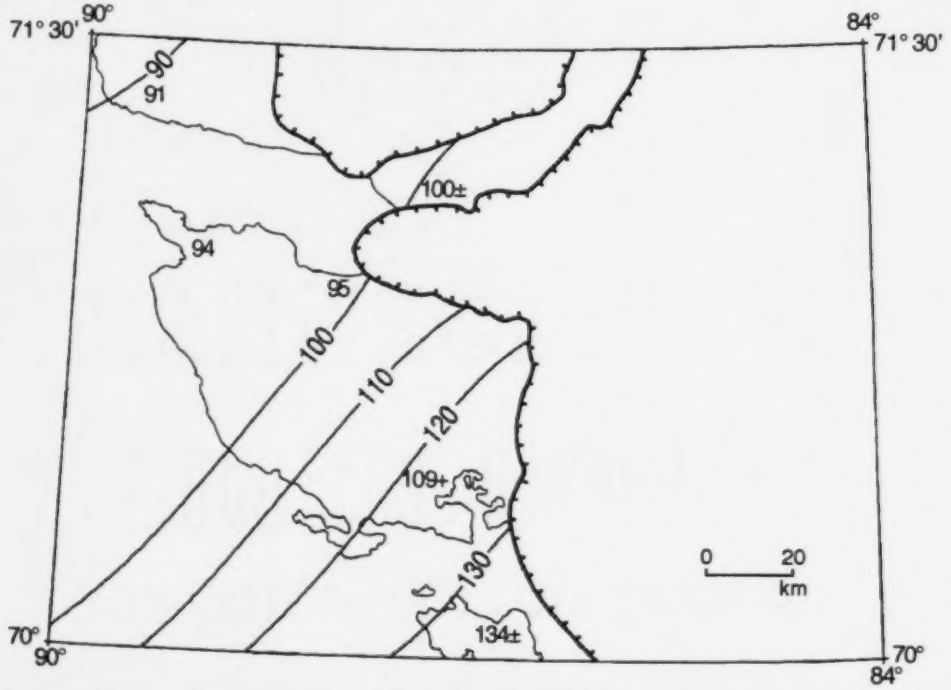

Figure 3-23. Isobases on the 8000 BP shoreline. Elevations followed by a plus sign (+) were estimated from minimum curve segments; elevations followed by a plus/minus sign (±) were estimated from extrapolated or weakly controlled curve segments.

By 7500 BP the ice had retreated eastward to the head of Bernier Bay (Fig. 3-24). The 7500 BP shoreline rises approximately 42 m, from 69 m asl in the northwest to about 111 m asl in the southeast. A minimum emergence estimate of 87 m for the area north of the head of Bernier Bay is provided by a date of 7560 ± 500 BP (I-1254, Craig, 1965). This is not corroborated by the data from the Bernier Bay northeast and Berlinguet River curve areas which indicate more modest emergence since 7500 BP. Considering its large 1 σ error of 500 years and noting that an unknown method was used to measure its elevation, the above date is probably not a reliable age for the 7500 BP shoreline. The minimum emergence for the Bernier Bay northeast area is 81 m, based on a similar date of 7620 ± 110 (GSC-5091). Emergence estimates for the Bernier Bay southeast area were lower than in adjoining areas to the north and west beginning at 7500 BP. The 7500 BP shoreline rises approximately 46 m across the area from northwest to southeast (Fig. 3-24).

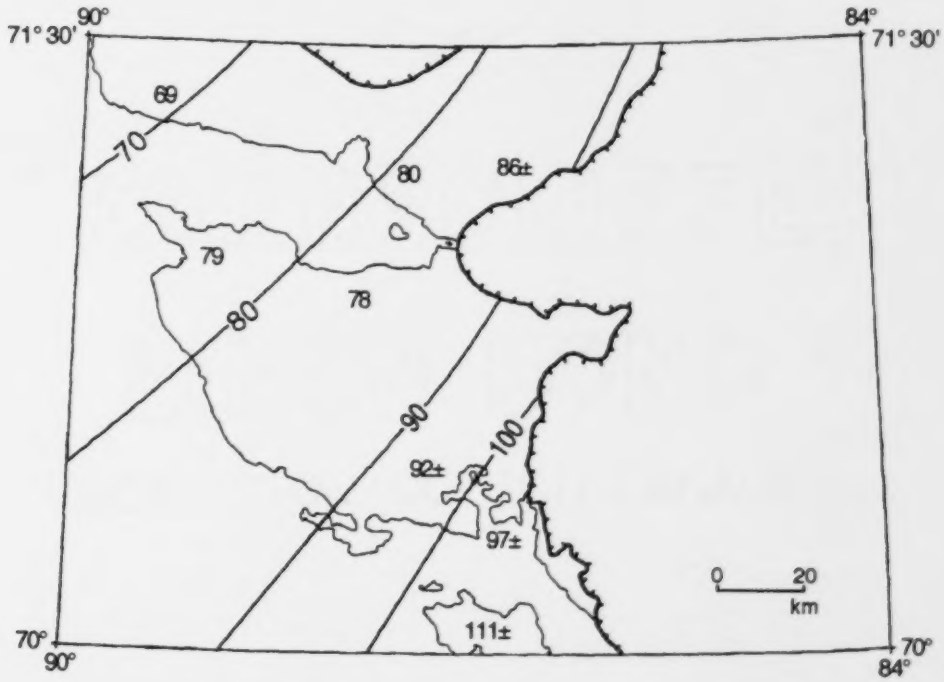

Figure 3-24. Isobases on the 7500 BP shoreline.

The margin of Foxe ice was located east of the head of Berlinguet Inlet at 7000 BP. The 7000 BP shoreline (Fig. 3-25) rises approximately 43 m to the southeast from 57 m at Morin Point to more than 97 m southeast of Agu Bay. By 6000 BP (Fig. 3-26) most of the marine-based ice in the study area had calved, but ice was still at or near tidewater around Bell Bay and Autridge Bay. Tilt on 6000 BP shoreline is less, approximately 31 m (Fig. 3-26), rising toward the southeast, and the isobases are more widely spaced.

The main features of the isobase pattern are the southeastward tilt of shorelines and the low shoreline gradients around Bernier Bay. The increase in gradients toward the southeast, where the isobases are more closely spaced, indicates that Foxe ice thickened in this direction. Interestingly, more steeply tilted shorelines, such as might be expected in the vicinity of an ice margin, were not found in the vicinity of the Bernier Bay Moraines; instead the opposite is found. This aspect of the emergence will be discussed below.

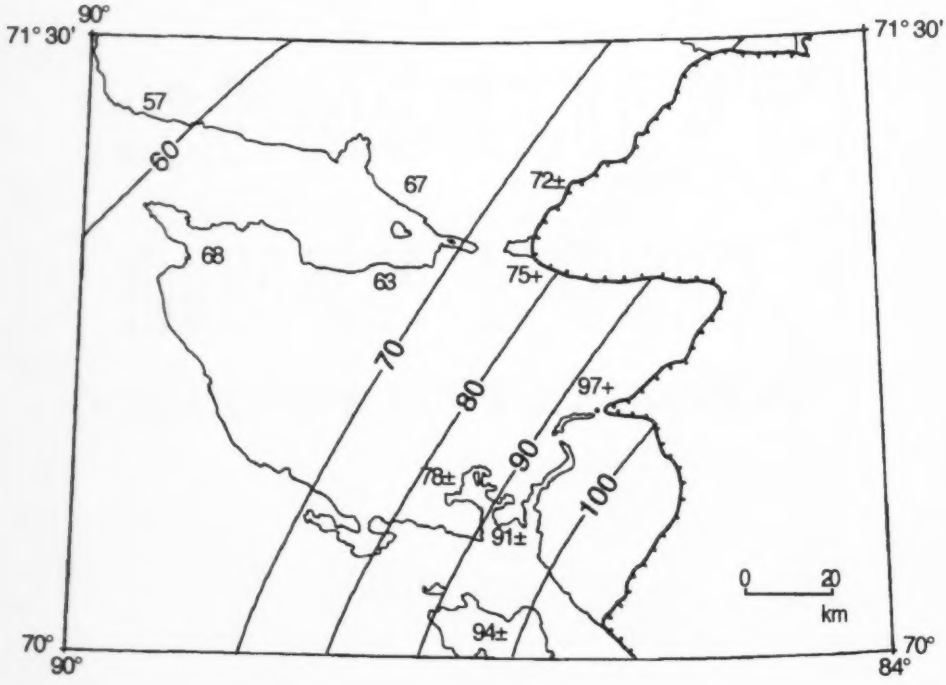

Figure 3-25. Isobases on the 7000 BP shoreline.

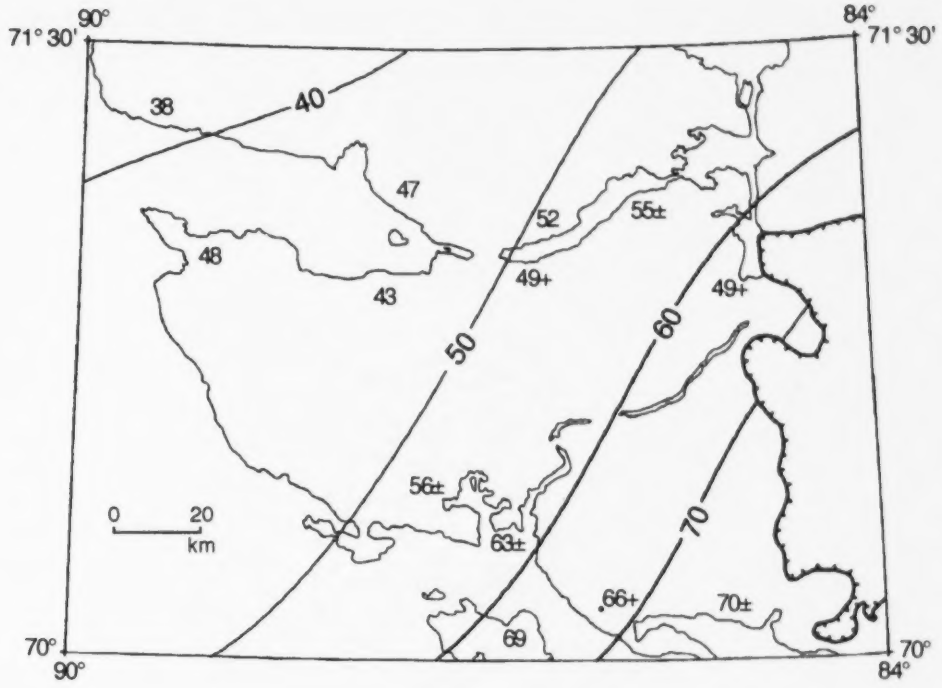

Figure 3-26. Isobases on the 6000 BP shoreline.

Discussion

The emergence curves display a normal exponential decline in sea level during the Holocene and are similar to others from formerly glaciated parts of Arctic Canada (e.g. Barr, 1971; Dyke, 1979,1984; Dyke et al., 1991 and others). The curves are normal in the sense that the rate of emergence decelerates smoothly from a maximum in the early postglacial period (Andrews, 1989). The emergence history is typical of Zone I of Clark et al., (1978) in which there is continual, though slowing, monotonic postglacial emergence. All Zone I curves have a similar shape (see below) but the total amount of emergence and the time of deglaciation varies. Much of Arctic Canada lies within Zone I (Andrews, 1989) except the outer fiords of eastern Baffin Island, where initial postglacial emergence is followed by a period of submergence. Andrews (1989) places the Zone I-II transition through the middle section of the eastern Baffin Island fiords. The amount of uplift due to thinning of the ice sheet prior to deglaciation, i.e. restrained rebound, is largely unknown.

The similarity in the form of uplift curves from Arctic Canada led Andrews (1968, 1970a) to develop a method of predicting uplift curves. He compared the form of 21 uplift curves from Arctic Canada, including one from the Bernier Bay southeast area, and found that their shape can be predicted by a function (Andrews, 1968) of the form:

$$U'p_t = \frac{A(1-i^t)}{(1-i)}$$

where $U'p_t$ is the uplift at time t after deglaciation, A is the total uplift multiplied by a constant that varies with the time of deglaciation and i is a constant having a value of 0.677 for Arctic Canada. Values of A and i were calculated from the 21 radiocarbon dated curves. In Andrews' (1968) study, sample elevations and marine limits were first corrected for eustatic rise in sea level based on the sea level curve of Shepard (1963), prior to deriving the values of A and i. The equation is significant because it allows accurate prediction of an entire curve from a single marine limit date.

The equation above was used to derive a predicted emergence curve for the Bernier Bay southeast area (Fig. 3-27). Only the height of marine limit (i.e. the total postglacial uplift) and the associated radiocarbon age were used. The predicted uplift curve was converted to a predicted emergence curve by subtracting the predicted uplift from the total uplift for each interval. Shepard's (1963) eustatic corrections (i.e. the ones used to derive constants in Andrews, 1968) were then removed to produce a relative sea level curve that agrees well with the form of the middle and lower part of the curve as revealed by the set of eight younger radiocarbon dates (Fig. 3-27). Despite this good prediction, well-dated multiple curves are still required to define any isobase irregularities.

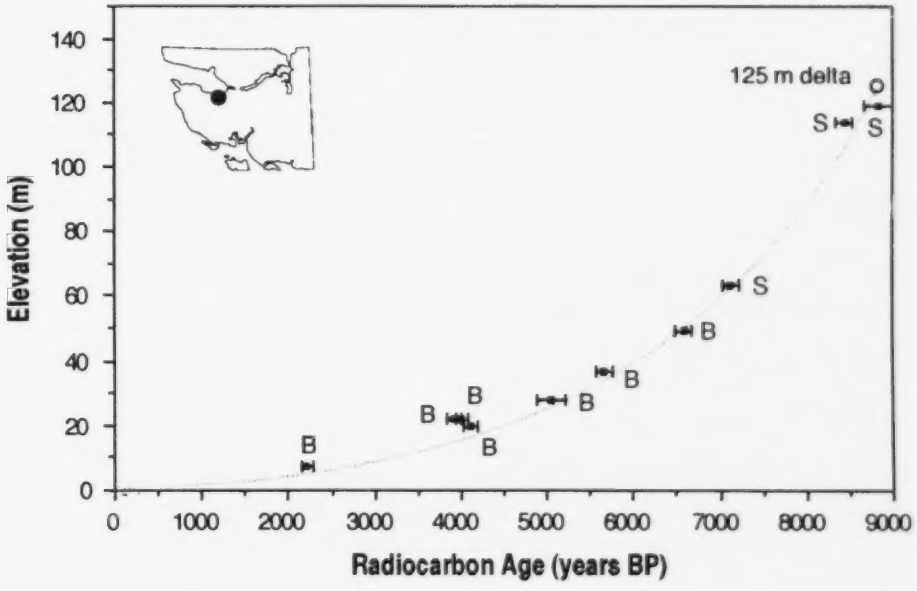

Figure 3-27. Predicted emergence curve for Bernier Bay southeast based on Andrews' (1968) method.

Emergence rates were measured using the well-controlled curve from Bernier Bay southeast. For the first 1000 years after deglaciation emergence occurred at about 3.5 m/century; in the last 1000 years the rate was an order of magnitude less, about 35 cm/century. The half-response time, the time during which half the remaining emergence is accomplished, is about 1800 years. Dyke et al., (1991) estimate the half-

response time of the Prince of Wales Island curves at 2000 years. The slightly shorter half-response time for the study area suggests more rapid isostatic recovery. The discrepancy suggests that the emergence curves, probably do not conform to a simple exponential function. Walcott (1970) suggests that the curves may conform to a complex function with two exponential terms. The departure from a simple exponential decay is accounted for in Andrews' (1968) method above by varying the constant in the equation according to the time since deglaciation.

No evidence was found for stable high sea levels following deglaciation, as occurred on eastern Ellesmere Island (England, 1983). Hence, the rate of emergence in the study area exceeded the eustatic rise throughout the postglacial. Eustatic sea level, as recorded by dated corals from Barbados, rose continuously but in steps from a minimum of -121 m at 17,000 BP but the most rapid rise occurred during two brief intervals (Fairbanks, 1989). During melt-water pulse IA, centred on 12,000 BP, sea level rose 24 m in less than 1000 years. The second interval of rapid rise is centred at 9,500 BP, melt-water pulse IB, when sea level rose 28 m (Fairbanks, 1989). Approximately 30 m of eustatic rise occurred between 9000 BP and 5000 BP (Fairbanks, 1989). Over the same interval, sea level in the study area fell by 100 m.

Several authors (Blake, 1975,1992; Dredge, 1990, 1991) have raised the possibility of minor marine transgressions or stepwise Holocene emergence. No geomorphic evidence was found in the area for temporarily stable relative sea levels or for transgressions. Instead only smooth exponentially declining forms can be used consistently for relative sea level curves. Although stepwise emergence or small transgressions are possible within the uncertainties of the radiocarbon data presented here, there is nothing to suggest events that are correlative between the curve areas. Attempting to fit such irregular curves to the radiocarbon data results in regionally inconsitent transgressions. If such adjustments did occur, their measurement would require techniques with more resolution than that employed here. Therefore, natural dating "noise" caused by the sinking of whale carcasses offshore or shells growing on the sea floor at variable depths below the corresponding sea level are the most conservative, hence preferred, explanation.

Raised shorelines in the study area tilt up, with increasing gradients, toward the southeast, whereas they are nearly level around Bernier Bay. Stronger tilting of shorelines is expected if the moraines marked the position of an ice margin unconfined by other ice masses. Geomorphic evidence indicates that Foxe and Brodeur ice were confluent along a broad zone of coalescence marked by the till sheet boundary parallel to the north side of Bernier Bay (Chapter 2). Since they were mutually buttressing, both ice masses were probably of similar thickness along this contact. The isostatic signature of two ice loads is expected to have been fully integrated into a single depression due to crustal rigidity. The depression created by the Brodeur Peninsula Ice Cap created a flattening of the isobase surface on the northwestern flank of the regional depression produced by the Foxe Dome. A similar effect was produced on the northeastern flank of the Foxe Dome by the Barnes Ice Cap (Dyke, 1974). Given a half-response time (the time for half the remaining emergence to be accomplished) of 1800 years, the early postglacial shorelines should carry an isostatic memory back to 13,000 BP (Dyke, pers. comm., 1995). Hence, the isobases reflect crustal loading conditions during the LGM implying that the Brodeur Peninsula Ice Cap is a maximal, as opposed to a residual, feature.

The widely spaced isobases over the northwestern part of the study area support the idea of a uniform ice cover with a low, flat profile during the last glaciation The small tilt of shorelines around Bernier Bay contrasts markedly with the very closely spaced isobases associated with the Cockburn Moraines on northeastern Baffin Island (Dyke, 1974; Miller and Dyke, 1974; Andrews, 1989). The lack of more pronounced shoreline tilts near the mouth of the bay is reasonable because ice from Bernier Bay was grounded offshore during the last glacial maximum, and had a gently sloping surface profile extending to the grounding line of an ice shelf in Prince Regent Inlet.

Comparison of bone and wood dates from three sites allow estimation of the marine reservoir effect for bowhead whales. The bone dates were first corrected for fractionation effects, assuming a $\partial^{13}C$ value of -15‰, the average for whalebone (see Appendix F). At Van Koenig Point, a date on a bowhead earbone from 4 m asl had an age of 1270 ± 60 BP (S-3099), 330 years older than a 3 m asl wood date at 940 ± 130 BP

(GSC-239) from the same area. Correcting for emergence (at 3.5 m/ka, from emergence curve) of 1 m gives an age of 1225 BP for the 4 m shoreline to suggesting a reservoir correction of 45 years for whalebone.

At Foss Fiord, an earbone from 38 m asl dated 5260 ± 90 BP (S-3345) while driftwood from 37 m asl dated 4680 ± 80 BP (GSC-5077). Correcting for 1 m of emergence, gives an age of 4780 BP for the 38 m shoreline, suggesting a reservoir correction of 480 years for whalebone.

At Crown Prince Frederick Island, an earbone from 72 m asl dated 6510 ± 130 BP (S-3433) while driftwood from 68 m asl dated 5870 ± 70 BP (GSC-5295). Correcting for 4 m of emergence yields an age of 6025 BP for the 72 m asl shoreline, suggesting a reservoir correction of 485 years for whalebone.

Also, at Crown Prince Frederick Island, a walrus tusk from 41 m asl dated 4940 ± 70 BP (TO-5016). This is similar to a wood date from 34.5 m asl of 4210 ± 170 BP (GSC-5294). Correcting for 6.5 emergence (from curve) yields an age for the 41 m shoreline of 4710 BP, suggesting a reservoir correction of 230 years for walrus. The above values should be considered maximum preliminary estimates and more precise measurement is possible with greater numbers of bone-wood pairs (Dyke et al., in prep.).

The reliability of whalebone dates was good with only 7 out of 57 falling more than 5 m below the emergence curves. This validates the original assumptions of the method that sinkage is general no more than the keel depth of a floating bowhead carcass. Contamination of bones is not a problem as long as the earbones are used.

Conclusions

The emergence history of the study area is characterized by exponentially declining emergence rates during the postglacial. The time-transgressive marine limit varies in elevation from 92 to 138 m asl. Differential emergence was most pronounced during the period of initial rapid emergence that followed deglaciation.

Emergence in the first 1000 years following deglaciation occurred at about 3.5 m/century. During the last 1000 years the rate dropped to 35 cm/century. The rate of ongoing emergence is probably similar.

Within the constraint provided by the radiocarbon dates, the relative sea level curves indicate a continuous, exponential decline in sea level with a half-response time of about 1800 years. Non-glacioisostatic tectonic movements do not appear to have influenced its emergence history. Hence, local emergence curves can be adequately predicted from height and age of marine limit. This technique is applicable to other areas for reconnaissance purposes. However, more radiocarbon dates on lower shorelines would be needed to ensure that the signals, if any, of tectonic movements are detected and to ensure that Andrews' (1968) equation is a good predictor elsewhere.

Shorelines tilt up toward the center of loading in Foxe Basin and shoreline gradients increase in the same direction. Crustal deformation, as expressed by the tilt on raised shorelines, is normally expected to be most pronounced near the ice margins. Here tilt increases toward the centre of loading and was modest in the area furthest from the centre of the Foxe Dome due to loading by the Brodeur Peninsula Ice Cap to the north. The isobase pattern suggests: 1) that the Brodeur Peninsula Ice Cap was a LGM feature, not a deglacial remnant, and 2) that the isostatic depression caused by ice in Bernier Bay extended offshore into Prince Regent Inlet.

References

Andrews, J.T., 1968. Postglacial rebound in Arctic Canada: similarity and prediction of uplift curves. *Can. J. Earth Sci.* 5(39):39-47.

Andrews, J.T., 1970a. *A geomorphological study of post-glacial uplift with particular reference to Arctic Canada.* Institute of British Geographers, Special Publication No. 2, 156 p.

Andrews, J.T., 1970b. Differential crustal recovery and glacial chronology (6700-0 BP), west Baffin Island, N.W.T., Canada. *Arct. Alp. Res.* 5:185-200.

Andrews, J.T., 1986. Elevation and age relationships, raised marine deposits and landforms in glaciated areas: examples based on Canadian Arctic data. In O. van de Plassche, (ed.) *Sea Level Research: a Manual for the Collection and Evaluation of Data*, Geo Books, Great Britain, p. 67-90.

Andrews, J.T., 1989. Quaternary geology of the northeastern Canadian Shield. In *Quaternary Geology of Canada and Greenland*. R.J. Fulton (ed.), Geological Survey of Canada, Geology of Canada, no. 1, p. 276-317.

Andrews, J.T. and Dugdale, R.E., 1970. Age prediction of raised strandlines based on their gradients. *Geol. Soc. Am. Bull.* 81:3769-3772.

Barr, W., 1971. Postglacial isostatic movement in northern Devon Island: a reappraisal. *Arctic* 24: 249-268.

Basham, P.W., Forsyth, D.A. and Wetmiller, R.J., 1977. The seismicity of northern Canada. *Can. J. Earth Sci.* 14:1646-1667.

Blake, W., Jr., 1975. Radiocarbon age determinations and postglacial emergence at Cape Storm, Southern Ellesmere Island, Arctic Canada. *Geografiska Annaler* 57A: 1-71.

Blake, W., Jr., 1992. Holocene emergence at Cape Herschel, east-central Ellesmere Island, Arctic Canada: implications for ice sheet configuration. *Can. J. Earth Sci.* 29:1958-1980.

Cathles, L.M., 1975. *The Viscosity of the Earth's Mantle*. Princeton University Press, 386 p.

Clark, J.A., Farrell, W.E. and Peltier, W.R., 1978. Global changes in postglacial sea level: a numerical calculation. *Quat. Res.* 9:265-287.

Craig, B.G., 1965. Notes on moraines and radiocarbon dates in northwest Baffin Island, Melville Peninsula and northeast District of Keewatin. *Geol. Surv. Can. Pap.* 65 20, 7 p.

Dredge, L.A., 1990. The Melville Moraine: sea-level change and response of the western margin of the Foxe Ice Dome, Melville Peninsula, Northwest Territories. *Can. J. Earth Sci.* 27: 1215-1224.

Dredge, L.A., 1991. Raised marine features, radiocarbon dates, and sea level changes, eastern Melville Peninsula, Arctic Canada. *Arctic* 44(1):63-73.

Dyck, W., Fyles, J.G. and Blake, W., Jr., 1965. Geological Survey of Canada Radiocarbon Dates V. *Radiocarbon* 7:24-46.

Dyck, W., Lowdon, J.A., Fyles, J.G. and Blake, W., Jr., 1966. Geological Survey of Canada Radiocarbon Dates V. *Geol. Surv. Can. Pap.* 66-48, 32 p.

Dyke, A.S., 1974. *Deglacial Chronology and Uplift History: Northeastern Sector, Laurentide Ice Sheet.* Colorado University Institute of Arctic and Alpine Research, Occasional Paper No. 12, 113 p.

Dyke, A.S., 1979. Radiocarbon dated Holocene emergence of Somerset Island, central Canadian Arctic. In Current Research, Part B, *Geol. Surv. Can. Pap.* 79-1B, p. 307-318.

Dyke, A.S., 1984. Quaternary geology of Boothia Peninsula and northern District of Keewatin, Central Canadian Arctic. *Geol. Surv. Can.* Memoir 407, 26 p.

Dyke, A.S., 1993. Glacial and sea level history of Lowther and Griffith Islands, Northwest Territories: a hint of tectonics. *Geographie physique et Quaternaire* 47(2): 133-145.

Dyke, A.S. and Dredge, L.A., 1989. Quaternary geology of the northwestern Canadian Shield. In *Quaternary Geology of Canada and Greenland*. R.J. Fulton (ed.), Geological Survey of Canada, Geology of Canada, no. 1, p. 189-214.

Dyke, A.S. and Morris, T.F., 1990. Postglacial history of the bowhead whale and of driftwood penetration: implications for paleoclimate, Central Canadian Arctic. *Geol. Surv. Can. Pap.* 89-24, 17 p.

Dyke, A.S., Morris, T.F. and Green, D.E.C., 1991. Postglacial tectonic and sea level history of the central Canadian Arctic. *Geol. Surv. Can. Bull.* 397, 56 p.

Dyke, A.S., McNeely, R.N. and Hooper, J., in prep. Indirect assessments of marine reservoir corrections for bowhead whale radiocarbon dates.

England, J., 1983. Isostatic adjustments in a full glacial sea. *Can. J. Earth Sci.* 20:895-917.

England, J., 1992. Postglacial emergence in the Canadian High Arctic: integrating glacioisostasy, eustasy, and late deglaciation. *Can. J. Earth Sci.* 29(5):984-999.

Fairbanks, R.G., 1989. A 17,000-year glacio-eustatic sea level record: influence of glacial melting rates on the Younger Dryas event and deep-ocean circulation. *Nature* (342):637-642.

Falconer, G., Ives, J.D., Løken, O.H. and Andrews, J.T., 1965. Late Wisconsin end moraines in northern Canada. *Science* 147:608-610.

Farrell, W.E. and Clark, J.A., 1976. On postglacial sea level. *Geophysical Journal of the Royal Astronomical Society* 46: 647-726.

Hooper, J., 1990. *Late Quaternary glacial and sea level history of the Bernier Bay area, northwestern Baffin Island, N.W.T.* Unpublished MSc. Thesis, 92 p.

Kerr, J.W., 1980. Structural framework of the Lancaster Aulocogen, Arctic Canada. *Geol. Surv. Can. Bull.* 319, 24 p.

Mangerud, J. and Gulliksen, S., 1975. Apparent radiocarbon ages of recent marine shells from Norway, Spitsbergen, and Arctic Canada. *Quat. Res.* 5:263-273.

McNeely, R. and Jorgensen, P.K., 1992. Geological Survey of Canada Radiocarbon Dates XXX. *Geol. Surv. Can. Pap.* 90-7, 84 p.

Miller and Dyke, 1974. Proposed extent of Late Wisconsin Laurentide Ice on eastern Baffin Island. *Geology* 2: 125-130.

Shepard, F.P., 1963. Thirty-five thousand years of sea level. *Essays in Marine Geology*. University of Southern California Press, Los Angeles, pp. 1-10.

Walcott, R.I., 1970. Isostatic response to loading of the crust in Canada. *Can. J. Earth Sci.* 7: 716-726.

Walcott, R.I., 1972. Past sea levels, eustasy and deformation of the earth. *Quat. Res.* 2:1-14.

Chapter 4:
Paleoclimatic Significance of Postglacial Whale and Walrus Fossils

Introduction

This chapter presents data on the relative abundance of fossils of bowhead whales (*Balaena mysticetus*) walrus (*Odebenus rosmarus*) and driftwood pieces (*Picea* sp.) on raised beaches of northwest Baffin Island. The original impetus for the research was the reconstruction of the Holocene relative sea level history based on radiocarbon-dated organic samples, primarily whale bones, from raised shorelines. Nearly half of the samples collected were dated. In addition to their value for measuring relative sea level change, the abundance of bones on radiocarbon-dated shorelines constitutes a record of the number of whales and walruses entering the area during postglacial time. Climatic and oceanographic conditions governed the extent of summer sea ice, which in turn controlled the occupation of the area by marine mammals.

The study area extends from Bernier Bay and Berlinguet Inlet in the north to Autridge Bay and Whyte Inlet in the south and lies generally west of Fury and Hecla Strait (Fig. 1-1). The area has an arctic climate with long, cold winters and short cool summers. Pack ice in marine channels bordering the field area is extensive and it is not until late summer and fall, when temperatures are already declining, that large areas of open water exist. Committee Bay, to the south, rarely opens.

Deglaciation started about 9000 BP with the calving of an extensive ice shelf or ice stream which occupied the Gulf of Boothia and Prince Regent Inlet (Dyke and Prest, 1987). This was followed by the Cockburn Substage (Andrews and Ives, 1963), during which a series of large moraines were deposited around the perimeter of the Foxe Dome, one of three primary ice dispersal centres of the Laurentide Ice Sheet. The moraine system includes the Cockburn Moraines on the northeast coast of Baffin Island, the Bernier Bay Moraines (Chapter 2) and the Melville Moraine on western Melville Peninsula (Dredge, 1990). Deposition of the moraines reflects a period of ice marginal stability along the western and

northern margins of the Foxe Dome. Stabilization of the margin at these moraines was a result either of the establishment of a terrestrial margin, i.e. after marine-based portions of the ice sheet had calved, a shift in climate resulting in positive mass balance conditions on the Foxe Dome, or both.

The moraine-building episode ended about 6500 BP. Ice in the interior of the study area retreated progressively and the entire area was deglaciated by 5500 BP (Fig. 2-14). The formation of the Holocene marine limit occurred at the instant of deglaciation. The 8500 BP shoreline is at 120 m asl in the north, around Bernier Bay, and at 138 m asl in the south. Flights of raised beaches are a common feature of the terrain below marine limit.

Past and Present Distribution of Bowheads

The distribution of bowhead whales is known from reports of recent sightings and records from the period of historic whaling 1719-1915 (Ross, 1979; Reeves et al. 1983; Burns et al., 1993). The bowhead whale, also called the Greenland right whale, is a baleen whale, up to 20 m long, adapted to an ice-edge environment. Bowheads are migratory, following the pack ice-edge northward in summer and southward in winter.

The remaining bowheads in Canadian Arctic waters consist of three stocks. The largest is in Bering Strait and the Beaufort Sea. Two stocks occur in eastern waters. One, the Davis Strait stock, winters along the pack ice edge between Labrador and West Greenland and migrates northward to Lancaster Sound, Admiralty Inlet and Prince Regent Inlet in summer. Another, smaller stock migrates through Hudson Strait to summer feeding grounds in northern Hudson Bay and Foxe Basin. Like other whales, the bowhead populations suffered considerable depredations during the period of historic whaling. Presently, the Bering Strait stock consists of about 7000 individuals, and the two stocks of the eastern arctic consist only of a few hundred individuals (Reeves et al., 1983).

It is not known whether the Davis Strait and Hudson Bay groups constitute biologically distinct populations. Some interbreeding may

occur since they share the same winter range. A fall migration route from the Gulf of Boothia through Fury and Hecla Strait to northern Foxe Basin has been speculated upon and would connect the Davis Strait and Hudson Bay stocks, if it exists (Reeves et al., 1983). Presently, there appears to be little likelihood of interchange between the Bering Strait stock and the eastern Arctic stocks. Summer sea ice conditions in the Central Arctic channels form an effective barrier separating eastern and western populations of bowhead whales as well as belugas, narwals, walrus and possibly seals (Harington, 1966). Dyke and Morris (1990) suggest that the Bering Strait and Davis Strait/Hudson Bay stocks have been effectively isolated for at least 3000 years.

Most of the bowhead skulls found were those of mature animals and from 180 to 200 cm in width (between ends of temporal processes). Hence, the most likely, though undifferentiated, causes of mortality in the sampled population are disease, old age and occasional ice entrapment, but not Inuit hunting. Bowheads are not subject to the enigmatic mass strandings as are some other whale species. However, they may become disoriented and strand in shallows with muddy bottoms which confuse their echolocation system (Barr, 1971). On the west side of Prince Regent Inlet, on Somerset Island, there is extensive evidence for the hunting of bowhead whales by Thule eskimos (McCartney and Savelle, 1985). From the size of the skulls, it is apparent that the Thule hunters preferred to take young bowheads for reasons of safety and ease of handling. McCartney and Savelle (1985) conservatively estimate the total number of Thule-killed bowheads represented in the Somerset Island archeological assemblage at 1000 to 1500. These whales were likely taken since 1000 A.D. Ice conditions in southern Prince Regent Inlet and the Gulf of Boothia appear to have prevented Thule whaling in the study area. Most of the whale bones collected in this study represent mature individuals that died of the aforementioned "natural" causes before 1000 BP. Several whalebone houses were found in the course of fieldwork; no skulls from these sites were sampled.

Dyke and Morris (1990) discussed the abundance of bowhead whales in the Central Arctic, primarily from their work on Prince of Wales Island. They found that large numbers of bowheads colonized the area as soon as it was deglaciated, with a dramatic peak in the number of

bowhead bones on beaches formed during the interval 11,000 to 8500 BP. Apparently, the ice-edge habitat preference of the bowhead is applicable to calving marine margins of an ice sheet as well as the edge of pack ice. Three other intervals were identified (Table 4-1).

Table 4-1. Postglacial abundance of whale bones and driftwood on raised beaches of Prince of Wales Island (Dyke and Morris, 1990).

Interval (ka BP)	Whalebone	Driftwood	Environmental Significance
11-8.5	abundant	absent	warm, deglaciation interval
8.5-5	absent	rare	cool, increasing sea ice
5-3	common	common	warmer than present
3-present	rare	abundant	cooler than present

An apparent contradiction in the record is the abundance of whales in the 11,000 to 8500 BP interval, at a time when driftwood was excluded. This has been explained by meltwater-driven currents which flowed out from the Archipelago. Such currents would have excluded driftwood while facilitating the entry of whales (Bering Strait bowheads initially) to the archipelago by exporting sea ice (Dyke and Morris, 1990).

Driftwood

Driftwood has been used to date raised shorelines and as a paleoenvironmental indicator on Ellesmere Island (Blake, 1972; Stewart and England, 1983), Prince of Wales Island (Dyke and Morris, 1990) and in Svalbard (Häggblom, 1982). Supply of wood to the Arctic Ocean is by large rivers of the circumpolar region, especially those of Siberia. Northward shifts in the position of treeline and degradation of permafrost along river channels increase the supply of wood. The wood is rafted by sea ice which is carried by ocean currents during its residence in the ocean. Sea ice rafting is required since the wood becomes waterlogged and sinks within two years whereas the drift takes approximately five years (Häggblom, 1982). Currents, winds, sea ice conditions and the configuration of coastlines and channels further influence the amount of driftwood stranding along a particular coastline. Hence, the paleoenvironmental signal provided is difficult to interpret.

Methods

Fieldwork was conducted during four seasons (1988-1991) utilizing camps located in coastal areas so the modern high tide line could be used as a benchmark for altimeter surveys. About half of the field time was spent surveying and investigating raised beaches for dateable materials.

When searching raised beaches, the intention was to obtain samples spanning the entire elevation range between sea level and marine limit. After good samples had been collected from a particular elevation, more time was spent searching at higher (or lower) elevations. Thus, the search pattern was not strictly random. Often, in the course of travelling to and from the modern beach to measure bone elevations, more bones were found on lower beaches. Given the large areas of raised beaches, the whale bones sampled probably represent only a fraction of the material present. Because of the priority placed on collecting samples from unique elevations (so that as many raised shorelines as possible would be dated), the relative numbers of bowheads from beaches with many whale bones are likely underrepresented.

Whenever possible earbones were collected from bowhead skulls. The earbone assemblage consists of a pair of periotic bones and otic capsules and is the best material from this animal for radiocarbon dating (Barr, 1971; Dyke et al., 1991). Unlike most other parts of the skeleton, the earbones are extremely dense and largely devoid of visible pore spaces. Pore spaces in other bones were commonly filled with humus and riddled by plant rootlets. These contaminants, containing radiometrically young carbon, were difficult to remove entirely. Only rarely were both periotic bones and both otic capsules retrieved from a single skull.

The radiocarbon dates (Table 3-1) were used to draw 12 emergence curves for different parts of the coast. This sea level history is the topic of a separate paper (Chapter 3), but the curves are used herein to assign minimum ages to undated bones. The method relies on the assumption that the number of bones, or skeletons, on beaches is a reflection of the number of whales present at a given time. Because the bowhead is migratory, these bones actually record the number of animals that died during the summer, the period of open water or loose ice between August

and September, in the northern part of their summer range. Also, each occurrence of bone is treated as though it represents a single animal and there is some possibility that different parts of the same skeleton were found at different sites. However, most of the finds were bowhead cranial bases, essentially the back of the skulls. These necessarily represent individual whales.

Results

In total, 139 samples of bowhead whale bone, a small narwal tusk, 18 walrus tusks and bones, and four driftwood pieces were gathered. Of these, 56 bowhead whale bones, four walrus tusks, and all four driftwood pieces were dated (Table 3-1; Fig. 3-6). Minimum ages were assigned to the undated whale and walrus bones by interpolating their ages from the local emergence curves (Chapter 3). Age assignments for undated bone are listed in Appendix H.

Four intervals are recognized in the postglacial record (Fig. 4-1). The earliest penetration of marine molluscs into the area occurred immediately upon deglaciation of Prince Regent Inlet and the Gulf of Boothia around 9000 BP. Between 9000 and 7000 BP, marine molluscs flourished but no bowheads or driftwood entered the area even though they were abundant less than 100 km farther north along the Prince Regent coast of Baffin Island (A.S. Dyke, pers. comm., 1994). Thus, during this interval, Prince Regent Inlet from the mouth of Bernier Bay south was likely blocked by sea ice.

Between 7000 and 4000 BP, bowheads, walrus and some driftwood entered the area. Figure 4-2 shows the approximate configuration of the sea and the margin of the Early Barnes Ice Cap at 6500 BP (cf. Chapters 2 and 3). At that time, there were three possible routes for whales entering the study area. Bowheads could swim south along Prince Regent Inlet and then either east into Bernier Bay and Berlinguet Inlet or south along the Gulf of Boothia coast. The east end of Berlinguet Inlet was deglaciated about 6500 BP after which bowheads would have been able to access the Gulf of Boothia from Admiralty Inlet via Berlinguet Inlet and Bernier Bay. This would have remained a viable access route until emergence of the isthmus separating Bernier Bay and Berlinguet Inlet.

The center of the isthmus is at about 10 m asl so Brodeur Peninsula was a large island until 2000 BP or later. Finally, some whales may have entered the area from Foxe Basin via Fury and Hecla Strait which became free of glacial ice between 6900 and 6500 BP (Dredge, 1990; Chapter 3).

The valley connecting Bell Bay to the head of Nybøe Fiord via Saputing and Ivisarak Lakes was blocked by glacier ice until after 6500 BP. By this time sea level had fallen below 66 m asl, the elevation of the valley floor west of the south end of Saputing Lake.

The oldest whalebone date was obtained on an earbone collected from a raised beach at 49 m asl (6585 ± 105 BP, S-3013) and is older than expected from its elevation. Nine other whale bones were found at higher elevations, up to 74 m asl[1], so the first bowheads probably entered Prince Regent Inlet, the Gulf of Boothia and Bernier Bay several hundred years earlier. The number of whale carcasses stranding on beaches in the area increased gradually until about 4000 BP (Fig. 4-1). Of the total 139 dated and undated specimens, 54 (39%) are from this 7000 to 4000 BP interval.

Between 4000 and 3000 BP, the number of strandings reached its postglacial maximum. During this 1000 year period, 59 (42%) of the finds stranded. The rate of strandings was at least three times as high during this period as during the preceding and subsequent intervals.

After 3000 BP, the numbers of bowheads dropped to levels slightly below those of the 7000 to 4000 BP period. Only 25 (18%) of the finds date from this interval. Interestingly, no whale bone dates were obtained in the age range 500 BP to the present, nor were any whale bones found at elevations corresponding to this interval, although some have been found along the coast of Admiralty Inlet (Dyke, pers. comm., 1994) to the north. Consequently, the number of carcasses stranding along coasts in the field area reached its late Holocene minimum *prior* to the period of historic and Thule whaling.

Many Thule and/or historic eskimo winter houses were encountered at low elevations (< 10 m asl) in the field area. Many of these contained bowhead skulls and ribs. It is not known whether these skulls represent

[1] Samples were selected for dating on the basis of quality (i.e. extent of contamination). Hence the highest (oldest) bones were not always selected.

animals which were killed in the course of Thule whaling or whether they are skulls of animals which died naturally and were later collected as building material. No bones from Thule habitation sites are included in Figure 4-1 or Appendix H. Two sites provide evidence that these people searched for, and retrieved, fossil material from raised beaches. In one instance, half a bowhead mandible was found which had been excavated from the beach and then left at the surface, presumably with the intention of returning to the site after the bone had been cleaned by the elements. Earbones were collected from an apparently undisturbed bowhead skull found near this site and dated 5520 ± 70 (S-3098). In the other instance, a mandible had been excavated and the anterior end sawn off and removed. Earbones were also collected from a skull at this site but were not dated.

The spatial distribution of whale bone is not uniform. Most of the skulls were found on the coasts of Bernier Bay, Berlinguet Inlet, Bell Bay and the northeast coast of the Gulf of Boothia between Van Koenig Point and Foss Fiord (Fig. 3-6). Five skulls were found on Crown Prince Frederick Island. No whalebone was found east of Nybøe Fiord despite extensive searching, nor are whale bones, walrus tusks or driftwood reported from western Melville Peninsula (Dredge, 1991). However, numerous whale bones occur at Thule sites along the eastern (Foxe Basin) coast of the peninsula (Ross, 1974). Sea ice drifting southward down Prince Regent Inlet tends to accumulate in the southern Gulf of Boothia (cf. the typical distribution of sea ice shown in Fig. 1-4). Hence, sea ice conditions in this channel become increasingly severe southward, effectively excluding bowheads from the southeastern part of the study area.

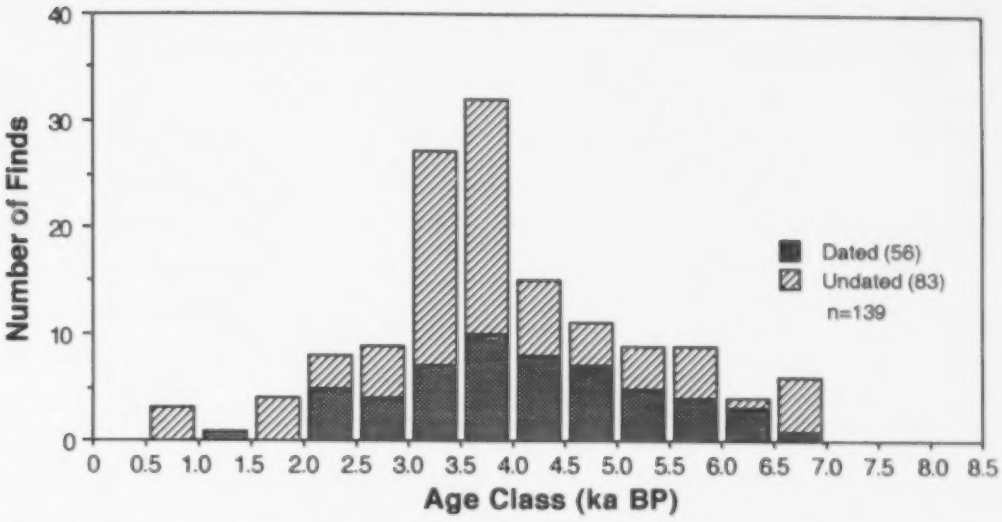

Figure 4-1. Abundance of whale bones on raised beaches. Ages assigned to undated samples are minimum ages.

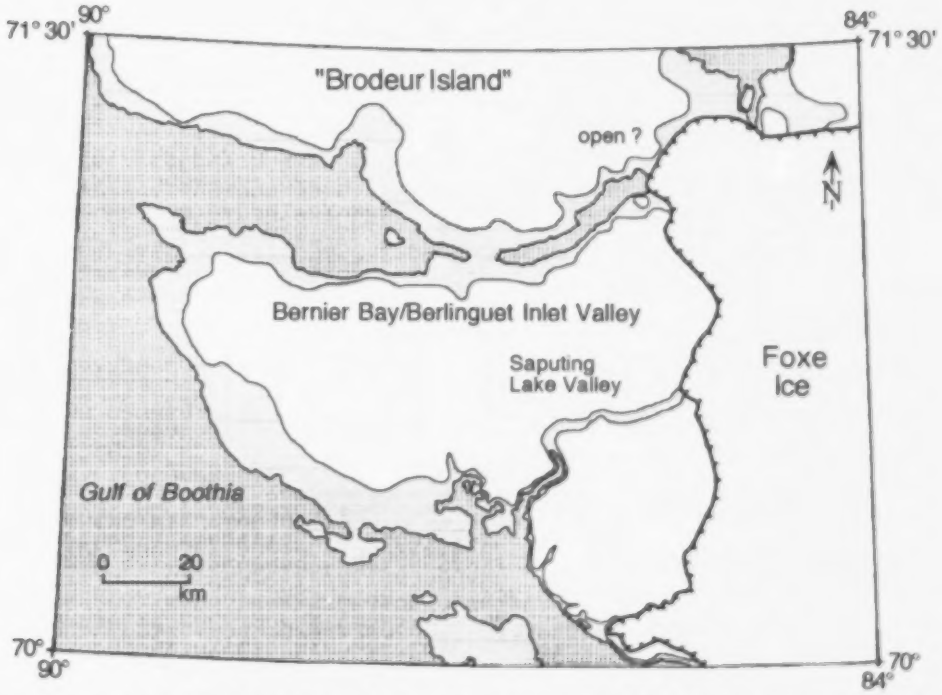

Figure 4-2. Paleogeography of the study area at 6500 BP. The area of marine overlap is based on local emergence curves and contour data (cf. Chapters 2, 3). Dark shading is the modern sea, lighter shading is the 6500 BP sea.

The histogram of walrus abundance (Fig. 4-3) generally resembles that of bowheads though walrus fossils are much less numerous. The field area is presently well within the range of Atlantic walrus (Harington, 1966; Perry, 1967) but it seems that the area has never sustained a large walrus population, if such can be inferred from the scarcity of walrus fossils on raised beaches. Unlike bowheads, walrus sink after death and may be greatly underrepresented in beach sediments. There is also greater risk in assigning minimum ages to undated walrus fossils than bowhead fossils because of their lower stranding potential (A.S. Dyke, pers. comm., 1994) and because they may wander inland before dying (Dyke, 1979a and unpublished radiocarbon dates). The earliest documented penetration of walrus into the study area is recorded by a date of 6200 ± 80 BP (S-3093) on the skull of an immature animal. The skull was found on a raised beach at 38 m asl and was slightly older than expected for its elevation. The peak in walrus abundance occurs between 4000 to 5000 BP. No material was found for the interval 500 to 3000 BP. There is limited evidence that these animals may have recently extended their range as recorded by three finds of walrus tusks (undated) just above the modern high tide line.

The greatest abundance of both walrus and bowheads occurred during the interval 3000 to 5000 BP. However, the maximum abundance of walrus appears to have occurred earlier, between 4000 and 5000 BP, whereas the maximum abundance of bowheads occurred between 3000 and 4000 BP. Hence, the expansion of walrus into the area in response to less severe sea ice conditions may have occurred more quickly than the expansion of bowheads in response to the same environmental change. Alternatively, walrus may be more tolerant of ice than bowheads. The closest modern population of Atlantic walrus is in northern Foxe Basin where they overwinter in a large polynya (Smith and Rigby, 1981; Stirling et al., 1981). If this population was also large during the mid Holocene, wanderers may have travelled westward, reaching the field area via Fury and Hecla Strait. Indeed, the radiocarbon dates reported here may reflect the establishment of this polynya, and its related walrus population, shortly after deglaciation of Foxe Basin ca. 6900 BP.

Most of the walrus tusks were found on Van Koenig Point where a large scatter of walrus bones, appearing to represent near-complete skeletons of several individuals, was found at a hilltop site. The extraordinary abundance of bones suggests that the site may have been a hauling-out beach or rookery. When occupied by walrus, the hilltop was a small sandy island. A few tusks were found on the northeast coast of the Gulf of Boothia and Crown Prince Frederick Island. Also, a mandible and some low-elevation tusks were found near Morin Point. Finally, one tusk was found on the south shore of Berlinguet Inlet just above the modern high tide line.

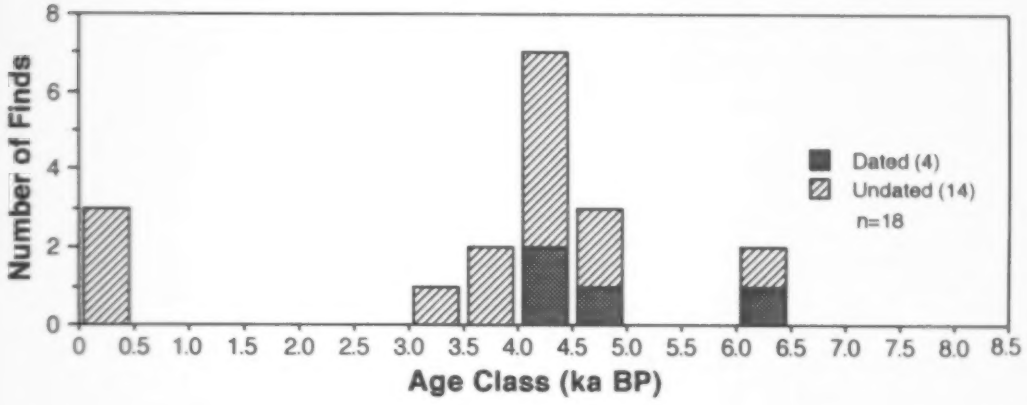

Figure 4-3. Relative abundance of walrus during the postglacial interval. Ages assigned to undated specimens are minimums.

All four pieces of driftwood were found on Crown Prince Frederick Island and, to the north, on the adjacent coast of Baffin Island (Fig. 3-6). Wood was not found on the raised beaches around Bernier Bay and Berlinguet Inlet. The earliest penetration of driftwood is recorded by a date of 5870 ± 70 BP (GSC-5295) on a small log found at 68 m asl on Crown Prince Frederick Island. One piece of driftwood was found on a raised beach at Thiboult Bay by B.G. Craig (Dyck et al., 1965). Because so little wood was found, it is difficult to draw meaningful inferences from it. The distribution of wood suggests that it drifted south down Prince Regent Inlet to strand on the Gulf of Boothia coast. The presence of driftwood on Prince of Wales Island was interpreted as indicating coverage of marine channels by moving pack ice (Dyke and Morris, 1990)

and similar conditions are assumed for the study area. The scarcity of wood in the area is not surprising because the wood would have to drift through Barrow Strait or Lancaster Sound before drifting south down Prince Regent Inlet. During this journey, the wood would have considerable opportunity to strand on other, more exposed, coasts. Driftwood is common, though not particularly abundant, on modern beaches in the area.

Discussion

Variations in the number of bowhead fossils on raised beaches with elevation could be due to (a) changes in the absolute size of the Davis Strait bowhead stock or (b) changes in its summer range which was largely controlled by summer sea ice severity. It is possible that the large numbers of bones from the early Holocene on Prince of Wales Island and the mid Holocene on Prince of Wales, Somerset and Baffin Islands represent much larger bowhead populations than existed in the historic period. Nevertheless, sea ice conditions, which became more severe during periods of climatic cooling, appear to have been the main control on bowhead occupation of channels in the central Arctic.

None of the bowheads of the early Holocene population documented in the central Arctic Islands (Dyke and Morris, 1990) and in Lancaster Sound and Prince Regent Inlet reached the field area. Hence, sea ice conditions were likely severe in the period (9000 to 7000 BP), following deglaciation. This is in marked contrast to the record from Prince of Wales Island where bowheads lived in close proximity to the retreating margin of the Laurentide Ice Sheet (Dyke and Morris, 1990). The gradual increase in bowhead numbers in the field area during the subsequent interval (7000 to 4000 BP) suggests slowly improving sea ice conditions.

The mid Holocene bowhead and walrus peak, 5000 to 3000 BP, is most likely a response to less severe sea ice conditions. This peak in bowhead numbers correlates well with the mid Holocene peak in the bowhead population of Prince of Wales Island (Dyke and Morris, 1990). Hence, the mid Holocene was a period of increased numbers of whales throughout their summer range in response to warmer than average summer temperatures and diminished sea ice cover. During this same

interval, the remnant Laurentide ice (the proto-Barnes Ice Cap) retreated from the fiord heads of eastern Baffin Island.

The onset of cooler conditions records the beginning of the Neoglacial about 3000 BP which resulted in a sharp decline in bowhead use of these channels. The same pattern was observed in the Prince of Wales Island bowhead record (Dyke and Morris, 1990). This cool period is also apparent in the pollen record of Baffin Island (Short et al., 1985). Cooling is also recorded by ice-cored terminal moraines of alpine glaciers and ice caps on eastern Baffin Island which advanced to their late Holocene maximum positions during this interval (Davis, 1985). An early Holocene warm interval is recorded by rapid retreat of the outlet glaciers of the Penny Ice Cap on southeastern Baffin Island followed by a period of moraine stabilization beginning at 3200 BP and the onset of Neoglacial conditions by 2100 BP (Dyke, 1979b). A similar pattern was recorded by lichenometric studies of moraines on southeastern Baffin Island (Miller, 1973).

In the Flint Lake area, Andrews (1970) identified a major depositional event during the Flint Phase at about 5000 BP, marking the end of the hypsithermal. This was followed by the King Phase which was a Neoglacial readvance of the western margin of the Barnes Ice Cap. The stabilization of the King Phase moraines following renewed glacier retreat was lichenometrically dated at 1700 BP (Andrews and Webber, 1964). The record of bowhead fossils suggests that the Flint Phase was a period of reduced summer sea ice. Hence, deposition of the Flint Moraines may be more a response to increased precipitation on the Barnes Ice Cap brought about by more open water conditions in the central Arctic and possibly Baffin Bay rather than the onset of Neoglacial conditions.

The peak in the number of bowheads between 5000 and 3000 BP and their subsequent gradual decline can also be correlated with the paleoclimatic record ($\partial\ ^{18}O$) of ice cores from the Devon Island Ice Cap, which reveals a prolonged cooling trend from a mid Holocene optimum at 5000 BP (Koerner, 1977; Paterson et al., 1977).

The earliest entry of whales to the study area probably occurred through Prince Regent Inlet, possibly while the east end of Berlinguet Inlet was still blocked by glacial ice. After this ice calved, whales could also enter the area via Admiralty Inlet. Raised beaches along Admiralty

Inlet have very large numbers of bowhead whale skeletons (Dyke, pers. comm., 1991). For reasons as yet unknown, Admiralty Inlet appears to have been occupied (in summer) by more bowheads than any other water body in the central Arctic. One possibility is that melting ice of the proto-Barnes ice cap persisted on plateaux bordering the head of the inlet. Large quantities of meltwater flowing north out of the inlet may have kept sea ice cover to a minimum. This is the same mechanism proposed to explain the abundance of early Holocene bowheads in channels bordering Prince of Wales Island by Dyke and Morris (1990). Differences in the distribution of walrus fossils suggest that Fury and Hecla Strait was likely a more important access route for walrus than for bowheads.

The complete absence of whale bone east of Nybøe Fiord, and on western Melville Peninsula, suggests that this area has been prone to sea ice conditions sufficiently severe to exclude these animals throughout the postglacial. Contrary to the theory of whalers (Reeves et al., 1983), Fury and Hecla Strait does not appear to have been a significant migration route for whales of the Davis Strait stock returning to the south via Foxe Basin, nor is there evidence for an interchange between the Davis Strait and Hudson Bay bowhead stocks via this channel during the Holocene. A less likely explanation is that the occupation of the Gulf of Boothia and Fury and Hecla Strait by migrating bowheads was so brief that they suffered no significant mortality in these waters.

References

Andrews, J.T., 1970. Differential crustal recovery and glacial chronology (6700-0 BP), west Baffin Island, N.W.T., Canada. *Arct. Alp. Res.*, 5:185-200.

Andrews, J.T. and Ives, J.D., 1972. Late- and post-glacial events (<10,000 BP) in the eastern Canadian Arctic with particular reference to the Cockburn Moraines and break-up of the Laurentide Ice Sheet. In: Y. Vasari, H. Hyvarinen and S. Hicks (eds.); *Climatic Changes in Arctic Areas During the Last 10,000 Years*. Acta Universitatus Ouluensis, Series A, Geologica No. 1, p. 149-176.

Andrews, J.T. and Webber, P.J., 1964. A lichenometrical study of the northwestern margin of the Barnes Ice Cap: a geomorphological technique. *Geog. Bull.* 22:80-104.

Barr, W., 1971. Postglacial isostatic movement in northern Devon Island: a reappraisal. *Arctic* 24: 249-268.

Blake, W., Jr., 1972. Climatic implication of radiocarbon-dated driftwood in the Queen Elizabeth Islands, Arctic Canada. In: Y. Vasari, H. Hyvarinen and S. Hicks (eds.); *Climatic Changes in Arctic Areas During the Last 10,000 Years*. Acta Universitatus Ouluensis, Series A, Geologica No. 1, p. 77-104.

Burns, J.J. Montague, J.J. and Cowles, C.J. (eds.), 1993. *The Bowhead Whale*. Special Publication Number 2, The Society for Marine Mammology, Lawrence, KS, 787 p.

Davis, P.T., 1985. Neoglacial moraines on Baffin Island. In J.T. Andrews (ed.) *Quaternary Environments: Eastern Canadian Arctic, Baffin Bay and West Greenland*. Allen and Unwin, Boston, p. 682-718.

Dredge, L.A., 1990. The Melville Moraine: sea-level change and response of the western margin of the Foxe Ice Dome, Melville Peninsula, Northwest Territories. *Can. J. Earth Sci.* 27: 1215-1224.

Dredge, L.A., 1991. Raised marine features, radiocarbon dates, and sea level changes, eastern Melville Peninsula, Arctic Canada. *Arctic* 44(1):63-73.

Dyke, A.S., 1979a. Radiocarbon dated Holocene emergence of Somerset Island, central Canadian Arctic. In Current Research, Part B, *Geol. Surv. Can. Pap.* 79-1B, p. 307-318.

Dyke, A.S., 1979b. Glacial and sea level history of southwestern Cumberland Peninsula, Baffin Island, N.W.T., Canada. *Arct. Alp. Res.* 11(2):179-202.

Dyke, A.S. and Morris, T.F., 1990. Postglacial history of the bowhead whale and of driftwood penetration: implications for paleoclimate, Central Canadian Arctic. *Geol. Surv. Can. Pap.* 89-24, 17 p.

Dyke, A.S. and Prest, V.K., 1987. Late Wisconsin and Holocene history of the Laurentide Ice Sheet. *Geographie physique et Quaternaire* 41: 237-264.

Dyke, A.S., Morris, T.F. and Green, D.E.C., 1991. Postglacial tectonic and sea level history of the central Canadian Arctic. *Geol. Surv. Can. Bull.* 397, 56 p.

Häggblom, A., 1982. Driftwood in Svalbard as an indicator of sea ice conditions. *Geografiska Annaler* 64A:81-94.

Harington, C.R., 1966. Extralimital occurrences of walruses in the Canadian Arctic. *Journal of Mammology* 47(3): 506-513.

Hooper, J., 1990. *Late Quaternary glacial and sea level history of the Bernier Bay area, northwestern Baffin Island, N.W.T.* Unpublished MSc. Thesis, 92 p.

Ives, J.D. and Andrews, J.T., 1963. Studies in the physical geography of north-central Baffin Island, N.W.T., *Geog. Bull.* 19:5-48.

Koerner, R.M., 1977. Devon Island Ice Cap: core stratigraphy and paleoclimate. *Science* 196:15-18.

Miller, G.H., 1973. Late Quaternary glacial and climatic history of northern Cumberland Peninsula, Baffin Island, N.W.T., Canada. *Quaternary Research* 3:561-583.

Paterson, W.S.B., Koerner, R.M., Fisher, D., Johnsen, S.J., Clausen, H.B., Dansgaard, W., Bucher, P. and Oeschger, H., 1977. An oxygen-isotope climatic record from the Devon Island Ice Cap, Arctic Canada. *Nature* 266:508-511.

Perry, R., 1967. *The World Of the Walrus.* Cassell and Company Ltd., London, 162 p.

Reeves, R., Mitchell, E., Mansfield, A. and McLaughlin, M., 1983. Distribution and migration of the bowhead whale, *Balaena mysticetus*, in the eastern North American Arctic. *Arctic* 36(1): 5-64.

Ross, W.G., 1974. Distribution, migration and depletion of bowhead whales in Hudson Bay, 1860-1915. *Arct. Alp. Res.* 6:85-98.

Ross, W.G., 1979. The annual catch of Greenland (bowhead) whales in waters north of Canada 1719-1915: a preliminary compilation. *Arctic* 32: 91-121.

Short, S.K., Mode, W.N. and Davis, P.T., 1985. The Holocene record from Baffin Island: modern and fossil pollen studies. In J.T. Andrews (ed.) *Quaternary Environments: Eastern Canadian Arctic, Baffin Bay and West Greenland.* Allen and Unwin, Boston, p. 608-642.

Stewart, T.G. and England, J.H., 1983. Holocene sea ice conditions and Paleoenvironmental change, northernmost Ellesmere Island, N.W.T., Canada. *Arct. Alp. Res.* 15: 1-17.

Stirling, I., Cleator, H. and Smith, T.G., 1981. Marine Mammals. In I. Stirling and H. Cleator (eds.), *Polynyas in the Canadian Arctic.* Canadian Wildlife Service Occasional Paper No. 45, p. 44-58.

Williams, L.D. and Bradley, R.S., 1985. Paleoclimatology of the Baffin Bay region. In J.T. Andrews (ed.) *Quaternary Environments: Eastern Canadian Arctic, Baffin Bay and West Greenland.* Allen and Unwin, Boston, p. 741-772.

Chapter 5: Conclusions

The landscape and sediments of northwest Baffin Island contain a relatively complete record of recent deglacial events but evidence of earlier glacial and nonglacial events is fragmentary. Evidence for falling postglacial sea level, in the form of raised beaches and marine sediments, is abundant. Comparatively little is known about pre-Foxe glaciation(s) and earlier (Tertiary) fluvial dissection. Tectonic modification of the landscape since the Late Tertiary appears to have been minimal although there is growing evidence in the form of anomalous emergence histories (Dyke et al., 1991) and continuing seismicity (Basham et al., 1977) that tectonic movements are continuing in other parts of the central Arctic.

Large terminal moraines of Cockburn age mark the former position of a stable margin of the Bernier Bay Lobe. The moraine system also contains interlobate elements deposited between the Bernier Bay Lobe and ice on Brodeur and Agu Peninsulas. The gradient of the moraines indicates that the ice lobe in Bernier Bay was grounded but fed into an ice shelf in Prince Regent Inlet. Thaw flowslides, kettles and large ice wedge troughs in the larger moraines indicate substantial cores of buried glacier ice may exist within these deposits. Melting of the ice cores ceased when till accumulated on its surface to a depth equal to the maximum depth of summer thawing.

The retreat of ice across the plateaux of Brodeur and Agu Peninsulas is recorded by numerous ice marginal channels inscribed on an otherwise minimally-altered surface.

The westward dispersal of Precambrian erratics is consistent with prevailing westward flow of ice from the Foxe Dome during the last glaciation. However, the scarcity of these erratics on southern Brodeur Peninsula indicates that the Brodeur Peninsula Ice Cap maintained an independent flow regime throughout the last glaciation, agreeing with Dyke and Prest's (1987) reconstruction. Unlike the Brodeur Peninsula ice, there is no evidence that ice on Agu Peninsula had an independent flow regime.

Granule lithology was more effective for distinguishing till dispersal patterns than matrix carbonate content (Chittick) analysis which is

complicated by unknown background levels of insoluble impurities in the local carbonate bedrock. The best-documented aspects of the dispersal pattern are the westward dispersal of shield clasts in three plumes by Foxe Ice and the exclusion of this ice from southern Brodeur Peninsula by the local ice. The two northern plumes formed alongside the Bernier Bay Ice Stream. More limited westward dispersal occurred over the plateau of Agu Peninsula possibly because the area was covered by cold-based ice. The widespread occurrence of sparse Precambrian erratics in the field area suggests these erratics may have been deposited during earlier regional glaciation(s).

Between 9000 and 6500 BP, the Bernier Bay Lobe maintained a relatively stable margin with a calving terminus offshore and a shallow marine moat along its south side during a period when the climate was probably warmer than present. This could only have occurred if the supply of ice from the Foxe Dome was large, and supports the hypothesis that new moisture sources formed by the breakup of the McClintock Ice Divide to the west led to a period of renewed accumulation and strongly positive mass balance on the Foxe Dome during the Cockburn Substage.

The longitudinal gradient of the moraine crests and the bathymetry of Prince Regent Inlet indicate that a calving terminus was located near the mouth of Bernier Bay during the Cockburn Substage. If the ice in Bernier Bay was not a great deal thicker during the last glacial maximum, then an extensive ice shelf, rather than an ice stream, probably occupied Prince Regent Inlet throughout the last glaciation. The position of the moraines records the margin of the Bernier Bay Ice Stream during the LGM, when moraine deposition began.

The series of emergence curves record continuous isostatic rebound during the Holocene. The emergence history of the area is typical of formerly-glaciated areas (Zone I of Clark et al., 1978) and is characterized by an exponentially declining drop in sea level. Because wasting ice in the marine-based portion of the ice sheet was immediately replaced by the sea, marine limits formed at the same time an area was deglaciated. Total measured emergence varied between 120 m in the northwest and 138 m in the southeast. The rate of emergence (from the Bernier Bay southeast curve) was about 3.5 m per century in the first 1000 years following deglaciation and declined to 35 cm per century in the last 1000

years. The half-response time is approximately 1800 years, whereas Dyke et al., (1991) found a half-response time of 2000 years based on the extensively controlled driftwood curve from Prince of Wales Island. The above data corroborate the geomorphic evidence on the configuration of former ice loads and are relevant to geophysical modelling of the properties of the upper mantle, particularly its viscosity (e.g. Cathles, 1975; Walcott, 1972).

Good agreement was found between the emergence curve based on the radiocarbon dates and a predicted emergence curve based on a modified version of Andrews' (1970) method for predicting uplift curves. The uplift curve was converted to an emergence curve by subtracting the amount of uplift from the total uplift for each 1000-year interval and by removing the eustatic corrections. Only the height and age of the marine limit is needed to predict an emergence curve using this method. The close fit to the radiocarbon data from lower shorelines suggests that useful emergence curves can be derived for some areas where only a dated marine limit elevation is available. A significant drawback is that the method always generates smooth curves from the given input data and is therefore incapable of detecting anomalies caused by tectonic or other effects.

Isobase maps of the area show an increase in the elevation of raised shorelines toward the southeast, reflecting crustal loading by the Foxe Dome. Shoreline gradients are steepest for the immediate postglacial time and decline progressively thereafter. These gradients are difficult to measure precisely because only minimum curves are available in the southeastern part of the field area. Flattening of the isobase surface in the northwest of the study area is due to loading by the smaller Brodeur Peninsula Ice Cap, imposed on the much larger regional depression produced by the Foxe Dome. This flattening of the isobase surface supports the interpretation that the Brodeur Peninsula Ice Cap was a feature of the LGM rather than a deglacial residual. Presumably, the isobases curve westward at some point over Committee Bay in response to loading by Keewatin ice. However, the isobases still trend north-south on Melville Peninsula, parallel to the Melville Moraine (Dredge, 1990).

The earliest entry of bowhead whales to the area occurred about 7000 BP. Until then, bowheads had been excluded, likely by a pervasive

cover of sea ice. At this time, bowheads could have entered the area via Prince Regent Inlet, Admiralty Inlet, or through Fury and Hecla Strait. Small numbers of bowhead whale bones were found on shorelines dating between 7000 and 5000 BP and between 3000 BP and the present. The greatest number of bones were found on shorelines dating between 5000 and 3000 BP. Fluctuations in the numbers of bowheads could be due either to changes in the absolute population of bowheads in the North Atlantic, Baffin Bay and Lancaster Sound or changes in the amount of sea ice in channels bordering the study area. Hence, sea ice was probably least extensive between 5000 and 3000 BP during a mid Holocene warm period, and subsequently increased in response to Neoglacial cooling. No whalebone was found on or near the modern beach, indicating that the number of bowheads in the study area has declined to levels similar to those of the early Holocene. Beaches from the period of historic whaling during the last two centuries are also devoid of whalebone. Hence, the absence of bones on young beaches is not a result of depletion of the bowhead stocks by whaling in the North Atlantic and Baffin Bay. Again, more severe sea ice is the most likely explanation, but there remains the possibility that the prehistoric bowhead stocks may have been much larger than in historic time. It may eventually be possible to obtain estimates of the absolute size of the prehistoric population by counting the numbers of bones on raised beaches of known age throughout its former range.

References

Andrews, J.T., 1970. *A geomorphological study of post-glacial uplift with particular reference to Arctic Canada.* Institute of British Geographers, Special Publication No. 2, 156 p.

Basham, P.W., Forsyth, D.A. and Wetmiller, R.J., 1977. The seismicity of northern Canada. *Can. J. Earth Sci.* 14:1646-1667.

Cathles, L.M., 1975. *The Viscosity of the Earth's Mantle*. Princeton University Press, 386 p.

Clark, J.A., Farrell, W.E. and Peltier, W.R., 1978. Global changes in postglacial sea level: a numerical calculation. *Quat. Res.* 9:265-287.

Dredge, L.A., 1990. The Melville Moraine: sea-level change and response of the western margin of the Foxe Ice Dome, Melville Peninsula, Northwest Territories. *Can. J. Earth Sci.* 27: 1215-1224.

Dredge, L.A., 1991. Raised marine features, radiocarbon dates, and sea level changes, eastern Melville Peninsula, Arctic Canada. *Arctic* 44(1):63-73.

Dyke, A.S. and Prest, V.K., 1987. Late Wisconsin and Holocene history of the Laurentide Ice Sheet. *Geographie physique et Quaternaire* 41: 237-264.

Dyke, A.S., Morris, T.F. and Green, D.E.C., 1991. Postglacial tectonic and sea level history of the central Canadian Arctic. *Geol. Surv. Can. Bull.* 397, 56 p.

Walcott, R.I., 1972. Past sea levels, eustasy and deformation of the earth. *Quat. Res.* 2:1-14.

Appendix A. Lithologic constituents of till granule fractions.

Prefix	Number	carb.	s.stone	r. s.stone	gneiss	quartz	shell	shale	talc	diabase	volcanic	unknown	lithic f.
88 DCA	402	99.1%			0.9%								C
88 DCA	403	100.0%			+								C
88 DCA	411	99.0%		1.0%	+								C
88 DCA	412	99.0%			+	1.0%							C
88 DCA	414	98.0%		2.0%									C
88 DCA	415	100.0%											C
88 DCA	416	100.0%			+								C
88 DCA	417	99.0%			+	1.0%							C
88 DCA	418	100.0%			+								C
88 DCA	419	100.0%			0.0%								C
88 DCA	420	100.0%			+								C
88 DCA	428	100.0%			+								C
88 DCA	429	100.0%			+								C
88 DCA	455	88.1%		+	11.0%	0.9%							MCC
88 DCA	457	89.3%			3.4%	1.7%	5.6%						MCC
88 DCA	459	64.1%			16.3%	1.7%	17.1%					0.8%	M
88 DCA	460	98.1%		0.9%	0.9%								C
88 DCA	463	99.0%		+	1.0%								C
88 DCA	464	71.0%		2.0%	18.0%	3.0%	6.0%						MC
88 DCA	467	88.0%		1.0%	9.0%		2.0%						MCC
88 DCA	472	100.0%		+	+								C
88 DCA	473	98.9%		+	+								C
88 DCA	474	97.0%		+	+		3.0%						C
88 DCA	475	100.0%		+	+								C
88 DCA	476	100.0%		+	+								C
88 DCA	481	100.0%	+	+	+								C
88 DCA	482	100.0%	+	+	+							+	C
88 DCA	483	100.0%			+								C

Appendix A. Lithologic constituents of till granule fractions (cont.)

Prefix	Number	carb.	s.stone	r. s.stone	gneiss	quartz	shell	shale	talc	diabase	volcanic	unknown	lithic f.
88 DCA	485	95.1%			3.3%		1.7%						C
88 DCA	486	100.0%			+								C
88 DCA	487	100.0%			+								C
88 DCA	488	98.7%			0.6%	0.6%							C
88 DCA	489	100.0%			+								C
88 DCA	490	96.9%	+	+	3.1%								C
88 DCA	491	98.5%			1.5%								C
88 DCA	492	98.2%	0.6%	+	1.2%								C
88 DCA	494	99.0%			1.0%								C
88 DCA	496	100.0%			+								C
88 DCA	497	100.0%			+								C
88 DCA	498	99.0%			1.0%								C
88 DCA	507	96.1%			3.0%	1.0%							C
88 DCA	508	97.0%			2.0%	1.0%							C
88 DCA	509	94.5%			4.4%	1.1%							C
88 DCA	510	87.4%			12.6%								MCC
88 DCA	511	88.9%			9.1%	2.0%							MCC
88 DCA	512	96.3%			2.9%		0.7%						C
88 DCA	513	90.9%			9.1%								C
88 DCA	514	93.4%			5.7%		0.9%						C
88 DCA	515	96.8%			3.2%								C
88 DCA	516	98.0%	0.5%		1.0%	0.5%							C
88 DCA	517	98.1%		+	1.9%								C
88 DCA	518	87.3%		1.9%	6.8%	2.9%	1.0%						MCC
88 DCA	519	96.4%			2.1%		0.7%					0.7%	C
88 DCA	520	99.0%			1.0%								C
88 DCA	521	100.0%			+								C
88 DCA	525	100.0%			+								C

Appendix A. Lithologic constituents of till granule fractions (cont.)

Prefix	Number	carb.	s.stone	r. s.stone	gneiss	quartz	shell	shale	talc	diabase	volcanic	unknown	lithic f.
88 DCA	526	98.7%		+	1.4%								C
88 DCA	532	100.0%			+								C
88 DCA	533	99.3%			+	0.7%							C
88 DCA	534	100.0%			+								C
88 DCA	535	83.0%		0.7%	5.6%	10.6%							MCC
88 DCA	536	100.0%			+								C
88 DCA	554	96.2%		+	3.1%		0.8%						C
88 DCA	556	90.1%		+	0.9%	4.5%	4.5%						C
88 DCA	557	98.0%		+	+	2.0%							C
88 DCA	558	100.0%		+	2.0%								C
88 DCA	559	97.6%		1.6%			0.8%						C
88 DCA	560	100.0%		+	+								C
88 DCA	561	100.0%			0.0%								C
88 DCA	562	100.0%	+		+								C
88 DCA	563	99.0%	+	1.0%	+								C
88 DCA	564	100.0%											C
88 DCA	567	96.9%		+	+	3.1%							C
88 DCA	570	100.0%		+	+								C
88 DCA	571	99.0%				1.0%							C
88 DCA	573	92.0%		+	2.0%	1.0%	5.0%						C
88 DCA	574	98.1%		+	+		1.8%						C
88 DCA	575	100.0%		+	+								C
89 DCA	403	100.0%											C
89 DCA	404	65.0%	5.9%		27.9%					1.2%			M
89 DCA	406	86.1%	2.8%		9.2%		1.9%						MCC
89 DCA	409	88.0%	2.8%		8.7%			0.4%					MCC
89 DCA	410	99.8%	0.0%		0.2%								C
89 DCA	411	91.4%	0.3%		5.4%		0.1%				2.9%		C

Appendix A. Lithologic constituents of till granule fractions (cont.)

Prefix	Number	carb.	s.stone	r. s.stone	gneiss	quartz	shell	shale	talc	diabase	volcanic	unknown	lithic f.
89 DCA	412	97.0%	0.8%		2.1%		0.1%						C
89 DCA	414	96.6%	0.1%	0.1%	3.1%		0.1%						C
89 DCA	415	99.4%			0.6%								C
89 DCA	417	96.7%	0.4%		2.9%								C
89 DCA	420	80.1%	3.4%		15.9%		0.6%						MCC
89 DCA	422	81.5%	2.4%	0.1%	15.3%		0.8%						MCC
89 DCA	425	90.3%	4.4%		5.4%								C
89 DCA	427	58.1%	6.5%		35.3%								M
89 DCA	431	65.1%	23.8%		11.1%								M
89 DCA	436	48.4%	48.4%		2.1%	0.2%						0.9%	M
89 DCA	437	75.1%	24.7%		0.2%								MC
89 DCA	438	97.7%	2.0%		0.3%								C
89 DCA	439	100.0%											C
89 DCA	440	87.7%	5.5%		2.8%	3.1%						0.8%	MCC
89 DCA	441	77.3%	13.1%		8.6%	1.0%							MC
89 DCA	442	100.0%											C
89 DCA	447	99.8%			0.2%								C
89 DCA	448	98.7%	0.4%		1.0%								C
89 DCA	454	89.4%	4.5%		5.6%		0.6%						MCC
89 DCA	455	56.3%	13.2%		30.5%								M
89 DCA	456	96.5%	0.4%		3.2%								C
89 DCA	457	96.7%			3.3%								C
89 DCA	458	98.0%			2.0%								C
89 DCA	462	98.7%			1.3%								C
89 DCA	463	26.0%	1.4%		57.4%					15.2%			M
89 DCA	471	91.7%			8.1%	0.2%							C
89 DCA	473	99.8%			0.1%								C
89 DCA	474	5.1%	0.5%		94.4%								P

Appendix A. Lithologic constituents of till granule fractions (cont.)

Prefix	Number	carb.	s.stone	r. s.stone	gneiss	quartz	shell	shale	talc	diabase	volcanic	unknown	lithic f.
89 DCA	475	93.7%	0.3%		6.0%								C
89 DCA	476	62.1%	2.1%		35.3%				0.5%				M
89 DCA	483	75.5%	1.7%		22.6%	0.2%							MC
89 DCA	484	98.2%			1.8%								C
89 DCA	487	95.7%	0.7%		3.6%								C
89 DCA	488	75.7%	1.8%		22.5%								MC
89 DCA	489	4.7%	0.1%		95.2%								P
89 DCA	490	92.2%	1.8%		6.0%								C
89 DCA	491	90.6%	0.8%		8.7%								C
89 DCA	492	89.9%			10.0%	0.1%							MCC
89 DCA	493	51.3%	3.0%		45.7%								M
89 DCA	494	78.4%	4.5%		17.1%								MC
89 DCA	495	77.7%	2.4%		19.9%								MC
89 DCA	496	82.5%	0.8%		16.8%								MCC
89 DCA	516	83.4%	0.9%		15.7%								MCC
89 DCA	517	81.2%	0.7%		17.5%		0.1%				0.4%		MCC
89 DCA	522	88.7%			11.3%								MCC
89 DCA	523	75.5%	1.1%		23.3%	0.1%							MC
89 DCA	524	100.0%											C
89 DCA	525	91.5%	7.1%		1.3%								C
89 DCA	527	94.7%	4.1%		1.2%								C
89 DCA	528	97.3%	1.6%		1.1%	0.1%							C
89 DCA	529	99.2%	0.2%		0.5%								C
90 DCA	401	61.4%	12.7%		24.8%		1.0%					0.1%	M
90 DCA	402	79.3%	6.7%		11.9%			0.5%		1.2%		0.3%	MC
90 DCA	403	52.4%	9.9%		37.1%		0.7%						M
90 DCA	406	83.4%	5.7%	0.8%	9.7%		0.5%						MCC
90 DCA	407	98.3%	0.7%		1.0%								C

Appendix A. Lithologic constituents of till granule fractions (cont.)

Prefix	Number	carb.	s.stone	r. s.stone	gneiss	quartz	shell	shale	talc	diabase	volcanic	unknown	lithic f.
90 DCA	408	97.6%	0.6%	0.0%	1.6%		0.1%	0.1%					C
90 DCA	409	95.5%	1.3%		3.2%								C
90 DCA	410	82.0%	5.4%	0.1%	7.1%		4.4%	0.9%					MCC
90 DCA	415	67.3%	6.8%		25.4%		0.5%						M
90 DCA	418	95.7%	1.6%		2.7%								C
90 DCA	420	75.5%	2.1%		20.6%		1.9%						MC
90 DCA	421	83.0%	10.1%	0.1%	6.8%								MCC
90 DCA	423		46.7%		0.1%			53.2%					M
90 DCA	424	0.6%	86.8%	0.2%	12.5%								MSS
90 DCA	428	8.4%	40.5%		22.7%						28.4%		M
90 DCA	430	58.7%	1.5%		3.2%	2.1%		33.9%			0.6%		M
90 DCA	431	0.0%	0.1%		0.2%			0.0%			99.7%		M
90 DCA	433		98.6%		0.4%			0.9%					S
90 DCA	434		88.4%		1.6%	0.3%		9.8%					MSS
90 DCA	436	20.1%	72.9%		1.5%	5.2%						0.2%	MS
90 DCA	446	92.8%	1.6%		5.4%			0.1%					C
90 DCA	447	94.2%	0.8%		4.5%	0.1%	0.4%						C
90 DCA	448	99.1%	0.3%		0.6%								C
90 DCA	449	93.2%	2.7%		4.0%			0.1%					C
90 DCA	450	82.3%	1.9%		15.8%								MCC
90 DCA	454	95.1%	0.5%		4.4%								C
90 DCA	455	100.0%			0.1%								C
90 DCA	456	94.8%	2.2%		2.9%	0.1%							C
90 DCA	472	82.4%	2.4%		13.5%		1.7%						MCC
90 DCA	478	96.6%	1.7%		1.6%	0.0%		0.1%					C
90 DCA	479	98.0%			2.0%								C
90 DCA	480	97.8%	1.3%		0.9%								C
90 DCA	481	98.6%	0.1%		1.3%								C

Appendix A. Lithologic constituents of till granule fractions (cont.)

Prefix	Number	carb.	s.stone	r. s.stone	gneiss	quartz	shell	shale	talc	diabase	volcanic	unknown	lithic f.
90 DCA	482	98.9%	0.6%		0.4%			0.2%					C
90 DCA	483	99.7%			0.3%								C
90 DCA	484	97.2%	1.0%		1.9%								C
90 DCA	485	89.9%	3.0%		7.0%								MCC
90 DCA	486	98.9%	0.1%		1.0%								C
90 DCA	487	97.0%			3.0%								C
90 DCA	487	99.8%			0.2%								C
90 DCA	489	82.4%	3.8%		11.7%	2.1%							MCC
90 DCA	490	91.1%	3.5%		5.3%	0.1%							C
90 DCA	492	99.6%			0.4%								C
90 DCA	493	60.8%	8.3%	0.1%	30.4%				0.5%				M
90 DCA	494	86.3%			13.6%	0.1%							MCC
90 DCA	495	95.0%	0.3%	0.2%	4.4%								C
90 DCA	496	90.7%	0.6%		8.6%	0.1%							C
90 DCA	497	68.6%	13.8%		14.9%	0.1%	0.3%	2.4%					M
90 DCA	498	98.1%	1.5%		0.4%								C
90 DCA	499	99.7%	0.1%		0.2%								C
90 DCA	501	99.8%			0.2%								C
90 DCA	502	100.0%											C
90 DCA	503	89.5%	4.3%		5.5%							0.7%	MCC
90 DCA	505	88.8%	2.3%		9.0%								MCC
91 DCA	403	79.4%	9.2%		11.2%					0.2%			MC
91 DCA	404	77.0%	8.2%		12.0%			2.6%		0.2%			MC
91 DCA	406	80.9%	3.6%		15.5%								MCC
91 DCA	407	97.4%	0.6%		2.0%								C
91 DCA	408	70.0%	12.9%		16.6%		0.1%	0.4%					M
91 DCA	411	91.7%	2.0%		3.8%			2.5%					C
91 DCA	416	98.2%	0.3%		1.5%								C

Appendix A. Lithologic constituents of till granule fractions (cont.)

Prefix	Number	carb.	s.stone	r. s.stone	gneiss	quartz	shell	shale	talc	diabase	volcanic	unknown	lithic f.
91 DCA	417	89.2%	2.4%	0.1%	8.2%								MCC
91 DCA	418	83.8%	2.4%		13.4%		0.3%						MCC
91 DCA	419	93.9%	2.6%		3.5%								C
91 DCA	420	97.3%	0.8%		1.9%								C
91 DCA	421	78.8%	6.3%		14.5%	0.2%						0.3%	MC
91 DCA	423	5.3%	20.9%		73.0%					0.7%			MP
91 DCA	423	84.7%	7.6%		7.7%								MCC
91 DCA	424	72.4%	14.2%		13.5%								MC
91 DCA	425	79.4%	6.8%		13.5%							0.4%	MC
91 DCA	426	4.8%	72.3%		22.1%					0.8%			MS
91 DCA	427	36.2%	25.2%		34.3%		2.5%	0.6%		1.1%			M
91 DCA	428	0.6%	33.9%		65.5%								M
91 DCA	429	2.4%	4.2%		93.4%								P
91 DCA	431	2.7%	55.9%		37.0%	1.2%		3.2%					M
91 DCA	432		23.9%		75.0%			1.1%					MP
91 DCA	433		41.8%		53.4%					4.8%			M
91 DCA	434	1.5%	75.5%		17.8%	3.7%		0.7%				0.8%	MS
91 DCA	436	89.8%	3.1%		6.7%	0.2%	0.2%						MCC
91 DCA	437		77.7%		18.8%			2.8%		0.6%			MS
91 DCA	438		81.3%		18.4%			0.2%					MSS
91 DCA	439	1.8%	88.4%		9.1%	0.6%							MSS
91 DCA	440		71.4%		25.5%			3.0%		0.2%			MS
91 DCA	441	2.1%	75.9%		21.5%					0.6%			MS
91 DCA	442	6.0%	81.4%		12.6%								MSS
91 DCA	443	3.5%	89.8%		5.8%	0.8%							MSS
91 DCA	444	2.7%	54.5%		36.3%			5.8%		0.7%			M
91 DCA	446	4.9%	71.9%		23.2%								MS
91 DCA	447	3.0%	82.9%		14.1%								MSS

Appendix A. Lithologic constituents of till granule fractions (cont.)

Prefix	Number	carb.	s.stone	r. s.stone	gneiss	quartz	shell	shale	talc	diabase	volcanic	unknown	lithic f.
91 DCA	448	0.4%	72.2%		27.0%					0.4%			MS
91 DCA	449	0.3%	81.0%		15.7%	0.8%						2.2%	MSS
91 DCA	450		53.6%		46.4%								M
91 DCA	451		92.2%		7.8%								S
91 DCA	452	0.6%	60.9%	3.9%	34.6%								M
91 DCA	457		67.7%		19.8%	0.3%		3.0%			9.1%		M
91 DCA	458		71.8%		26.8%	0.5%		0.9%					MS
91 DCA	459		76.7%		15.1%			8.2%					MS
91 DCA	463	7.9%	23.9%		56.5%			11.8%					M
91 DCA	464	0.3%	72.7%		17.4%	0.3%		5.1%			4.3%		MS
91 DCA	465		68.1%		22.7%			1.9%			7.3%		M
91 DCA	466	7.7%	56.6%	3.5%	32.3%			0.0%					M
91 DCA	467	0.7%	83.8%		15.5%								MSS
91 DCA	468	3.0%	46.5%		38.1%			8.3%			4.1%		M
91 DCA	469		81.4%		9.5%	0.1%		1.0%			8.0%		MSS

Appendix B. Carbonate content of tills

Prefix	Number	Calcite (%)	Dolomite (%	Total (%)	Cal/Dol
88 DCA	402	35.8	53.8	89.6	0.66
88 DCA	403	23.8	71.8	95.6	0.33
88 DCA	411	42.0	51.1	93.1	0.82
88 DCA	412	34.3	52.0	86.3	0.66
88 DCA	414	26.2	56.1	82.3	0.47
88 DCA	415	14.2	73.2	87.4	0.19
88 DCA	416	16.6	64.9	81.5	0.26
88 DCA	417	17.0	64.0	81.0	0.27
88 DCA	418	14.2	67.7	81.8	0.21
88 DCA	419	15.1	64.9	80.0	0.23
88 DCA	420	16.1	66.7	82.8	0.24
88 DCA	428	17.0	64.9	81.9	0.26
88 DCA	429	24.7	45.5	70.2	0.54
88 DCA	455	29.5	50.1	79.7	0.59
88 DCA	457	23.8	50.1	73.9	0.47
88 DCA	459	15.1	39.1	54.2	0.39
88 DCA	460	19.0	53.8	72.8	0.35
88 DCA	463	37.2	40.0	77.2	0.93
88 DCA	464	11.3	63.1	74.3	0.18
88 DCA	467	29.5	23.4	52.9	1.26
88 DCA	472	27.6	49.2	76.8	0.56
88 DCA	473	25.7	49.2	74.9	0.52
88 DCA	474	22.8	37.2	60.0	0.61
88 DCA	475	28.3	53.8	82.1	0.53
88 DCA	476	29.2	45.1	74.3	0.65
88 DCA	481	24.2	52.8	77.0	0.46
88 DCA	482	24.2	48.3	72.5	0.5
88 DCA	483	15.8	63.6	79.4	0.25
88 DCA	485	16.7	51.0	67.7	0.33
88 DCA	486	18.6	56.4	75.0	0.33
88 DCA	487	37.4	32.0	69.4	1.17
88 DCA	488	29.9	39.2	69.1	0.76
88 DCA	489	18.6	48.3	66.9	0.39
88 DCA	490	32.7	43.7	76.5	0.75
88 DCA	491	30.8	41.9	72.8	0.74
88 DCA	492	30.8	38.3	69.1	0.8
88 DCA	494	31.8	38.3	70.1	0.83
88 DCA	496	18.6	61.8	80.4	0.3
88 DCA	497	20.5	54.6	75.1	0.38
88 DCA	498	14.8	52.8	67.6	0.28
88 DCA	507	57.2	19.3	76.5	2.96
88 DCA	508	26.1	40.1	66.2	0.65
88 DCA	509	36.5	32.9	69.4	1.11
88 DCA	510	20.5	33.8	54.3	0.61

Appendix B. Carbonate content of tills (cont.)

Prefix	Number	Calcite (%)	Dolomite (%	Total (%)	Cal/Dol
88 DCA	511	26.1	32.9	59.0	0.79
88 DCA	512	42.1	25.6	67.8	1.64
88 DCA	513	13.9	33.8	47.7	0.41
88 DCA	514	28.9	30.2	59.1	0.96
88 DCA	515	32.7	33.8	66.5	0.97
88 DCA	516	22.4	41.0	63.4	0.55
88 DCA	517	29.9	39.2	69.1	0.76
88 DCA	518	19.5	41.0	60.6	0.48
88 DCA	519	29.9	35.6	65.5	0.84
88 DCA	520	12.0	61.8	73.8	0.19
88 DCA	521	16.7	62.7	79.5	0.27
88 DCA	525	20.5	51.0	71.5	0.4
88 DCA	532	20.5	70.0	90.5	0.29
88 DCA	533	33.4	36.3	69.7	0.92
88 DCA	534	43.1	38.3	81.4	1.12
88 DCA	535	17.7	35.6	53.2	0.5
88 DCA	536	13.9	51.9	65.8	0.27
88 DCA	554	35.5	47.4	82.9	0.75
88 DCA	556	18.6	45.5	64.1	0.41
88 DCA	557	23.3	61.8	85.1	0.38
88 DCA	558	13.9	67.3	81.2	0.21
88 DCA	559	9.2	79.0	88.2	0.12
88 DCA	560	7.3	80.8	88.1	0.09
88 DCA	561	13.9	77.2	91.1	0.18
88 DCA	562	4.5	89.9	94.4	0.05
88 DCA	563	22.4	70.0	92.3	0.32
88 DCA	564	29.9	44.6	74.5	0.67
88 DCA	567	38.4	52.8	91.1	0.73
88 DCA	570	9.2	79.0	88.2	0.12
88 DCA	571	7.3	76.3	83.6	0.1
88 DCA	573	28.0	51.9	79.9	0.54
88 DCA	574	18.6	61.8	80.4	0.3
88 DCA	575	27.1	54.6	81.7	0.5
89 DCA	403	43.9	30.8	74.7	1.43
89 DCA	404	16.7	26.9	43.6	0.62
89 DCA	406	56.0	13.3	69.3	4.19
89 DCA	409	33.7	27.3	61.0	1.23
89 DCA	410	48.0	25.2	73.2	1.9
89 DCA	411	54.0	26.4	80.4	2.05
89 DCA	412	33.7	34.8	68.5	0.97
89 DCA	414	42.5	36.8	79.2	1.16
89 DCA	415	47.8	24.3	72.1	1.97
89 DCA	417	30.5	45.5	76.0	0.67
89 DCA	420	51.6	10.5	62.1	4.94

Appendix B. Carbonate content of tills (cont.)

Prefix	Number	Calcite (%)	Dolomite (%)	Total (%)	Cal/Dol
89 DCA	422	34.7	20.3	54.9	1.71
89 DCA	425	3.2	82.4	85.6	0.04
89 DCA	427	2.2	38.0	40.2	0.06
89 DCA	431	5.1	45.0	50.1	0.11
89 DCA	436	3.2	70.2	73.3	0.05
89 DCA	437	3.6	54.3	58.0	0.07
89 DCA	438	3.6	60.4	64.0	0.06
89 DCA	439	1.2	44.1	45.3	0.03
89 DCA	440	4.1	51.1	55.1	0.08
89 DCA	441	3.1	45.1	48.2	0.07
89 DCA	447	3.1	67.2	70.3	0.05
89 DCA	448	3.6	73.2	76.8	0.05
89 DCA	454	3.6	68.6	72.2	0.05
89 DCA	455	2.6	46.4	49.1	0.06
89 DCA	456	4.1	65.4	69.4	0.06
89 DCA	457	4.0	63.4	67.4	0.06
89 DCA	458	3.1	65.2	68.3	0.05
89 DCA	462	3.6	70.2	73.8	0.05
89 DCA	471	3.6	51.1	54.7	0.07
89 DCA	473	13.1	42.3	55.4	0.31
89 DCA	474	1.7	8.5	10.2	0.2
89 DCA	475	4.5	51.9	56.5	0.09
89 DCA	476	2.6	39.1	41.8	0.07
89 DCA	483	2.6	54.2	56.8	0.05
89 DCA	484	1.7	76.7	78.4	0.02
89 DCA	486	2.2	48.8	50.9	0.04
89 DCA	487	2.2	75.3	77.5	0.03
89 DCA	488	3.6	46.0	49.6	0.08
89 DCA	489	1.7	10.6	12.3	0.16
89 DCA	490	5.5	65.2	70.7	0.08
89 DCA	491	6.1	51.6	57.6	0.12
89 DCA	492	3.2	42.7	45.9	0.07
89 DCA	493	1.2	35.7	36.9	0.03
89 DCA	494	4.1	42.2	46.4	0.1
89 DCA	495	4.1	48.3	52.4	0.08
89 DCA	516	10.4	60.9	71.3	0.17
89 DCA	517	7.0	64.6	71.6	0.11
89 DCA	522	9.7	49.7	59.4	0.2
89 DCA	523	1.2	41.4	42.6	0.03
89 DCA	524	6.4	64.3	70.7	0.1
89 DCA	525	4.0	62.9	66.9	0.06
89 DCA	527	5.0	66.1	71.1	0.08
89 DCA	528	4.6	58.4	63.0	0.08
89 DCA	529	4.6	65.8	70.4	0.07

Appendix B. Carbonate content of tills (cont.)

Prefix	Number	Calcite (%)	Dolomite (%)	Total (%)	Cal/Dol
90 DCA	401	20.9	28.4	49.3	0.73
90 DCA	402	21.4	23.4	44.7	0.91
90 DCA	403	8.9	19.2	28.1	0.46
90 DCA	406	58.3	37.2	95.5	1.57
90 DCA	407	41.0	48.3	89.3	0.85
90 DCA	408	54.5	40.9	95.4	1.33
90 DCA	409	36.2	41.8	78.1	0.87
90 DCA	410	38.2	18.8	56.9	2.03
90 DCA	415	18.5	46.9	65.4	0.39
90 DCA	418	59.3	19.7	79.0	3.01
90 DCA	420	7.4	57.5	65.0	0.13
90 DCA	421	5.5	56.1	61.7	0.1
90 DCA	423	0.7	2.6	3.3	0.28
90 DCA	424	0.7	1.7	2.4	0.43
90 DCA	428	0.0	7.5	7.5	0
90 DCA	430	13.7	4.0	17.7	3.43
90 DCA	431	0.7	0.3	1.0	2.42
90 DCA	433	0.7	3.8	4.5	0.19
90 DCA	436	0.7	3.1	3.8	0.24
90 DCA	446	9.8	52.4	62.3	0.19
90 DCA	447	16.6	39.1	55.6	0.42
90 DCA	448	48.7	23.4	72.1	2.08
90 DCA	449	18.0	42.8	60.8	0.42
90 DCA	450	10.3	29.8	40.2	0.35
90 DCA	454	27.1	33.1	60.2	0.82
90 DCA	455	60.2	26.1	86.4	2.3
90 DCA	456	26.6	25.7	52.3	1.04
90 DCA	472	15.1	28.0	43.1	0.54
90 DCA	478	33.4	37.2	70.6	0.9
90 DCA	479	48.7	28.0	76.7	1.74
90 DCA	480	35.3	53.8	89.1	0.66
90 DCA	481	42.0	39.1	81.1	1.08
90 DCA	482	36.2	55.7	91.9	0.65
90 DCA	483	46.8	46.4	93.2	1.01
90 DCA	484	22.8	58.4	81.2	0.39
90 DCA	485	22.8	54.7	77.6	0.42
90 DCA	486	30.0	43.7	73.7	0.69
90 DCA	487	40.1	42.8	82.8	0.94
90 DCA	489	56.4	18.8	75.2	3.01
90 DCA	490	15.1	56.6	71.7	0.27
90 DCA	492	49.7	31.7	81.4	1.57
90 DCA	493	10.3	36.8	47.1	0.28
90 DCA	494	19.0	51.1	70.0	0.37
90 DCA	495	44.9	28.9	73.8	1.55

Appendix B. Carbonate content of tills (cont.)

Prefix	Number	Calcite (%)	Dolomite (%	Total (%)	Cal/Dol
90 DCA	496	25.7	43.7	69.4	0.59
90 DCA	497	7.4	49.2	56.7	0.15
90 DCA	498	25.7	45.5	71.2	0.56
90 DCA	499	42.0	25.2	67.2	1.67
90 DCA	501	53.5	28.0	81.5	1.91
90 DCA	502	59.3	32.6	91.9	1.82
90 DCA	503	12.2	57.1	69.3	0.21
90 DCA	505	28.8	35.1	63.9	0.82
91 DCA	404	44.9	41.8	86.7	1.07
91 DCA	406	26.6	18.8	45.4	1.42
91 DCA	407	48.7	6.8	55.5	7.21
91 DCA	408	16.1	24.3	40.4	0.66
91 DCA	411	70.8	13.2	84.0	5.36
91 DCA	416	51.6	10.5	62.1	4.94
91 DCA	417	36.2	41.8	78.1	0.87
91 DCA	418	35.3	36.3	71.6	0.97
91 DCA	419	45.8	16.0	61.8	2.87
91 DCA	420	22.8	34.4	57.3	0.66
91 DCA	421	51.6	40.0	91.6	1.29
91 DCA	423	46.8	29.8	76.6	1.57
91 DCA	424	19.0	42.8	61.7	0.44
91 DCA	425	0.5	1.0	1.5	0.49
91 DCA	426	0.5	0.5	1.0	0.92
91 DCA	427	1.4	17.6	19.1	0.08
91 DCA	428	0.7	3.8	4.5	0.19
91 DCA	429	1.7	25.7	27.4	0.07
91 DCA	431	0.5	0.8	1.2	0.64
91 DCA	432	0.5	0.3	0.8	1.62
91 DCA	433	0.5	3.3	3.8	0.15
91 DCA	434	0.5	0.5	1.0	0.92
91 DCA	436	5.5	76.9	82.4	0.07
91 DCA	437	0.7	0.5	1.3	1.37
91 DCA	438	0.5	0.5	1.0	0.92
91 DCA	439	0.5	0.8	1.2	0.64
91 DCA	440	0.5	4.2	4.7	0.12
91 DCA	441	0.5	0.3	0.8	1.62
91 DCA	442	0.5	0.3	0.8	1.62
91 DCA	443	0.5	0.3	0.8	1.62
91 DCA	444	0.5	0.5	1.0	0.92
91 DCA	446	0.5	3.3	3.8	0.15
91 DCA	447	0.5	0.3	0.8	1.62
91 DCA	448	0.5	0.8	1.2	0.64
91 DCA	449	0.7	0.5	1.3	1.37
91 DCA	450	0.7	2.4	3.1	0.31

Appendix B. Carbonate content of tills (cont.)

Prefix	Number	Calcite (%)	Dolomite (%)	Total (%)	Cal/Dol
91 DCA	451	0.5	0.5	1.0	0.92
91 DCA	452	0.2	0.8	1.0	0.32
91 DCA	457	1.2	5.4	6.6	0.22
91 DCA	459	0.5	0.5	1.0	0.92
91 DCA	464	0.5	3.5	4.0	0.14
91 DCA	466	0.2	0.5	0.8	0.47
91 DCA	467	0.5	0.5	1.0	0.92
91 DCA	468	0.5	0.3	0.8	1.62
91 DCA	469	1.2	0.3	1.5	4.02

Appendix C. Sand, silt and clay content of tills

Prefix	Number	Sand(%)	Silt(%)	Clay(%)	Prefix	Number	Sand(%)	Silt(%)	Clay(%)
88 DCA	402	18.3	71.4	10.3	88 DCA	511	38.5	43.2	18.4
88 DCA	403	54.4	42.3	3.3	88 DCA	512	32.4	41.1	26.6
88 DCA	411	39.2	52.3	8.5	88 DCA	513	69.9	26.4	3.8
88 DCA	412	37.4	51.1	11.6	88 DCA	514	44.9	38.1	17.1
88 DCA	414	43.8	48.2	8	88 DCA	515	33.5	55.6	11.1
88 DCA	415	37.2	51.9	11.3	88 DCA	516	40	53.7	6.4
88 DCA	416	42.2	50.3	7.7	88 DCA	517	40	49.1	11
88 DCA	417	38.4	43.6	18.3	88 DCA	518	59.9	27.6	12.6
88 DCA	418	36.7	53.2	11.5	88 DCA	519	48	42.9	7.6
88 DCA	419	30	55.9	14.1	88 DCA	520	64.7	24	11.3
88 DCA	420	34.2	58.9	7.2	88 DCA	521	44	43	13
88 DCA	428	54.5	40.9	4.7	88 DCA	525	41.7	46.3	12.3
88 DCA	429	30.3	56.6	13.3	88 DCA	526	23.2	56.4	20.5
88 DCA	455	41	45.9	13.2	88 DCA	532	54.5	39.6	6
88 DCA	457	50.2	39.4	10.6	88 DCA	533	48.2	42.4	9.4
88 DCA	459	57.7	34.5	7.6	88 DCA	534	35.2	52.8	12.5
88 DCA	460	54	34.6	10.4	88 DCA	535	63.8	20.4	15.8
88 DCA	463	40.9	38.3	20.4	88 DCA	536	52.3	43.5	4.2
88 DCA	464	48.2	45.5	6.5	88 DCA	554	43.2	59.4	17.5
88 DCA	467	63.8	22.5	13.6	88 DCA	556	54.8	34.9	10.4
88 DCA	472	31.1	55.6	13.6	88 DCA	557	55.6	35.6	8.8
88 DCA	473	42.7	45.1	12.5	88 DCA	558	61.7	33.6	4.8
88 DCA	474	38.6	41.7	19.8	88 DCA	559	35	57.3	7.9
88 DCA	475	32.4	54.5	9.9	88 DCA	560	48.3	47.2	5.1
88 DCA	476	32.5	59.4	8.3	88 DCA	561	41.5	55.7	2.8
88 DCA	481	47.1	37.3	15.6	88 DCA	562	39.6	57.9	2.7
88 DCA	482	47.2	42.6	10.5	88 DCA	563	45.9	48.7	5.3
88 DCA	483	46.8	45	8.5	88 DCA	564	26.1	69.5	4.6
88 DCA	485	60.7	29.5	10	88 DCA	567	29.5	61.5	9.4
88 DCA	486	59.4	31.7	9.1	88 DCA	570	39.8	51.5	8.9
88 DCA	487	35.1	47.8	17.3	88 DCA	571	28.1	62.6	9.3
88 DCA	488	42.6	34.8	22.7	88 DCA	573	34.2	44.4	21.6
88 DCA	489	53.8	37.4	9	88 DCA	574	33.8	58.2	8.3
88 DCA	490	50.6	36.5	12.9	88 DCA	575	46.4	39.9	13.8
88 DCA	491	43.5	38.8	17.7	89 DCA	403	25	40	35
88 DCA	492	55.5	33.5	11.3	89 DCA	404	44	46	10
88 DCA	494	55.2	35.5	9.4	89 DCA	406	62	21	17
88 DCA	496	32.3	55.4	12.6	89 DCA	409	44	37	19
88 DCA	497	37.9	44.4	18.1	89 DCA	410	46	37	17
88 DCA	498	53.8	36.6	9.8	89 DCA	411	58	30	12
88 DCA	507	72.7	21.8	5.5	89 DCA	412	42	37	21
88 DCA	508	42	45.9	12.3	89 DCA	414	56	30	14
88 DCA	509	36.9	52.1	11.2	89 DCA	415	48	42	10
88 DCA	510	40.5	43.3	16.2	89 DCA	417	65	23	12

Appendix C. Sand, silt and clay content of tills (cont.)

Prefix	Number	Sand(%)	Silt(%)	Clay(%)	Prefix	Number	Sand(%)	Silt(%)	Clay(%)
90 DCA	484	40	51	9	91 DCA	439	93	7	1
90 DCA	485	56	32	12	91 DCA	440	94	6	1
90 DCA	486	42	41	17	91 DCA	441	86	14	0
90 DCA	487	48	42	10	91 DCA	442	89	11	0
90 DCA	489	59	29	12	91 DCA	443	65	29	6
90 DCA	490	59	31	10	91 DCA	444	93	6	1
90 DCA	492	48	34	18	91 DCA	446	74	25	1
90 DCA	493	66	25	9	91 DCA	447	84	14	2
90 DCA	494	60	26	14	91 DCA	448	66	29	5
90 DCA	495	70	21	9	91 DCA	449	62	32	6
90 DCA	496	60	28	12	91 DCA	450	86	13	1
90 DCA	497	53	32	15	91 DCA	451	78	18	4
90 DCA	498	56	30	14	91 DCA	452	83	16	1
90 DCA	499	40	29	31	91 DCA	457	88	4	8
90 DCA	501	47	26	27	91 DCA	458	97	0	3
90 DCA	502	20	50	30	91 DCA	459	81	15	4
90 DCA	503	57	31	12	91 DCA	463	98	1	1
90 DCA	505	71	21	8	91 DCA	464	85	14	1
91 DCA	403	not reported			91 DCA	465	98	1	1
91 DCA	404	not reported			91 DCA	466	88	11	1
91 DCA	406	63	25	12	91 DCA	467	93	6	1
91 DCA	407	40	32	28	91 DCA	468	91	7	2
91 DCA	408	57	22	20	91 DCA	469	95	4	1
91 DCA	411	22	71	7					
91 DCA	416	75	20	5					
91 DCA	417	59	33	8					
91 DCA	418	44	45	11					
91 DCA	419	68	22	10					
91 DCA	420	41	40	19					
91 DCA	421	48	48	4					
91 DCA	423	61	21	12					
91 DCA	424	48	37	15					
91 DCA	425	49	42	9					
91 DCA	426	93	6	1					
91 DCA	427	67	23	10					
91 DCA	428	74	20	6					
91 DCA	429	43	35	22					
91 DCA	431	88	10	2					
91 DCA	432	54	40	6					
91 DCA	433	64	30	6					
91 DCA	434	92	6	2					
91 DCA	436	56	34	10					
91 DCA	437	94	5	1					
91 DCA	438	93	6	1					

Appendix C. Sand, silt and clay content of tills (cont.)

Prefix	Number	Sand(%)	Silt(%)	Clay(%)	Prefix	Number	Sand(%)	Silt(%)	Clay(%)
89 DCA	420	58	30	12	89 DCA	523	42	54	4
89 DCA	422	66	22	12	89 DCA	524	43	46	11
89 DCA	425	50	46	4	89 DCA	525	51	41	8
89 DCA	426	58	35	7	89 DCA	527	49	40	11
89 DCA	427	67	24	9	89 DCA	528	57	35	8
89 DCA	431	31	61	8	89 DCA	529	47	40	13
89 DCA	436	64	28	8	90 DCA	401	51	33	16
89 DCA	437	62	31	7	90 DCA	402	55	30	15
89 DCA	438	55	38	7	90 DCA	403	68	23	9
89 DCA	439	46	41	13	90 DCA	406	47	36	17
89 DCA	440	77	18	5	90 DCA	407	48	32	20
89 DCA	441	29	70	1	90 DCA	408	49	33	18
89 DCA	447	45	46	9	90 DCA	409	55	31	14
89 DCA	448	34	54	12	90 DCA	410	47	36	17
89 DCA	454	44	48	8	90 DCA	415	54	31	15
89 DCA	455	71	23	6	90 DCA	418	54	36	10
89 DCA	456	52	42	6	90 DCA	420	53	35	12
89 DCA	457	49	40	11	90 DCA	421	62	28	10
89 DCA	458	44	46	10	90 DCA	423	85	12	3
89 DCA	462	53	40	7	90 DCA	424	not till?		
89 DCA	463	93	6	1	90 DCA	427	All pebbles		
89 DCA	471	54	34	12	90 DCA	428	not till?		
89 DCA	473	47	34	19	90 DCA	430	54	28	18
89 DCA	474	55	23	22	90 DCA	431	87	10	3
89 DCA	475	36	43	21	90 DCA	433	85	13	2
89 DCA	476	54	36	10	90 DCA	434	95	3	2
89 DCA	483	61	34	5	90 DCA	435	not reported		
89 DCA	484	26	63	11	90 DCA	436	83	10	7
89 DCA	486	50	43	7	90 DCA	437	insufficient sample		
89 DCA	487	43	50	7	90 DCA	446	53	31	16
89 DCA	488	64	29	7	90 DCA	447	61	28	11
89 DCA	489	60	29	11	90 DCA	448	57	27	16
89 DCA	490	49	41	10	90 DCA	449	51	33	16
89 DCA	491	44	37	19	90 DCA	450	58	29	12
89 DCA	492	53	33	14	90 DCA	454	50	36	14
89 DCA	493	32	51	17	90 DCA	455	not reported		
89 DCA	494	49	39	12	90 DCA	456	61	27	12
89 DCA	495	50	35	15	90 DCA	472	34	32	34
89 DCA	496	77	14	9	90 DCA	478	55	36	9
89 DCA	508	insufficient sample			90 DCA	479	31	34	35
89 DCA	509	insufficient sample			90 DCA	480	53	37	10
89 DCA	516	71	18	11	90 DCA	481	46	40	14
89 DCA	517	66	30	4	90 DCA	482	53	34	13
89 DCA	522	47	35	18	90 DCA	483	49	39	12

Appendix D: Altimetry

The elevations of the sample sites were measured with a Wallace and Tiernan surveying barometric altimeter with 2 m increments read to the nearest half meter. Measurement errors due to changes in barometric pressure were minimized by bracketing readings at sample points between two readings at a point of known elevation. The modern high tide line was used as a benchmark for these surveys. For most finds, an altimeter reading was taken at the sample site, followed by a reading at the high tide line and a third reading at the sample site. The elevation of the site was then calculated by averaging the difference between each of the two site readings and the sea level reading. Usually this procedure took only a few minutes so errors resulting from barometric pressure changes were negligible. Typically, the second site reading was within 1 m of the initial reading.

To save time travelling to and from modern sea level, camp elevations were usually used as reference points when measuring the elevation of sites far from the coast. Measurements at these sites were bracketed by readings taken when leaving and returning to the camp. Measured elevations were corrected to compensate for barometric pressure change that occurred during the traverse. To apply the correction, it was assumed that the pressure change was linear over the duration of the traverse. For the 1989-91 field seasons, the average elapsed time on altimeter traverses tied to camp elevations was 6.5 hours and the longest was 10.8 hours. The average change in barometric pressure that occurred during these traverses, expressed in metres, was 13 m; the minimum was 0 m. Such measurements are less accurate than those with only a few minutes of closure.

The approximate range of errors expected for this type of altimetry is given by Dyke (1979, see reference list, Chapter 3), who assigned errors of ±4 m to elevations above 40 m, ±3 m to elevations between 10 and 40 m, and ±1 m to elevations below 10 m. These errors, in light of hundreds of more recent measurements, are generous.

Appendix E: Sample Preparation

The risk of contamination of samples by radiometrically young carbon, particularly plant rootlets, was the main factor evaluated in selecting whalebone samples for radiocarbon dating. Plant rootlets proved capable of penetrating all but the densest bone. Other organic contaminants include black crustose lichens and a species of green algae. This was a serious concern because the introduction of small amounts of modern carbon into an old sample will result in an erroneous (too young) age (Dyke 1979; Dyke et al., 1991; see reference list, Chapter 3). The outer surfaces of many bones and shells were contaminated by hard crusts of brown redeposited carbonate. Surface contaminants on earbones were removed by grinding and sandblasting prior to submission to the radiocarbon laboratory. When earbones could not be found, other bones were collected. These were usually more porous, and were cleaned by sawing the bone into small cubes and then blasting dirt out of the pore spaces with compressed air.

Shells are prone to contamination by redeposited calcium carbonate crusts and, in the case of surface shells, a species of black lichen capable of growing within the shell as well as on the surface. Surface contaminants were removed using a cavitron, which combines an ultrasonic probe with a jet of water to scrub contaminants from the valves. Shells contaminated by black lichens were discarded. Shells excavated from sediment usually required minor cleaning with the cavitron to remove silt adhering to the valves. The shells were leached in HCl at the radiocarbon laboratory prior to dating.

Shell and wood samples were dated at the Radiocarbon Laboratory of the Geological Survey of Canada in Ottawa. Bone samples were dated at the Saskatchewan Research Council laboratory, Saskatoon. All of the bone dates given in this report are conventional age estimates, uncorrected for reservoir effects. The shell dates are corrected by 400 years to account for the marine reservoir effect.

Appendix F: $\partial^{13}C$ for dated shells, wood and bone

Table F-1. Measured $\partial^{13}C$ values for shell and wood samples

Number	Material	$\partial^{13}C$ (‰)
GSC-4695	shells	1.8
GSC-4703	shells	0.9
GSC-4721	shells	1.8
GSC-4754	shells	1.3
GSC-4775	shells	0.9
GSC-4776	shells	1
GSC-4777	shells	1.5
GSC-4894	shells	1
GSC-4897	shells	0.4
GSC-4898	shells	2.4
GSC-5086	shells	0.9
GSC-5087	shells	1.9
GSC-5088	shells	1
GSC-5089	shells	1.1
GSC-5090	shells	1.5
GSC-5091	shells	1.8
GSC-5311	shells	2.3
GSC-5316	shells	2.1
GSC-5331	shells	3
GSC-5345	shells	2.1
GSC-5364	shells	2
GSC-5372	shells	3.1
GSC-5373	shells	2.7
GSC-5374	shells	1.9
GSC-5395	shells	2.6
GSC-5076	wood	-24.9
GSC-5077	wood	-24

Table F-2. Measured $\partial^{13}C$ values for bone samples.

Number	Elevation (m asl)	Age (years BP)	$\partial^{13}C$ (‰)	Corrected Age (years BP)
S-3345	39	5110 ± 90	-15.7	4859 ± 90
S-3346	31	4610 ± 60	-15.9	4356 ± 60
S-3347	19	3340 ± 80	-15.5	3092 ± 80
S-3348	18	3280 ± 80	-15.8	3027 ± 80
S-3349	21	4090 ± 80	-15.6	3840 ± 80
S-3350	21	3700 ± 80	-14.7	3465 ± 80
S-3351	23	4010 ± 80	-15.8	3757 ± 80
S-3352	9	2290 ± 70	-14.8	2053 ± 70
S-3353	19	3880 ± 80	-15.7	3629 ± 80
S-3354	21	3740 ± 80	-14.9	3502 ± 80
S-3355	28	4530 ± 80	-16.0	4274 ± 80
S-3356	17	3330 ± 100	-15.2	3087 ± 100
S-3357	19	3780 ± 80	-15.3	3535 ± 80
S-3358	30	4860 ± 80	-16.4	4598 ± 80
S-3359	47	6150 ± 90	-16.2	5891 ± 90
S-3360	37	5200 ± 90	-16.2	4941 ± 90

*Corrected ages were calculated using the equation:

Corrected Age = uncorrected age + 16 x ($\partial^{13}C$ - -25‰) - 400 years.

where -25‰ is the wood standard and 400 years is the correction for the reservoir effect (for shells since the reservoir effect for bone is unknown).

Appendix G: Radiocarbon Dates From Northwestern Melville Peninsula

Lab Number	Elevation (m)	Age (yrs BP)
BREVOORT RIVER		
GSC-4123	165	8970 ± 90
GSC-4517	110	6930 ± 80
GSC-4454	110	6730 ± 80
GSC-4222	110	6730 ± 80
GSC-4232	75	6000 ± 80
GSC-4184	60	5650 ± 60
GSC-4126	20	3280 ± 60
BAKER BAY		
GSC-4324	220	9110 ± 100
GSC-4348	174	8750 ± 80
GSC-4465	190	8570 ± 100
GSC-4147	160	7970 ± 100
GSC-4429	161	7440 ± 120
GSC-4446	124	6760 ± 70
GSC-4221	120	6920 ± 80
GSC-4225	100	6810 ± 80
GSC-4583	80	6830 ± 130
GSC-4450	61	5900 ± 80
GSC-4169	60	6150 ± 80
GSC-4365	22	4920 ± 70
GARRY BAY		
GSC-4831	100	6920 ± 90
GSC-4464	97	6300 ± 90
GSC-4816	82	6250 ± 80
GSC-4817	69	6700 ± 70
GSC-4463	50	4960 ± 80
GSC-4818	49	5350 ± 80
GSC-4819	30	5240 ± 80
GSC-4825	18	2800 ± 70
GSC-4827	8	2930 ± 60

Appendix G (cont.)

Lab Number	Elevation (m)	Age (yrs BP)
SELKIRK BAY		
GSC-4786	92	6450 ± 70
GSC-4857	45	6150 ± 90
PURFUR COVE/FURY AND HECLA STRAIT		
GSC-4378	121	6520 ± 70
GSC-4562	112	6320 ± 100
GSC-4441	96	6300 ± 80
GSC-4455	79	6320 ± 80
GSC-4549	51	5960 ± 70
GSC-4389	40	5590 ± 60
GSC-4430	22	3960 ± 70

Source:

Dredge, L.A., 1990. The Melville Moraine: sea-level change and response of the western margin of the Foxe Ice Dome, Melville Peninsula, Northwest Territories. *Can. J. Earth. Sci.* 27: 1215-1224.

Appendix H: Dated and Undated Whale and Walrus Samples

Table H-1. Whalebone Dates (cf. Figure 3-6 for locations)

Lab No.	Material	El.	Age	Location
VAN KOENIG POINT:				
S-3099	earbone	4 m	1110 ± 60	71° 02' N, 89° 22' W
S-3044	earbone	11 m	2570 ± 60	71° 01' N, 89° 20' W
S-3096	earbone	23 m	4250 ± 70	70° 55' N, 89° 06' W
S-3098	earbone	27 m	5520 ± 70	70° 55' N, 89° 03' W
S-3045	earbone	28 m	4500 ± 80	70° 58' N, 89° 07' W
SOUTHEAST BERNIER BAY:				
S-3015	earbone	20 m	4115 ± 85	70° 56' N, 87° 45' W
S-3097	skull	22 m	4010 ± 70	70° 57' N, 87° 19' W
S-3075	bone	22 m	3930 ± 80	70° 56' N, 87° 14' W
S-3040	earbone	28 m	5050 ± 165	70° 56' N, 87° 56' W
S-3014	earbone	37 m	5670 ± 100	70° 56' N, 87° 47' W
S-3013	earbone	49 m	6585 ± 105	70° 56' N, 87° 42' W
MORIN POINT:				
S-3041	vertebra	5 m	2175 ± 130	71° 19' N, 89° 31' W
S-3043	earbone	21 m	3950 ± 70	71° 21' N, 89° 52' W
S-3074	earbone	24 m	4350 ± 70	71° 22' N, 89° 41' W
S-3042	earbone	33 m	5600 ± 90	71° 28' N, 89° 52' W
BELL BAY				
S-3177	earbone	9	2060 ± 100	70°56' N, 84°58' W
S-3179	earbone	21	3790 ± 80	70°56' N, 85°00' W
S-3257	earbone	22.5	3190 ± 90	70°53' N, 84°54' W
S-3256	earbone	22.5	3230 ± 80	70°53' N, 84°54' W
S-3176	earbone	28	4500 ± 100	70°55' N, 85°01' W
S-3098	earbone	31	4930 ± 80	70°57' N, 85°00' W
S-3180	earbone	44	6070 ± 90	70°57' N, 85°05' W
BERLINGUET INLET EAST				
S-3260	earbone	12	2310 ± 80	71°07' N, 85°51' W
S-3183	earbone	16	3990 ± 80	71°07' N, 85°51' W
S-3259	earbone	17	2800 ± 70	71°08' N, 85°40' W
S-3258	earbone	18	3320 ± 80	71°08' N, 85°44' W
S-3181	earbone	19	4220 ± 80	71°08' N, 85°40' W

Table H-1 (cont.)

Lab No.	Material	El.	Age	Location
S-3182	earbone	20.5	3870 ± 80	71°08' N, 85°40' W
S-3124	earbone	26.5	4300 ± 110	71°08' N, 85°40' W
S-3125	earbone	33	4520 ± 100	71°07' N, 85°37' W
BERLINGUET INLET WEST				
S-3262	earbone	15	2700 ± 90	70°58' N, 86°40' W
S-3261	earbone	16	2650 ± 80	70°59' N, 86°26' W
S-3263	earbone	19.5	3250 ± 80	70°58' N, 86°41' W
S-3134	earbone	19.5	3940 ± 90	70°58' N, 86°41' W
S-3128	earbone	29.5	5080 ± 80	70°57' N, 86°39' W
BERLINGUET RIVER				
S-3348	earbone	18	3280 ± 80	71°03' N, 86°21' W
S-3347	earbone	18.5	3340 ± 80	71°05' N, 86°14' W
S-3350	earbone	20.5	3700 ± 80	71°04' N, 86°20' W
S-3349	earbone	20.5	4090 ± 80	71°02' N, 86°41' W
S-3351	earbone	23	4010 ± 80	71°01' N, 86°46' W
BERNIER BAY NORTHEAST				
S-3352	earbone	9	2290 ± 70	71°02' N, 87°17' W
S-3356	earbone	17	3330 ± 100	71°07' N, 87°36' W
S-3353	earbone	18.5	3880 ± 80	71°07' N, 87°40' W
S-3357	earbone	19	3780 ± 80	71°07' N, 87°36' W
S-3354	earbone	20.5	3740 ± 80	71°09' N, 87°45' W
S-3355	earbone	27.5	4530 ± 80	71°09' N, 87°42' W
S-3358	earbone	30	4860 ± 80	71°08' N, 87°37' W
S-3360	earbone	37	5200 ± 90	71°03' N, 87°17' W
S-3359	earbone	47	6150 ± 90	71°03' N, 87°17' W
FOSS FIORD				
S-3346	earbone	31	4610 ± 60	70°25' N, 87°10' W
S-3345	earbone	37.5	5110 ± 90	70°24' N, 87°15' W
CROWN PRINCE FREDERICK ISLAND				
S-3434	earbone	47	5120 ± 120	70°00' N, 86°40' W
S-3431	earbone	50	5310 ± 120	70°00' N, 86°40' W
S-3432	earbone	50	5700 ± 120	70°05' N, 86°43' W
S-3433	earbone	72	6350 ± 130	70°04' N, 86°40' W

Table H-2. Walrus Dates (all are from the Van Koenig Point area)

Laboratory No.	Material	Elevation	Age (yrs BP)	Location
S-3101	walrus tusk	23 m	4320 ± 90	71° 03' N, 89° 02' W
S-3094	walrus tusk	26 m	4440 ± 70	71° 03' N, 89° 22' W
S-3095	walrus tusk	30 m	4810 ± 90	70° 44' N, 89° 06' W
S-3093	walrus skull	38 m	6200 ± 80	70° 58' N, 89° 57' W

Table H-3. Driftwood Dates

Laboratory No.	Material	Elevation	Age (yrs BP)	Location
VAN KOENIG POINT				
GSC-239	wood	2	940 ± 130	70°55' N, 89° 11' W
FOSS FIORD				
GSC-5076	wood	3	1140 ± 80	70°22' N, 87°16' W
GSC-5077	wood	36.5	4660 ± 80	70°22' N, 87°42' W
CROWN PRINCE FREDERICK ISLAND				
GSC-5294	wood	34.5	4210 ± 70	70°04' N, 86°46' W
GSC-5295	wood	68	5870 ± 70	70°02' N, 86°37' W

Table H-4. Undated bowhead samples

Sample Number	Material	Elevation (m)	Location	Assigned Age (ka BP)
88 DCA 404	vertebra	7	71°15' N, 88°32'W	1.5-2
88 DCA 551	vertebra	11	71°18' N, 89°21' W	2.5-3
88 DCA 410	bone	15	71°14' N, 88°06' W	3-3.5
88 DCA 435	rib	19	71°02' N, 89°24' W	3.5-4
88 DCA 425	vertebra	19	71°15' N, 88°30' W	3.5-4
88 DCA 439	skull fragment	20	70°58' N, 89°09' W	3.5-4
88 DCA 478	bone	20	71°03' N, 89°22' W	3.5-4
88 DCA 480	earbone	20	70°01' N, 87°30' W	3.5-4
88 DCA 493	rib	20	70°56' N, 87°54' W	3.5-4
88 DCA 504	skull fragment	20	70°56' N, 87°54' W	3.5-4
88 DCA 529	earbone	20	70°57' N, 87°24' W	3.5-4
88 DCA 553	skull fragment	20	71°18' N, 89°07' W	3.5-4
88 DCA 441	mandible	21	71°02' N, 89°22' W	3.5-4
88 DCA 506	earbone	21	70°57' N, 87°43' W	4-4.5
88 DCA 545	rib	21	71°28' N, 89°50' W	4-4.5
88 DCA 443	skull fragment	25	71°03' N, 89°22' W	4-4.5

Table H-4 (cont.)

Sample Number	Material	Elevation (m)	Location	Assigned Age (ka BP)
88 DCA 576	skull fragment	25	71°18' N, 89°20' W	4.5-5
88 DCA 433	vertebra	27	70°59' N, 89°12' W	4-4.5
88 DCA 479	skull fragment	27	70°58' N, 89°07' W	4-4.5
88 DCA 427	skull fragment	27	71°15' N, 88°13' W	4.5-5
88 DCA 426	skull fragment	27	71°15' N, 88°13' W	4.5-5
88 DCA 422	skull fragment	30	71°17' N, 88°42' W	5-5.5
88 DCA 470	skull fragment	34	70°47' N, 89°17' W	5-5.5
88 DCA 552	earbone	39	71°18' N, 89°08' W	5.5-6
88 DCA 421	vertebra	39	71°16' N, 88°39' W	5.5-6
88 DCA 544	skull fragment	40	71°26' N, 89°47' W	5.5-6
88 DCA 451	bone	41	70°59' N, 89°04' W	5.5-6
88 DCA 437	mandible	44	70°54' N, 89°12' W	5.5-6
88 DCA 423	rib	53	71°17' N, 88°52' W	6.5-7
88 DCA 548	skull fragment	54	71°23' N, 89°40' W	6.5-7
88 DCA 543	skull fragment	58	71°25' N, 89°46' W	6.5-7
88 DCA 452	rib	61	70°59' N, 89°03' W	6.5-7
88 DCA 453	skull fragment	61	70°58' N, 89°01' W	6.5-7
89 DCA 470	skull fragment	2.5	71°07' N, 85°49' W	0.5-1
89 DCA 464	skull fragment	4	71°08' N, 85°34' W	0.5-1
89 DCA 531	earbone	4	70°58' N, 86°34' W	0.5-1
89 DCA 513	earbone	8	70°58' N, 86°39' W	1.5-2
89 DCA 480	skull fragment	10	71°08' N, 85°43' W	1.5-2
89 DCA 419	skull fragment	11	70°27' N, 88°20' W	2-2.5
89 DCA 421	vertebra	11	70°27' N, 88°23' W	2-2.5
89 DCA 506	earbone	13.5	70°59' N, 86°26' W	2.5-3
89 DCA 479	skull fragment	14	71°08' N, 85°40' W	2.5-3
89 DCA 501	earbone	17	71°01' N, 85°51' W	2.5-3
89 DCA 465	earbone	18	71°08' N, 85°36' W	3-3.5
89 DCA 469	skull fragment	18	71°08' N, 85°42' W	3-3.5
89 DCA 510	rib	18.5	70°59' N, 86°18' W	3-3.5
89 DCA 520	earbone	18.5	70°58' N, 86°41' W	3-3.5
89 DCA 402	rib	19	70°23' N, 88°03' W	3-3.5
89 DCA 424	earbone	19.5	70°52' N, 84°52' W	3-3.5
89 DCA 521	earbone	19.5	70°58' N, 86°44' W	3-3.5

Table H-4 (cont.)

Sample Number	Material	Elevation (m)	Location	Assigned Age (ka BP)
89 DCA 478	earbone	20	71°08' N, 85°40' W	3-3.5
89 DCA 482	earbone	20	71°07' N, 85°49' W	3-3.5
89 DCA 500	earbone	20	71°07' N, 85°49' W	3-3.5
89 DCA 518	earbone	20	70°57' N, 86°37' W	3-3.5
89 DCA 401	skull fragment	22.5	70°26' N, 88°18' W	3-3.5
89 DCA 433	skull fragment	22.5	70°53' N, 84°54' W	3-3.5
89 DCA 435	earbone	22.5	70°05' N, 84°04' W	3-3.5
89 DCA 450	earbone	22.5	70°53' N, 84°54' W	3-3.5
89 DCA 451	earbone	22.5	70°53' N, 84°54' W	3-3.5
89 DCA 467	earbone	23.5	missing	3-3.5
89 DCA 461	skull fragment	25	71°08' N, 85°09' W	3.5-4
89 DCA 418	skull fragment	25.5	70°26' N, 88°17' W	3.5-4
89 DCA 468	earbone	26.5	71°08' N, 85°41' W	3.5-4
89 DCA 452	earbone	27	70°54' N, 84°56' W	3.5-4
89 DCA 446	skull fragment	31.5	70°55' N, 85°10' W	4-4.5
90 DCA 468	skull fragment	6	71°05' N, 87°27' W	1.5-2
90 DCA 465	skull fragment	7	71°02' N, 87°17' W	2-2.5
90 DCA 439	earbone	13	71°06' N, 86°14' W	2.5-3
90 DCA 441	earbone	17.5	71°03' N, 86°26' W	3-3.5
90 DCA 452	earbone	18	71°01' N, 86°44' W	3-3.5
90 DCA 463	earbone	18	71°02' N, 87°09' W	3.5-4
90 DCA 467	skull fragment	19	71°05' N, 87°26' W	3.5-4
90 DCA 470	earbone	19.5	71°08' N, 87°37' W	3.5-4
90 DCA 444	earbone	20	71°02' N, 46°38' W	3.5-4
90 DCA 464	rib	20	71°02' N, 87°05' W	4-4.5
90 DCA 442	earbone	20.5	71°02' N, 86°34' W	3.5-4
90 DCA 462	skull fragment	22	71°10' N, 87°23' W	3.5-4
90 DCA 443	earbone	22.5	71°02' N, 86°36' W	3.5-4
90 DCA 413	mandible	23.5	70°22' N, 87°29' W	3.5-4
90 DCA 461	skull fragment	33	71°05' N, 86°16' W	4.5-5
90 DCA 477	skull fragment	38.5	71°09' N, 87°44' W	5-5.5
91 DCA 405	skull fragment	74	70°04' N, 86°40' W	6-6.5

Table H-5. Undated walrus finds

Sample Number	Material	Elevation (m)	Location	Assigned Age (ka BP)
89 DCA 505	tusk	1	70°59' N, 86°25' W	0-0.5
88 DCA 539	bone	2	71°20' N, 89°40' W	0-0.5
88 DCA 550	tusk	2	71°18' N, 89°25' W	0-0.5
88 DCA 442	bone	21	71°02' N, 89°22' W	3.5-4
88 DCA 445	tusk	26	71°03' N, 89°22' W	4-4.5
88 DCA 447	tusk	26	71°03' N, 89°22' W	4-4.5
88 DCA 448	tusk	26	71°03' N, 89°22' W	4-4.5
91 DCA 414	tusk	26	70°02' N, 86°33' W	3-3.5
89 DCA 408	tusk	26.5	70°17' N, 87°45' W	3.5-4
89 DCA 407	tusk	31.5	70°17' N, 87°46' W	4-4.5
88 DCA 468	tusk	32	70°44' N, 89°06' W	4.5-5
91 DCA 402	tusk	36	70°02' N, 86°30' W	4-4.5
91 DCA 415	tusk	41	70°02' N, 86°35' W	4.5-5
88 DCA 547	jaw	52	71°23' N, 89°42' W	6-6.5